UNIVERSITY OF GÄVLE

FACULTY OF ENGINEERING AND SUSTAINABLE DEVELOPMENT
Department of Building, Energy and Environmental Engineering

Analysis of the Solarus C-PVT solar collector and design of a new prototype

Solarus C-PVT eguzki kolektorearen analisia eta prototipo berri baten diseinua

Analisis del collector solar Solarus C-PVT y diseño de un nuevo prototipo

Xabier Saizar Zubeldia
Gerard Vila Montagut

2015-2016
Student thesis, Master degree (one year), 15 HE
Energy Systems
Master Programme in Energy Systems
2015-2016

Supervisor: Björn Karlsson
Examiner: Nawzad Mardan

Abstract

Finding cleaner and sustainable energy resources is one of the most important concerns for the development of humanity. Solar energy is taking an essential role in this matter as the production cost of solar collectors is decreasing and more solar installations are being set up every year throughout the world. One way of reducing the cost of solar panels is by using concentrators that are cheaper than the costly photovoltaic cells and can increase their output. Solarus AB designed a Photovoltaic Thermal (PVT) hybrid collector that uses this principle and which is a variation of the Maximum Reflector Collector (MaReCo) design and is a Compound Parabolic Collector (CPC).

This thesis has two main objectives. The first one is to design variations of the actual Solarus' design and some alternative MaReCo designs and pure parabola designs. These designs include new solar cell cuts which are based on 4 busbar solar cells. In this way a future in-depth analysis may be carried out by comparing different receiver designs and collector boxes. The second goal is to investigate the current electrical and thermal performance of the collectors from Solarus AB which are installed in the Hus 45 of HiG. The appropriate data of the installation has been obtained using simulations and specific software, and it has been analysed with Microsoft Excel®.

Concerning the new designs of the receivers and boxes, everything has been prepared for the future construction of the prototypes. All the measurements and their adjustments have been taken into account to define the size of the components and the process of building has been set up. Moreover, some future work has been planned in order to move forward the project.

Regarding the analysis of the HiG installation, both electrical and thermal performance have resulted to be significantly lower compared with their estimated simulation, being their real output around 60 % of the estimated one. In the thermal part, the losses in the pipeline result to be more than a third part of the produced heat. In the electrical part, the production varies a lot between different collectors due to some of them do not work properly, consequence of poor condition of the solar panels (broken cells, dirt, shading, etc.).

Keywords: Solar Collector, Photovoltaic Thermal Hybrid, MaReCo, Concentrating PVT

Acknowledgements

Firstly, we would like to thank the organizations that gave us the opportunity of going on an Erasmus course to perform the Master in Energy Systems in Högskolan i Gävle. The "Euskal Herriko Unibertsitatea" and "Universitat Politècnica de Catalunya", where we have been studying our Master's degree in Industrial Engineering, have enabled us to perform the Erasmus studies thanks to their agreements with international universities. Secondly we thank Högskolan i Gävle for accepting us and evaluating our thesis. Thirdly, we would like to express our gratitude to our families for encouraging us and giving us the necessary support for this experience.

We are also very thankful to our supervisor Dr. Björn Karlsson, who has transmitted us his enthusiasm, passion and extensive knowledge of the MaReCo design. He has contributed with valuable comments on our work and has guided us with his wisdom.

We owe much gratitude to Solarus AB and concretely to João Santos Leite Cima Gomes who offered us the opportunity to work with them and develop this thesis there. We have not only learnt a lot about solar energy, but also we have been involved in a working environment. As we have been working in real projects that the company has developed, we expect that this thesis work can be useful to Solarus AB. We must also thank João for all the time and resources that he and the company have devoted while providing us the necessary equipment for this study.

Last but not least, we would like to thank all the people who have collaborated with the work performed during this stay. Our thanks also extend to the staff members of Solarus AB that have cooperated with these tasks and concretely to Tony Björklund, Olle Olsson and Patrick Maier, for their collaboration and great work while performing the research.

Contents

List of Figures

List of Tables

Nomenclature

Roman symbols

$A_{absorber}$	Absorber area of the collector [m^2]
$A_{aperture}$	Aperture area of the collector [m^2]
A_{gross}	Total area of the collector [m^2]
a_1	First order heat loss coefficient [$W/m^2 \cdot K$]
a_2	Second order heat loss coefficient [$W/m^2 \cdot K^2$]
C	Area concentration ratio
$C_{circular}$	Geometric concentration ratio of a circular CPC (3D)
C_{linear}	Geometric concentration ratio of a linear CPC (2D)
C_p	Specific heat [kJ/kg·K]
E_{el}	Electrical energy [kWh]
E_{th}	Thermal energy [kWh]
G_T	Solar irradiance [W/m^2]
I_{mp}	Maximum power point current [A]
I_{sc}	Short circuit current [A]
Q	Thermal power output [kW]
T_a	Ambient temperature [ºC]
T_{in}	Inlet water temperature of the collector [ºC]
T_m	Average temperature in the panel [ºC]
T_{out}	Outlet water temperature of the collector [ºC]
U	Heat loss coefficient [$W/m^2 \cdot K$]
V_{mp}	Maximum power point voltage [V]

V_{oc}	Open circuit voltage [V]
$\dot{V}$	Volumetric flow rate [m^3/s]
W_p	Peak power at STC [W]

Greek symbols

η_0	Zero-loss thermal efficiency
η_{th}	Thermal efficiency
θ_{accept}	Acceptance angle of the CPC [rad o deg]
ρ	Density [kg/m^3]

Glossary

AM	Air Mass ratio. Its value shapes the spectral distribution of solar irradiance.
CPC	Compound Parabolic Collector
C-PVT	Concentrating Photovoltaic Thermal
HiG	Högskolan i Gävle
IAM	Incidence Angle Modifier
MaReCo	Maximum Reflector Collector
PV	Photovoltaic
PVT	Photovoltaic Thermal. Hybrid systems combining electricity and heat generation in a single module.
STC	Standard Test Conditions. For solar modules: T=25 ºC, I=1000 W/m^2, and solar spectrum of AM1,5.

Chapter 1

Introduction

Energy is one of the most important concerns for the future and development of humanity, as the economic activity is strongly related with the availability of energy. It is known that fossil fuels reserve (which are actually the main source of energy) are declining, which arises the need of finding other sources of energy production. The increase of concentration of CO_2 in the atmosphere that comes from the combustion of fossil fuels is the main reason of global warming, and makes it more urgent the search of "clean" energy production like renewable energy. Solar energy is a good alternative to fossil fuels as solar radiation can be considered infinite (at a human scale) and it is environmentally friendly due to the non-production of pollutants in energy conversion.

Current solar energy generation is increasing a lot due to high investigation in the area and the decreasing cost of their production. The efficiency of PV modules is still low, but there have been plenty of improvements in the last years. In this thesis, the new designs of the concentrating solar panel are analyzed owing to the change of sizes of solar cells. With this research, it is intended to optimize the arrangement of solar cells in a C-PVT solar panel. Moreover, the current performance of the installation located in HiG is examined to detect the possible need of improvements.

1.1. Motivation

It is commonly known that all societies require energy services to meet basic human needs and to serve productive processes. Sustainable social and economic development requires affordable and guaranteed access to the energy resources necessary to provide indispensable and sustainable energy services. Access to clean and reliable energy

establishes an important prerequisite for basic determinants of human development, contributing, for instance, to economic activity, poverty alleviation, education, health and gender equality [1]. However, the majority of current primary energy driving global economies comes from the combustion of fossil fuels or/and from the controversial nuclear energy. Renewable energy plays a key role in providing energy in a sustainable manner and in mitigating climate change, contributing in that way to the transition to modern energy access.

Solar energy can be obtained in several ways and technologies such as simple flat-plate collectors or concentrating systems, having each technology its different characteristics. In order to be more competitive in the market, PV systems need to reduce their costs and since the solar cells are the most expensive component of an entire module, a reduction of their area would highly diminish overall costs.

On the other hand, the possibility to perform the Master Thesis in a company is considered as a huge opportunity. It allows the authors to be completely involved in a work atmosphere and it is really attractive to see that the project is real and it is useful for the company as well. The authors also prefer more practical research rather than pure theoretical and literature study. Moreover, the research is not only related with the energy area but also with an industrial field, which means that the research combines both background knowledge that the authors have acquired during their studies in Barcelona/Bilbao and in Gävle.

1.2. Objectives and limitations

The main objectives of this thesis are listed as it follows:

- Understand the operation of a hybrid concentrating collector and comprehend all its parts and their functions.
- Design the new prototype of the C-PVT collector in order to analyze how the cell cuts influence the performance.
- Analyze and evaluate the operating installation located at HiG of the collectors from Solarus AB. Verify its correct behavior and/or identify possible deficient points.
- Study the production process of the actual Solarus collectors and make a representative guideline. Define all the tasks involved in the assembly process and their pertinent times.

- Investigate the actual PVT market to detect the strengths and drawbacks of the Solarus' collector.

Although doing the thesis in a company has its advantages, there are some limitations which affect the development of the thesis. For instance each step has to be agreed with the superiors and this may lead to variations with the initial ideas and prolong the project.

1.3. About Solarus AB

1.3.1. The company

Solarus AB is a private small-medium company which develops, produces and sells hybrid solar PowerCollectors^{TM} and integrated project solutions. Hybrid means that the PowerCollectors^{TM} combines generation of thermal energy with the photovoltaic generation of electricity.

Solarus is headquartered in Venlo (Netherlands) with a Research & Development center in Gävle (Sweden). It operates worldwide with business development, assembly distribution and installation partners. Innovative local solutions to local needs are provided with these licensees.

Solarus' promise is to create general public benefit by alleviating energy poverty as well as leaving a material positive impact on society and the environment. Some of their objectives can be listed as:

- Reducing energy poverty by providing access to low-cost, efficient and environmentally sustainable electrical and thermal energy
- Addressing climate change by increasing the use of low-carbon C-PVT technology and decreasing global dependency on fossil fuel-based energy sources.
- Creating local employment opportunities in developing countries in manufacturing, assembly, distribution and installation.

Moreover, Solarus is a certified B Corp. This means that it is a for-profit company certified by the nonprofit B Lab to meet rigorous standards of social and environmental performance, accountability and transparency.

1.3.2. Our place in the company

The Solarus Company is divided in four main departments:

- The direction which manages the company, transfers information to the others departments and finds new investors.
- The marketing department which is in charge of the sales, products advertisings and communications.
- The production area which assembles and builds collectors.
- The Research & Development (R&D) develops designs of collectors and performs their simulations and tests.

During the performance of this master thesis, the authors have been integrated into the R&D department and have been highly involved in the projects of the company. This department is composed by a team of eight people: three employees of which two are PhD students, and five interns.

Furthermore, the authors have been in contact with the supervisor Björn Karlsson in Högskolan i Gävle. He worked alongside Solarus for several years and he is still now in contact with the company mainly because he is the responsible of one of the PhD students. So, the organization of the company and place where the authors have been located can be described in the Figure 1.1.

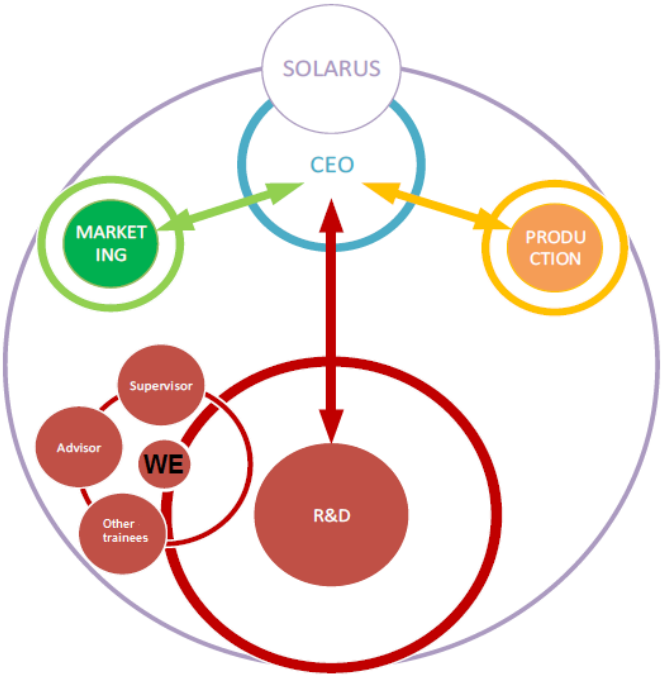

Figure 1.1. Place in the company of the authors

1.4. Organization of the Thesis

The chapters presented in this thesis have been arranged thematically. Here, a brief description of each one is presented.

Chapter 2 gives the reader a theoretical background, starting from the fundamentals of solar energy, photovoltaic modules and hybrid systems, and ending with a more specific study of concentrating solar panels explaining the basics of CPC technology and the MaReCo family.

Chapter 3 details a description of the Solaurs C-PVT collector. It contains the explanations of its purpose, its parts and its performance.

Chapter 4 contains the descriptions of all the 4 projects done in this thesis, the design of the new prototype, the analysis of the HiG installation, the market review and the production process guideline.

In *Chapter 5* the method used in each project is explained, all the important parameters that were taken into account for each of them and the realization of them.

Chapter 6 contains the results gotten from each research and they have been displayed in tables, graphs and images for a better understanding.

In *Chapter 7* the results achieved in the previous chapter are discussed trying to get a clear conclusion out of them.

Finally, *Chapter 8* includes the recommendations that the authors make in order to go straight on with the projects. The future work is planned and detailed for the main projects.

Chapter 2

Theoretical Background

2.1. Solar Energy

The sun emits energy to the earth in the form of solar radiation. This solar radiation interacts with the atmosphere, decreasing the radiation that arrives at the earth's surface. As a result, around 1000 W/m^2 of irradiance reaches the surface at sea-level on a clear day [2].

This solar radiation can be used to generate electricity and/or heating by a solar panel. The photovoltaic solar panels are the ones who generate electricity out of solar radiation, the thermal panels are the ones who generate heat, and lastly, the hybrid PVT panels can generate simultaneously electricity and heating in the same module. In a PVT solar panel, by combining a PV module and a solar thermal collector, more solar radiation can be harvested and the total efficiency of the module is increased [3].

2.2. PV modules

A photovoltaic module consists of solar cells connected in an assembly usually of 6x10 solar cells. The cells are connected in series for achieving the desired voltage output, or in parallel for the desired current output. The modules generate electricity through the photovoltaic effect, which happens when some radiation hits a material surface and the crystallized atoms are ionized, unbalancing the chemical bonds of the material [4].

90 % of the solar cells used in the world consist of Crystalline Silicon (c-Si) solar cells [5], most of them wafer-based. The output of the module is DC power, so in case it is desired to connect to the grid, an inverter is necessary to install among other devices as it can be seen in Figure 2.1.

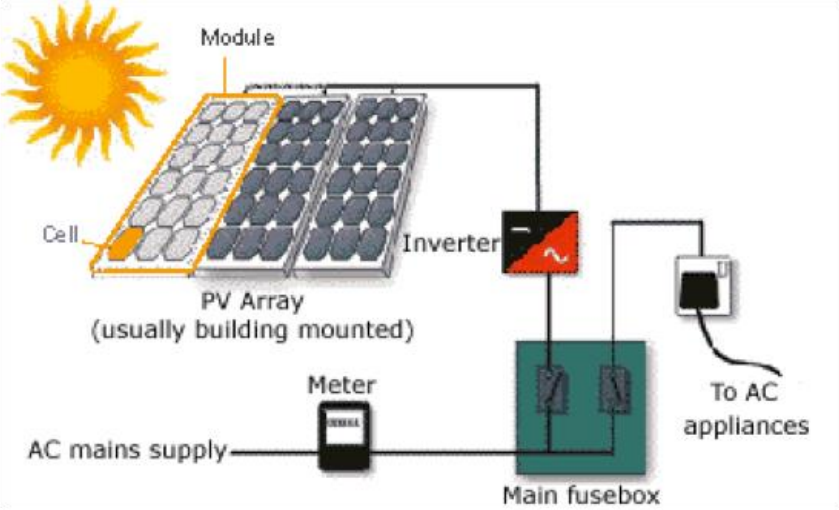

Figure 2.1. Solar panel components [6]

Solar modules cannot produce electricity from all the frequencies of light, just from a range of them, which means that a lot of solar energy is wasted. The range of the frequencies of light in which a solar cell can produce electricity, defines the efficiency of the cell. The highest efficiency that has been achieved in commercial products is 22.5 % [7]. With the efficiency defined, the power output of the module is then determined by the area that the solar cells cover. With a radiation of 1000 W/m^2 and a solar panel of 15 % efficiency, the output power of a panel with an area of 1 m^2 would be 150 W. So 150 W per square meter of solar panels can be harvested with cells of that efficiency. Knowing this fact, it can be seen that a large area is needed to be able to generate a practical power. The other problem that the conventional PV modules have, is that they are still too expensive with long payback periods [8].

2.3. PVT solar panels

A photovoltaic-thermal hybrid solar panel (PVT for simplicity) is a combination of photovoltaic and solar thermal systems which produce both heat and electricity from one unified module (see Figure 2.2). There are a lot of alternative approaches in PVT such as the selection among air, water or evaporative collectors, flat-plate or concentrator types, glazed or unglazed panels, building-integrated or stand-alone units, etc. All these

characteristics and options are summarized in several reference guides as [9,10]. Moreover, a noteworthy amount of research and development on PVT technology has been conducted in the last half century [11,12].

In solar PVT panels, more solar radiation is harvested by using the waste heat that is generated in photovoltaic modules. If the temperature of the PV cells increases, they become less efficient. So by having a cooling system for the solar cells, the temperature of the cells does not increase much (so the efficiency is maintained) and the waste heat can be used for a heating system [13]. Combining both two technologies, less material and space is used as well as the installation time.

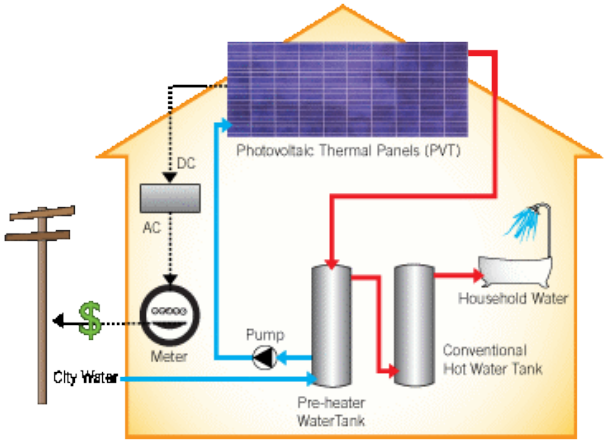

Figure 2.2. PVT solar panel [14]

Moreover, there are other important parameters that should be taken into account for the solar energy, which are the energy payback time and the greenhouse gases payback time. The energy payback time, is the operation time needed for the system to compensate the energy that was needed for the production of the system itself. The greenhouse gases payback time, is the operation time needed for the system to compensate the CO_2 that was emitted in the production of the system itself. The energy payback time of a PVT system ranges between 1-4 years, and the greenhouse gases payback time ranges between 0.8-4 years. Regarding the lifetime of solar panels, several companies give a product warranty of 5-10 years, and an energy performance warranty of 20-25 years, so this the payback times are achieved with ease. The return of investment (ROI) is shorter for PVT panels compared to PV panels, as less material is needed, and the efficiency and the output are much higher [3].

2.4. Concentrator solar panels

In concentrator solar panels, reflectors are used to focus solar radiation to the solar cells, increasing their efficiency. So by increasing the concentration, the efficiency can be augmented. The efficiency of the system is usually improved in two ways: the first one is that a more concentrated solar radiation hits the cells, and the second one is that the solar cells are replaced by cheaper elements as reflectors (Figure 2.3). The concentration ratio can vary much and it is determined by suns (1 sun = 1000 cm^2), from low concentrations (1-10 suns) to very high concentration (larger than 1000 suns) [5]. With concentrator solar panels, it has been achieved experimental total system efficiencies as high as 65.1 % [8].

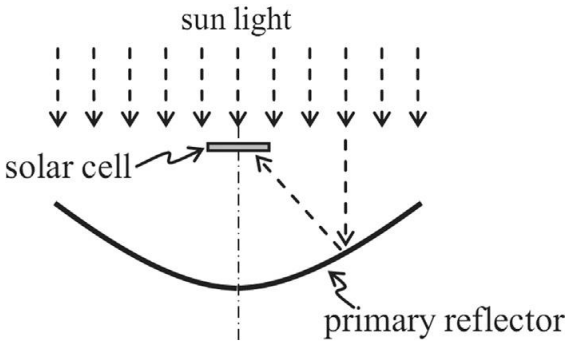

Figure 2.3. Concentrator solar panel [5]

A little drawback that concentrator solar panels have, is that the current increases lineally with concentration ratio, which cause increased power loss caused by series resistance (which is equal to the square of current multiplied by series resistance) [15].

In addition, some of the C-PVT systems include, apart from the trough concentrator and the receiver, a sun tracking system in order to collect the direct radiation. In addition, the installation can encompass a thermal energy storage system to store the heated liquid flowing inner the cavity (absorber) [16].

2.4.1. Compound Parabolic Collectors

The Compound Parabolic Collector (CPC) is a non-imaging concentration technology which is composed of two parabolic reflectors with different focal points (see Figure 2.4). Because of its design, they can function at its maximum performance without tracking the Sun. This fact simplifies their mechanical structure and diminishes difficulties associated with complex and multiple-compounded systems. It also allows a seasonal load-adaption for high latitude climates [17]. However, it is highly important to properly orientate them to the south in order to maximize their output.

One issue that can be found in CPC is the uneven illumination on the receiver due to the existence of individual focus for each parabola [18].

The study of the effects of non-uniform illumination on silicon solar cell performance started as early as in 1984 [19]. Later on, some authors worked with computational ray-tracing techniques in AutoCAD® to detect hotspots on a tubular receiver in a CPC trough [20]. The hotspots caused by non-uniform illumination are not desirable for photovoltaic and heat transfer purposes due to they can critically affect the performance of photovoltaic cells. Moreover, few years ago [21] used optical ray-tracing techniques to study the possibility of utilizing strategically situated diffusers inside the collector in order to alleviate uneven illumination.

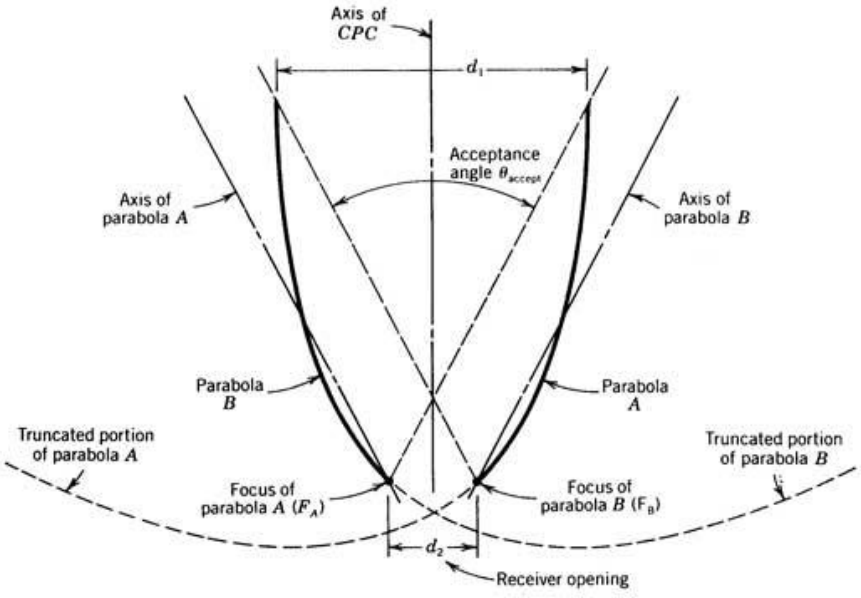

Figure 2.4. The Compound Parabolic Collector (CPC) [22]

A basic design of a CPC can be seen in Figure 2.4, in which the receiver is located in a region called as receiver opening which is situated between both focus of parabolas A and B. The focal point for parabola A lies on parabola B, whereas the focal point of parabola B lies on parabola A. Parabolas redirect and concentrate the incoming radiation on the receiver which can be either cylindrical tubes passing through the region below the focus or flat plates at the base of the intersection of the two parabolas.

The acceptance angle of the CPC is defined by the two parabolas' axis which are also shown in Figure 2.4. The axis of parabola A passes through the focal point of parabola A and the axis of parabola B likewise passes through the focal point of parabola B. This angle has an outstanding importance because it is the one that limits the incident radiation

that is reflected to the receiver. Light with an incidence angle less than one-half the acceptance angle is reflected through the receiver opening (see Figure 2.5a). On the other hand, light with an incidence angle greater than one-half the acceptance angle is not be reflected to the receiver opening (see Figure 2.5b) and could eventually be reflected back out through the aperture of the CPC [22].

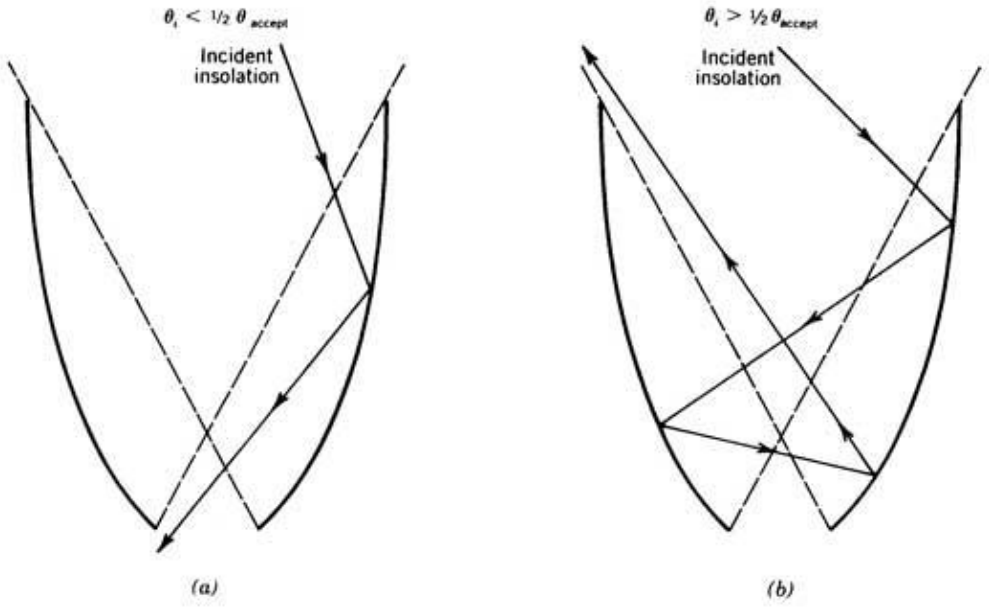

Figure 2.5. Light reflection from the CPC. a) Incidence angle less than one-half the acceptance angle; b) Incidence angle greater than one-half the acceptance angle [22].

Furthermore, if beam solar irradiance parallel to the axis of parabola A were incident on the CPC shown in Figure 2.4, the light would be dreamily focused to the focal point A.

The aperture of the CPC is usually tilted toward the south thus the incident solar irradiance enters within the acceptance angle of the CPC. Moreover, the CPC's aperture does not need to be tracked due to the sun's apparent motion does not cause the incident solar irradiance falling outside the CPC's acceptance angle. Normally, since the declination of the sun does not vary more than the acceptance angle during a day, a CPC's aperture need not be tracked on an hourly basis throughout a day. However, if the incident solar irradiance moves outside the acceptance angle of the CPC, its tilt might have to be adjusted periodically during the year.

2.4.2. The MaReCo

The MaReCo (Maximum Reflector Collector) design is based on an asymmetrical truncated CPC with a flat receiver [23]. It is a non-tracking concentrating collector

developed for northern latitudes (Swedish conditions) and bifacial absorbers are supposed to be used to minimize the absorber area. In this way, it is possible to replace some of the expensive absorber material with cheaper reflectors.

The general design of the MaReCo reflector trough (Figure 2.6) is conceived with two parabolas with their optical axes defining the upper and lower acceptance angles. The reflector consists of three parts [23]:

- Part A, extended from point 1-4, is the lower parabolic reflector. The optical axis of this parabola is situated along the upper acceptance angle and its focus on top of the absorber (point 5).
- Part B, extended from point 1-2, is the connecting circular reflector. This part transfers the light onto absorber's rear side. It substitutes an absorber between point 2 and focus (shown as a dotted absorber in Figure 2.6) with the absorber's rear side between points 1 and 5. In addition, the lower tip of the absorber can be located anywhere between points 1 and 2.
- Part C, extended from point 2-3, is the upper parabolic reflector. The optical axis of this parabola is placed along the lower acceptance angle and its focal point at point 5.

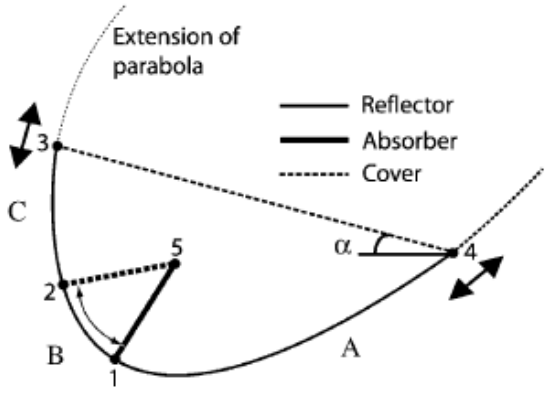

Figure 2.6. Sketch of the basic MaReCo design [23]

Moreover, to determine the position of the truncation, the cover glass (line from point 3 to 4 in Figure 2.6), it is necessary to vary the position of the reflector sheet along the extended parabolas in order to discover the location where maximum annual irradiation onto the aperture is obtained. Owing to the non-symmetrical form of the annual irradiation on a northern latitude, the front reflector is longer than the rear reflector to optimize the annual output.

Taking as a reference the design presented previously, several configurations of the MaReCo collector have been studied and some of them are presented here [23].

- **The Stand-Alone MaReCo**: it is based on the general design pattern and is dimensioned using simulation software to determine the configuration for the desired annual yield. Figure 2.7 shows a schematic section of the stand-alone MaReCo for Stockholm conditions. It has an aperture tilt of 30º while the upper acceptance angle is 65º and the lower is 20º (defined from the horizon).

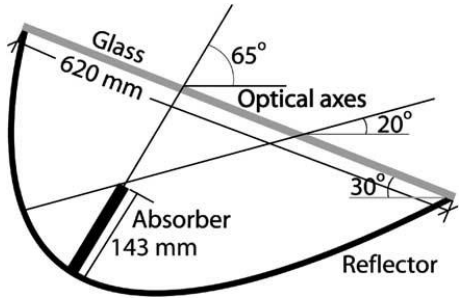

Figure 2.7. Section of the stand-alone MaReCo for Stockholm conditions [23]

- **The Roof-Integrated MaReCo**: the standard roof-integrated MaReCo is shown in Figure 2.8. It is designed by permitting the cover glass start where the circular part of the collector ends. In this way, no upper reflector is used and the inverted absorber is located just underneath the cover. The entire design is tilted to the roof angle.

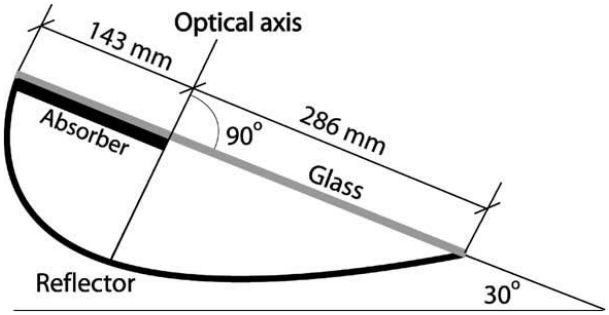

Figure 2.8. Section of the roof-integrated MaReCo design.
Roof angle of 30º and optical axis 90º from the cover glass [23]

Apart from the standard roof-integrated MaReCo, other designs have been performed to adapt them to new conditions. For instance, Figure 2.9 shows the specially designed roof MaReCo for east/west facing roofs which has the

concentrator axis situated in the east/west direction. It accepts radiation in the range of 20 to 90º from the cover glass normal.

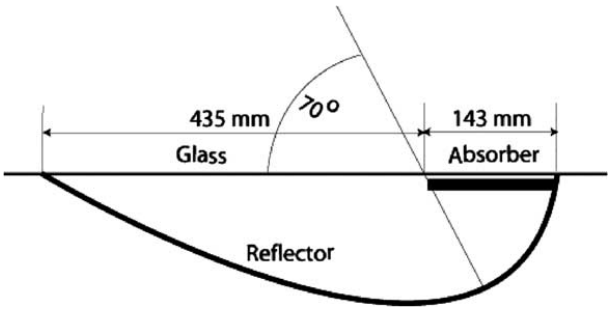

Figure 2.9. Section of the east/west roof MaReCo designed for a roof facing west.
Optical axis 70º from the cover glass [23]

Another example, is the load adapted roof integrated MaReCo, denoted as the spring/fall MaReCo, which is shown in Figure 2.10. Compared to the standard roof-integrated MaReCo, it has the optical axis tilted. This fact implies that beam radiation that hits the reflector with an angle smaller than 15º from the aperture normal will be reflected out of the collector.

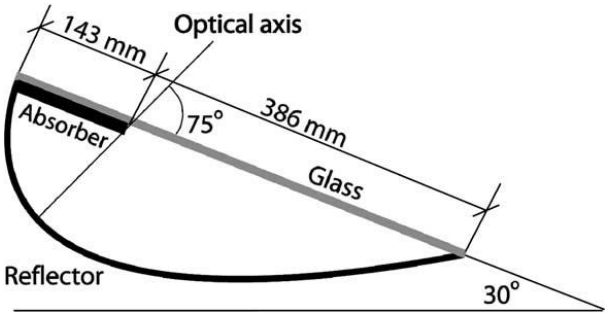

Figure 2.10. Section of the spring/fall MaReCo design.
Roof tilt 30º and optical axis at 45º from the horizon [23]

- **The wall MaReCo**: it is an alternative for a vertical installation which has an acceptance angle interval from 25º to 90º from the horizon, as seen in Figure 2.11. The absorber is also located just underneath the cover glass. It has an optical axis of 25º.

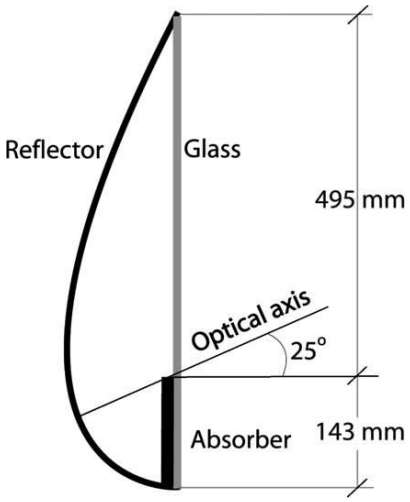

Figure 2.11. Section of the wall MaReCo designed for a south facing wall.
Optical axis at 25º from the horizon [23]

2.4.3. Concentration factor

The concentration factor depends on whether the concentrating system is a two-dimensional concentrator (linear) such as parabolic collector, or a three-dimensional concentrator (circular) such as a parabolic dish. Then, the geometric concentration ratio of a CPC is related to the acceptance angle by

$$C_{linear} = \frac{1}{\sin\left(\frac{1}{2}\theta_{accept}\right)} \qquad \text{(eq. 1)}$$

$$C_{circular} = \frac{1}{\sin\left(\frac{1}{2}\theta_{accept}\right)^2} \qquad \text{(eq. 2)}$$

where θ_{accept} is the acceptance angle of the CPC (see Figure 2.4) [24,25].

However, these formulas are difficult to apply for an anisotropic light source and that is why the ratio of reflector area to aperture area is used [23].

$$C = \frac{Aperture\ Area}{Receiver\ Area} \qquad \text{(eq. 3)}$$

2.5. Solar cell cuts

Normal size solar cells, have a resistive power loss due to the ribbons and the configuration of silicon wafer solar cells (Figure 2.12). This resistive power loss can be reduced by using smaller PV cell cuts.

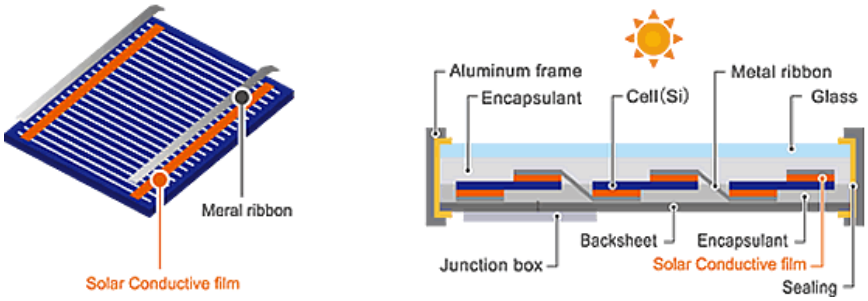

Figure 2.12. Configurations of a silicon wafer solar cell [26]

The cuts have been done perpendicular to the direction of the ribbons. Cutting the module in “n” pieces, makes the current flowing through the module to be”1/n” times [27]. So as it has been seen in the previous section, the power loss is proportional to the square of the current, so the power loss in the ribbon will be “$1/n^2$” times (this can be seen more clearly in Figure 2.13). Making this type of cut, the open circuit voltage (V_0) of the module is expected to be doubled, whereas the short circuit current (I_{sc}) is expected to be halved. So the power output should be the same, but as the power loss is smaller, the power output is higher in the halved cell [27]. Another benefit of cutting the size of solar cells is that the current generation increases, this way increasing the output power. So the current going through the cell will be a little higher than “1/n” times. This may affect the power loss but it also affects the power output in a bigger way. So a halved cell has 4.6 % more power due to this increase is being affected in 32 % by the power loss reduction and 68 % by the short-circuit current increase [28].

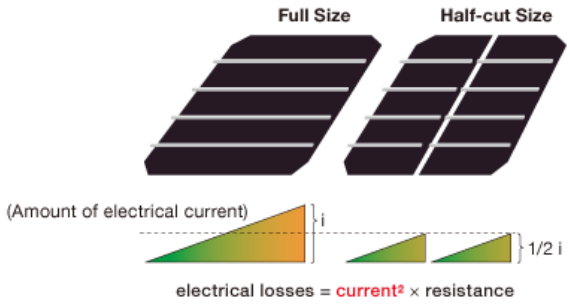

Figure 2.13. Decrease in losses in solar cell cuts [29]

But cutting a solar cell has its drawbacks, because there is additional cost for the laser cutting step, which is a harmful process and additional mismatch losses can be introduced. More space is needed also because there are additional gaps due to more cells and the cost of the ribbons increases [27]. But even though all this drawbacks, the advantages are still important and to be taken into account.

Moreover, it has been tested that the length of the solar cell strings has an important impact on the duration of peak power performance of a panel. Although larger cells slightly decrease the peak power, their peak power lasts for a significantly longer period. In an overall view, the net result is a gain in power production over the day with the use of larger cells [30].

Chapter 3

The Solarus C-PVT collector

3.1. General description

The Solarus C-PVT collector, also called hybrid, is a solar collector that is able to produce both heat and electricity. It is based on an asymmetric Compound Parabolic Collector (CPC) in which the receiver is located to the side of the concentration through rather than in the center as it would be in a symmetric CPC (see Figure 3.1). More specifically, the collectors manufactured and marketed by Solarus AB are from the roof-integrated MaReCo reference design.

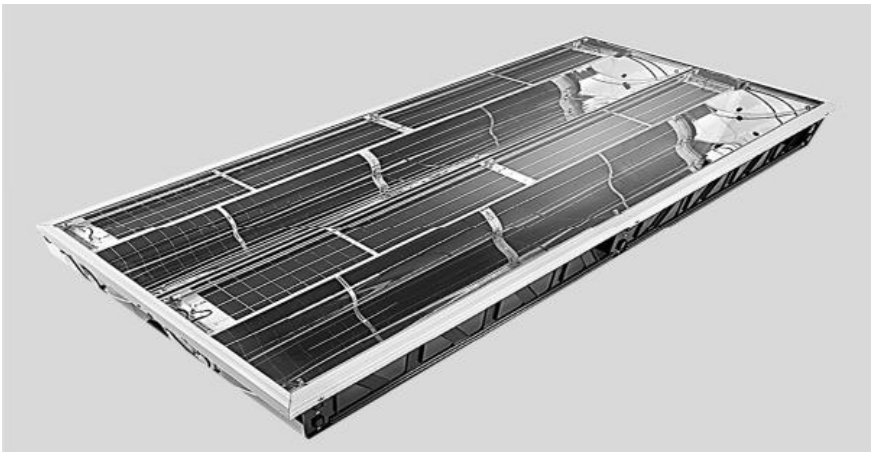

Figure 3.1. Solarus C-PVT collector overview

The collector is a combination of a thermal collector and a standard PV panel and is presented as an alternative to the side-by-side PV modules and thermal collector. The Solarus C-PVT consists of a two-sided PV module, a thermal absorber and a compound reflector as illustrated in Figure 3.2. The upper PV side of the receiver works like a standard module which does not have concentration, while the lower side does.

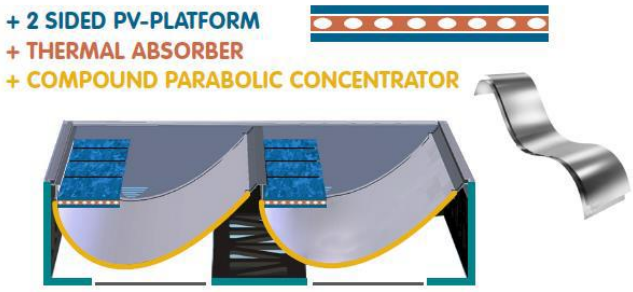

Figure 3.2. General components of the C-PVT collector [31]

The Solarus C-PVT is designed to be installed on south-facing roofs at high latitudes as explained in section 2.4.2. It was developed to provide maximum thermal power in the winter while reducing the supply during summer when the heating load is really low. As it combines both heat and electricity production it has a lot of possible applications and the Figure 3.3 summarizes some of them.

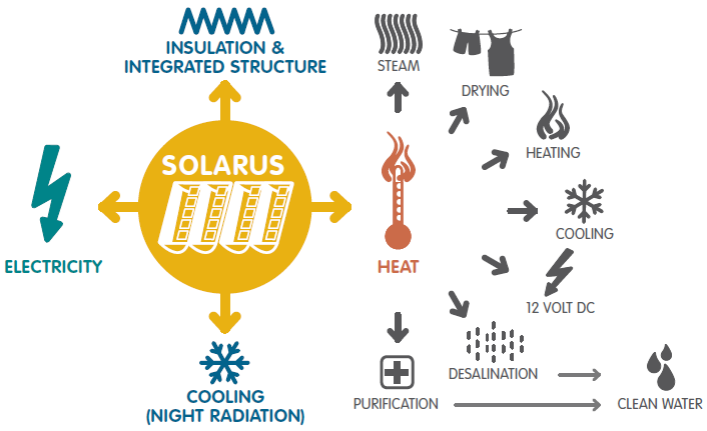

Figure 3.3. Several applications of the Solarus C-PVT collector

3.2. Parts of the collector

3.2.1. The structure

The structure, as it can be seen in Figure 3.4, is based in a plastic frame which provides structural support to the reflector. The glass cover is made of low iron glass with a 95% solar transmittance according to ISO9050 for solar thermal technologies [32]. It is mounted together and with the help of aluminum frames. Moreover, acrylic transparent gables are used at the ends of the troughs.

In addition, three metallic holders are located along the length of the receiver in order to hold the receiver. Three flexible metallic straps are used to keep the reflectors in the appropriate and designed shape.

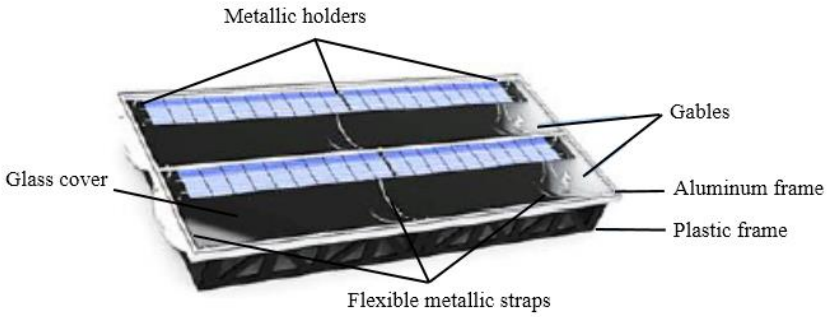

Figure 3.4. Collector structure

3.2.2. The reflector

The reflector is the key component for the concentration part of the collector. It is crucial to develop an optimum reflector that redirects sunlight properly to the receiver. The reflector is composed by two different shapes: circular and parabolic. As it can be observed in Figure 3.5 the circular part corresponds to a quarter of a circle and its radius is 144,86 mm.

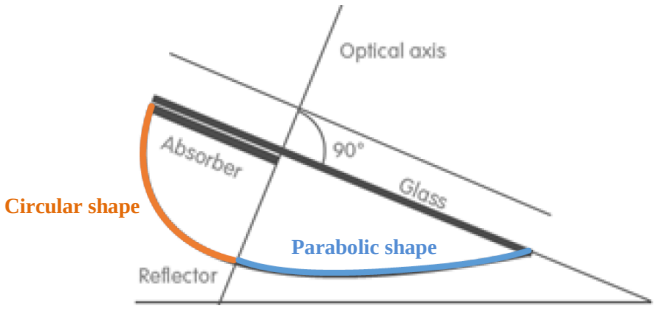

Figure 3.5. Cross section of the Reflector

Both circular and parabolic shapes have the same focus point and the point where the shape changes from circular (cylindrical once extruded) to parabolic matches with the intersection of the optical axis. This optical axis which is perpendicular to the glass cover is critical to determine the acceptance angle. If the incident radiation falls outside this interval, the reflector does not reflect the incoming beam radiation to the absorber and thus collector's efficiency is reduced. Hence, the optical efficiency of the collector during a year depends on the projected solar altitude. In consequence, the tilt of the collector determines the total amount of annual radiation that directed inside the acceptance angle. Studies and researches have been performed about the optimal tilt of the collector [33].

Furthermore, the reflector is made of anodized aluminium with a 95% of total solar reflectance for solar thermal (measured according to norm ASTM891-87) and a total light reflectance of 98% for PV (measured according to norm DIN 5036-3) [34,35].

Following what is explained in Section 2.4.3, using the equation (eq. 4) and the dimensions of the collector, the sunlight is reflected by the compound reflector with a concentration factor of 1,728 in the Solarus PVT.

$$C = \frac{0{,}273 \cdot 2{,}31}{0{,}158 \cdot 2{,}31} = 1{,}728 \qquad \text{(eq. 4)}$$

It has to be stated that the aperture area is taken in the same plane as the receiver.

3.2.3. The receiver

The receiver is 2310 mm long and 157 mm wide and it has two distinctive functions: the electrical and the thermal.

The electrical part is based on a four cell strings connected in series in each side of the receiver (eight cell strings per trough). In total, taking into account that each collector is composed by two troughs, sixteen cells strings are installed per collector. The last design of the collector considers that bottom and top sides are completely separated and their connections with the inverter can be seen in Figure 3.6.

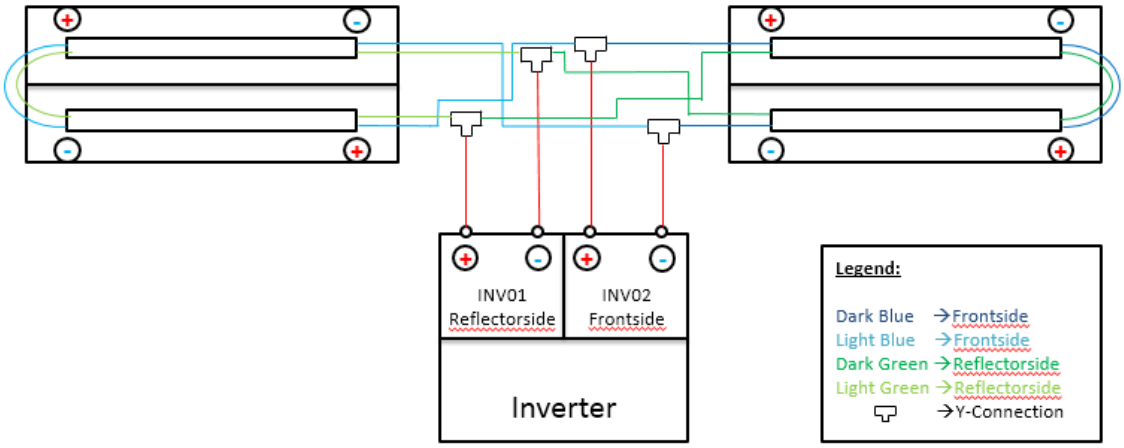

Figure 3.6. Electrical connections of the collector

Monocrystalline cells from Big Sun Energy are used and they have a nominal efficiency of 19,2 % and a temperature dependence of 0,43 %/ºC and their dimensions are 156 mm x 156 mm [36]. But in order to fit with the width of the absorber, the solar cells are cut in 148 mm x 156 mm. After that first step, it is necessary to cut the cells to reduce the current in order to avoid current capacity losses because of the concentration on the collector. So, both troughs have the cells cut one third the size they had previously (52 mm x 148 mm).

In both troughs, each side of the receiver contains 38 cells connected in series organized in four strings of 8-11-11-8 cells respectively. Each receiver has the same cell area: 0,585 m^2 (2 x 38 x 0,148 m x 0,052 m). So, the collector has 1,17 m^2 of solar cell area.

On the other hand, the thermal part is used as a thermal heat sink as well as a support for the PV cells. The absorber is made of aluminum and its design is based on eight elliptic channels whereby a heat-transport fluid (antifreeze, water or both mixed) circulates in order to remove heat. The Figure 3.7 shows the design of the Solarus PVT collector's absorber.

Figure 3.7. Cross section of the Solarus PVT collector's absorber

The total thermal absorber area per receiver, including both sides of a receiver, amounts to 0,7253 m^2 (0,157 m x 2,310 m x 2). It is also interesting to see in the Figure 3.7 that the receiver has two higher lateral edges which are useful for the lamination and the stabilization of the silicone. Solar cells are laminated on both sides of the thermal absorber with an electrically insulated and extremely transparent silicone (transparency of 93% for solar thermal and 96% for PV [37]).

3.3. Characteristics and performance

The characteristics of the Solarus C-PVT collector are listed in the Table 3.1. These parameters describe the performance of an entire module, i.e. two troughs.

Table 3.1. Technical specifications of the Solarus C-PVT collector [31]

Technical Specifications	
General specifications	
Dimensions (L x W x H)	2374 x 1014 x 235 mm
Weight	55 kg
Aperture area	2,2 m^2
Gross area	2,4 m^2
Cover	4 mm anti-reflective coated glass, super transparent, hailstone safe
Frame	Anodized aluminum & ABS ASA plastic
Price	550 €
Electrical properties	
Number of cells	152
Cell dimension	52 mm x 148 mm x 240 µm
Maximum Electrical Power at STC	250 W_p
Maximum Power Voltage (V_{mp})	40 V
Maximum Power Current (I_{mp})	3,7 A
Open Circuit Voltage (V_{oc})	51 V
Short Circuit Current (I_{sc})	4,1 A
Cells' efficiency	19,2 %

Thermal properties	
Peak Power	1250 W
Maximum working Pressure	10 bar
Operating Pressure	6 bar
Stagnation Temperature	180 ºC
Capacity antifreeze	1,4 l/powercollector
Thermal insulation	4,8 $W/m^2 \cdot K$
Absorber material	Aluminum
Zero Loss Efficiency	0,447
1st Order heat loss coefficient	4,48 $W/m^2 \cdot K$
2nd order heat loss coefficient	0,0034 $W/m^2 \cdot K^2$

Chapter 4

Description

4.1. Design of the new C-PVT prototype

One of the main purpose of this thesis is to analyze the effect of different solar cell cuts in the efficiency of a C-PVT solar panel. The size of the cell defines the dimensions of the receiver which, at the same time, influences the size of the reflector and the whole box. So, first of all, the arrangement of the solar cells on the receiver is decided, with the required spacing between cells and between the cells and the edges. Once the measurements are known, the design of the receiver is made by using the program SolidWorks® [38]. After having identified the size of the receiver, the dimensioning of the reflector is made, which consists of a quarter of a circle followed by a parabola. This will be made for the three different solar cell cuts. The ribs of the solar collector are going to be made by including the three reflector designs in the same rib. The reason of this is to use the cover glass of the older solar collectors, so that there is no need to buy a new one.

Apart from this designs, five more designs have been made with the symmetric MaReCo design (3 of them) and pure parabola design (2 of them).

4.2. Analysis and evaluation of the HiG installation

The solar collector installation at Högskolan i Gävle consists of 20 Solarus PVT V.11 solar collectors Figure 4.1, each collector having an aperture area of 2,1761 m^2 and a total collector area of 2,4 m^2 (the total area is used in the several calculations). These collectors feed electricity to the grid and hot water to the local district heating grid. The thermal and electrical systems have been designed and installed by local firms and the collectors have been delivered by Solarus. The installation was finished in 2013, but due to problems with the thermal and electrical controllers, full thermal production of the system has only been achieved since March 2014 and the electrical production since May 2014.

Figure 4.1. C-PVT collector's installation at HiG

4.2.1. Thermal Installation

The thermal installation is done by installing 5 parallel loops with four collector units in each loop as seen in the Figure 4.2. The 5 loops come together and are taken to a heat exchanger for feeding hot water to the district heating system.

The district heating grid requires a minimum temperature of hot water of 70 ºC, which limits the output of the system. As the there is no hot water production at night and almost in the whole winter, two valves are installed in the system for allowing water to the heat exchanger, one on the collector side and the other one in the district heating grid side. Other necessary equipment are the pumps, the filters, the flow meters (which are accumulative) and the expansion tank. All the symbols used are presented in Table 4.1.

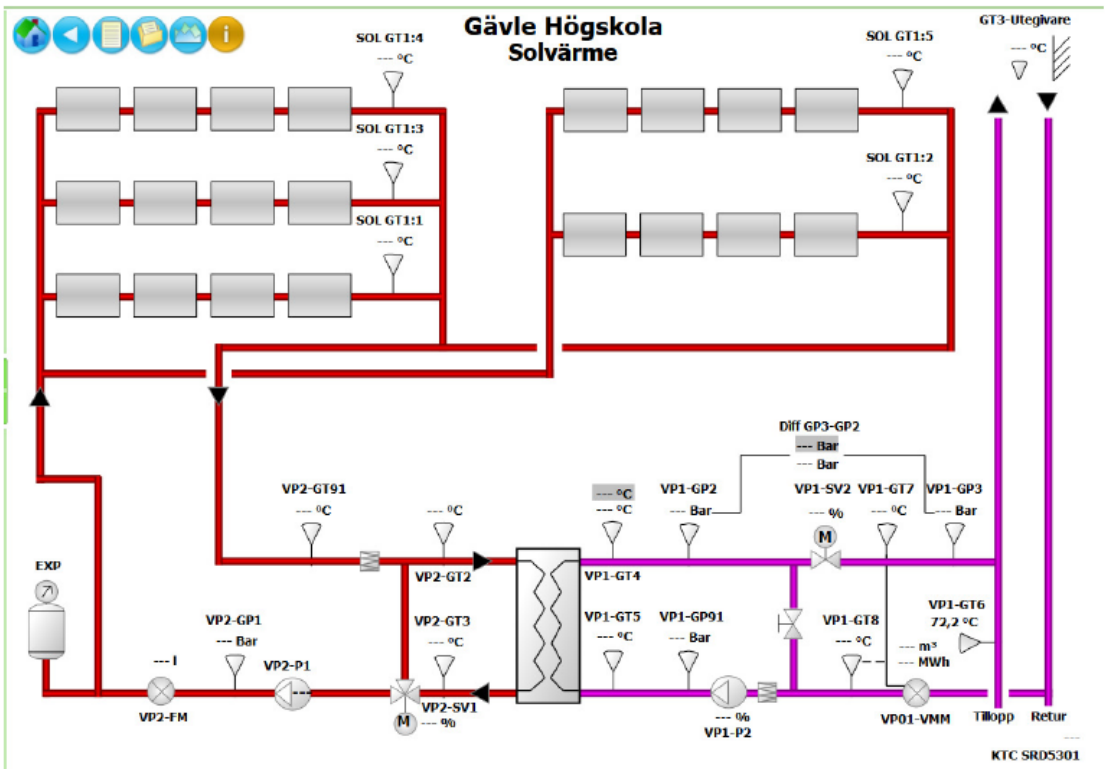

Figure 4.2. Thermal system of the installation at HiG

Table 4.1. Nomenclature of the symbols

Symbol	Nomenclature	Symbol	Nomenclature
	Sensor (T or P)		Filter
	Three-way valve		Valve
	Expansion tank		Flowmeter
			Pump

All the sensors are located indoor except the 5 temperature sensors located next to the solar collectors (SOL GT1:1-5), so these sensors may be affected by the outdoor climate.

The names of the sensors vary depending in which side of the heat exchanger they are. The sensors that are on the side of the district heating grid start by VP1, and the ones that are located on the side of the collectors start by VP2.

The symbol of the temperature and pressure sensors are the same, but they can be differentiated by having a look at their names. After the first name of the sensor (VP1 for district heating side and VP2 for the collector side), the temperature sensors are named by GTX (where X is the number) and the pressure sensors are named GPX.

The thermal fluid used in the installation consists of 30 % propylene glycol and 70 % water. With this fractions, the density of the fluid is 1010,53 kg/m^3, the heat capacity is 3,9147 kJ/kg*K and the freezing point is -14 ºC.

4.2.2. Electrical Installation

The electrical installation is divided in two loops, one consisting of 12 solar panels with a maximum output of 3 kW, and the other one consisting of 8 solar panels with a maximum output of 1,8 kW. They are connected to a Steca grid inverter. DC-DC optimizers are connected to each panel. An overview of the electrical connections can be seen in Figure 4.3 and in Figure 4.4.

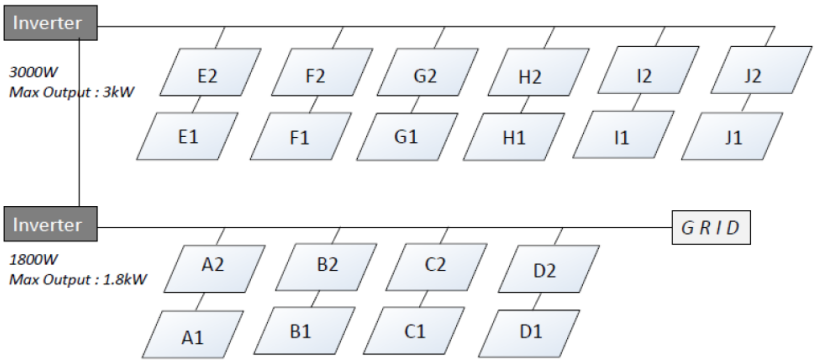

Figure 4.3. Physical layout of the electrical installation

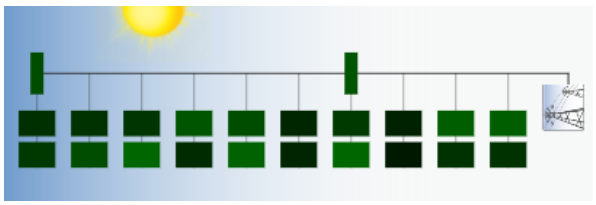

Figure 4.4. Electrical layout of the electrical installation in Tigo

4.2.3. Solar cells

The characteristics of the solar cells used in the solar panels are shown in Table 4.2.

Table 4.2. Characteristics of the solar cells

Data from manufacturer			
Efficiency	18,5-18-69 %	**Power**	4.52 W
Size	156 mm x 156 mm	**Composition**	Poly-c-Si

4.3. Market review and competitor analysis

Competitor analysis is an essential component of corporate strategy [39]. It consists of an assessment of the strengths and weaknesses of current and potential competitors. This analysis permits to identify opportunities and threats based on both offensive and defensive strategic context. With this evaluation, the company is able to establish what makes their product or service unique and therefore what attributes they play up in order to attract their target market.

Obviously, superior knowledge of rivals offers a legitimate source of competitive advantage. A common technique is to create detailed profiles on each of major competitors [40]. These profiles provide an in-depth description and analysis of the competitor's background, finances, products, markets, personnel, strategies, etc. This can involve some of the following listed characteristics:

- **Background**
  - Location of offices, plants and online presences
  - Ownership, corporate governance and organizational structure
  - History, dates and trends
- **Finances**
  - Various financial ratios: liquidity, cash flow, efficiency, debt…
  - Price-Earnings ratio, profitability and dividend policy
  - Profit growth profile and method of growth
- **Products**
  - Products offered with their parameters and performance
  - New products developed and R&D strengths
  - Reverse engineering and patents and licenses
- **Marketing**
  - Segment served, customer base, customer loyalty and market shares
  - Distribution channels used, geographical coverage
  - Pricing, discounts and sales
- **Personnel**
  - Number of employees and skill sets
  - Management style and its strength
  - Benefits and compensations
- **Strategies**
  - Objectives, mission statement and growth plans
  - Marketing strategies

4.4. Production process guideline

Nowadays, numerous companies have relocated their factories in developing countries that have cheaper labor costs. This fact is essentially related to a highly competitive environment and society where money makes the world go round. So, any measure that can be applied in a company and which implies a cost reduction is always welcomed. Probably, one of the most important actions is the optimization of the production process line. Its goal is to reduce the non-added value activities by: redesigning parts of the product, using alternative techniques in some tasks, decreasing lag time between assemblies' steps, improving the internal logistic design, optimizing both workspaces and operators' allocations, etc. [41],[42].

In order to analyze the current production process of Solarus' collectors, a guideline is generated. With its help, it is possible to recognize key points in the assembly process that could be modified and would facilitate the mounting procedure or would reduce the overall production time. The guideline can be considered the first step to optimize the assembly process.

Chapter 5

Method

5.1. Design of the new C-PVT prototype

As stated before, SolidWorks® is used to design the shape of the solar collector for each solar cell cut and for the symmetric MaReCo and pure parabola.

5.1.1. Solar cells

The first step before starting designing the box of the solar collector is to have a look at the solar cell cuts that are provided for analyzing the efficiency. The cell cuts are going to be done by starting from a 4 busbar solar cell, whose measurements are 156 mm x 156 mm. The solar cells are monocrystalline cells with an efficiency of 19,2 %. The electrical characteristics of the solar cells are shown in Table 5.1.

Table 5.1. Electrical characteristics of the standard solar cell

Full Size	
Isc	**9,15 A**
Imp	**8,48 A**
Voc	**0,64 V**
Vmp	**0,54 V**

Having the base solar cell described, three different cell cuts are made to analyze the efficiency of the whole solar collector with them.

5.1.2. Parabolic reflector

The shape of the reflector is a combination of a quarter of a circle and a parabola. The parabola is suitable for concentrating because all irradiation is reflected to the focal point. The mathematical design of the parabola is described by the (eq. 5) [43], where the y and x axes are described in the Figure 5.1 and p is related to the radius of the circular part.

$$y = \frac{x^2}{4 * p} \qquad \text{(eq. 5)}$$

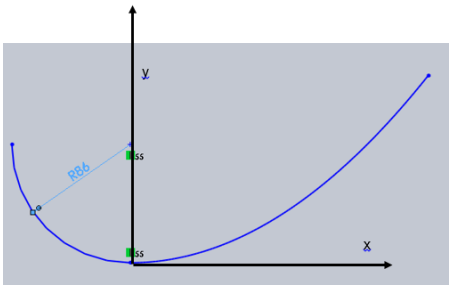

Figure 5.1. Parabolic design

5.1.3. Symmetric MaReCo and pure parabola design

Apart from the comparison between the solar cell cuts, other variations of the MaReCo family collectors are designed. In another collector box, 3 MaReCo symmetric designs are made with a specific arc angle and different reflector heights, and also 2 pure parabola designs are designed with different focus height and same reflector heights Table 5.2. For this, a research paper of Solarus is used where these two designs are analyzed, with different arc angles and focus height, where the efficiencies of them were gotten and compared to the Solarus MaReCo asymmetric design [44].

The different MaReCo designs are with 30º arc angle (θ_c) and reflector heights (Z) of 75 mm, 100 mm and 125 mm, see Figure 5.2.

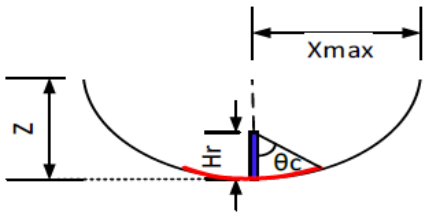

Figure 5.2. MaReCo parameters [44]

The pure parabola designs are both with 75 mm reflector height (Z) and focus lengths (H_r) of 25 mm one and 20 mm the other one, see Figure 5.3.

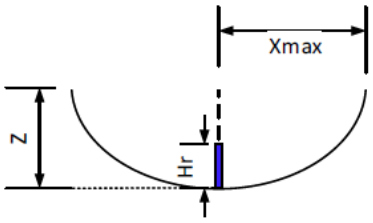

Figure 5.3. Pure parabola parameters [44]

Table 5.2. Different MaReCo and pure parabola designs

Design Number	Reflector Design	Arc circle angle / focus length	Reflector height (mm)
1	Symmetric MaReCo	30º	100
2	Pure Parabola	25 mm	75
3	Symmetric MaReCo	30º	75
4	Symmetric MaReCo	30º	125
5	Pure Parabola	20 mm	75

The shape of the parabola in these designs follows the same equation as in (eq. 5). For the MaReCo type, the arc is drawn first and the parabola is made tangent to the end of the arc. For the pure parabola, the focus length is put in the parameter “p”.

In these designs, the receiver of 78 mm x 39 mm is used and the pipe’s size varies. Three different receivers are made for these designs and as they are of the same size, they can be tested in all the designs. One consists of a 6 mm diameter pipe, putting the receiver sheets in a triangular shape; another one of a 10 mm diameter pipe, the receiver sheets in triangular shape also; and the last one is of 6 mm diameter pipe but the receivers are parallel to each other.

5.2. Analysis and evaluation of the HiG installation

5.2.1. Styr och staller

The thermal data of the Installation at HiG is obtained from the website Styr och staller [45]. In the website, all the data from every sensor in the system is stored, and the data that wants to be displayed has to be chosen from a list, as seen in Figure 5.4.

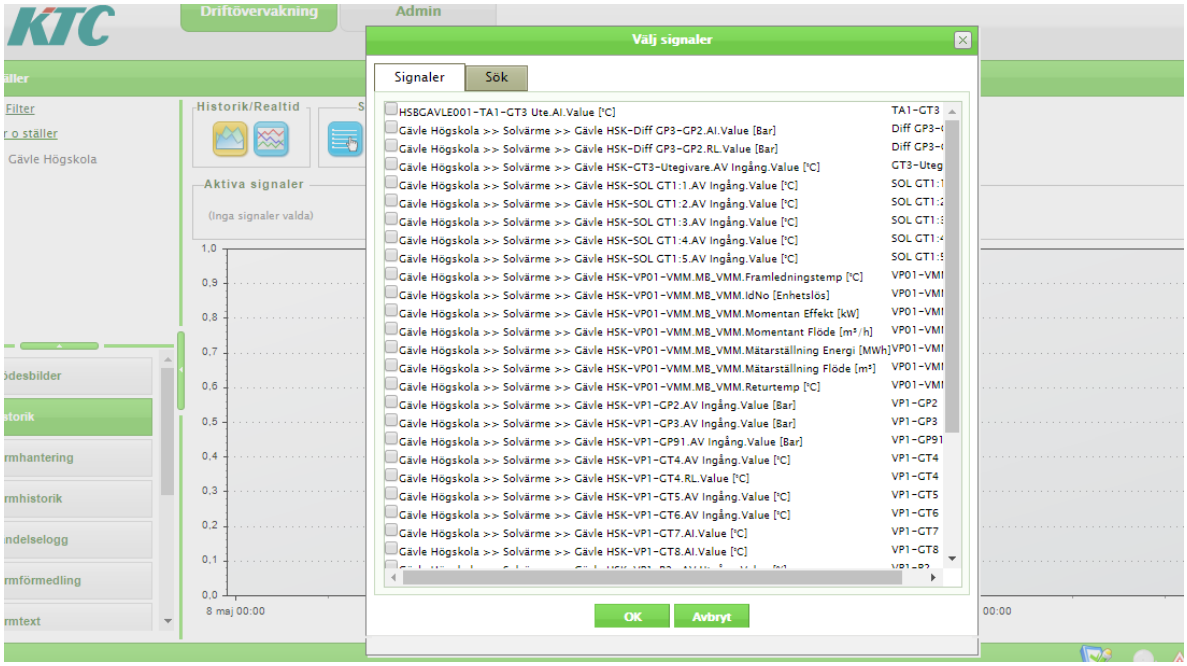

Figure 5.4. Data list in Styr och staller

After selecting the data, the desired time span has to be selected and its interval. In this way a diagram will appear with the different data variation throughout the time (as seen in Figure 5.5) and all the data can be exported to an excel book, to make the treatment of the data easier.

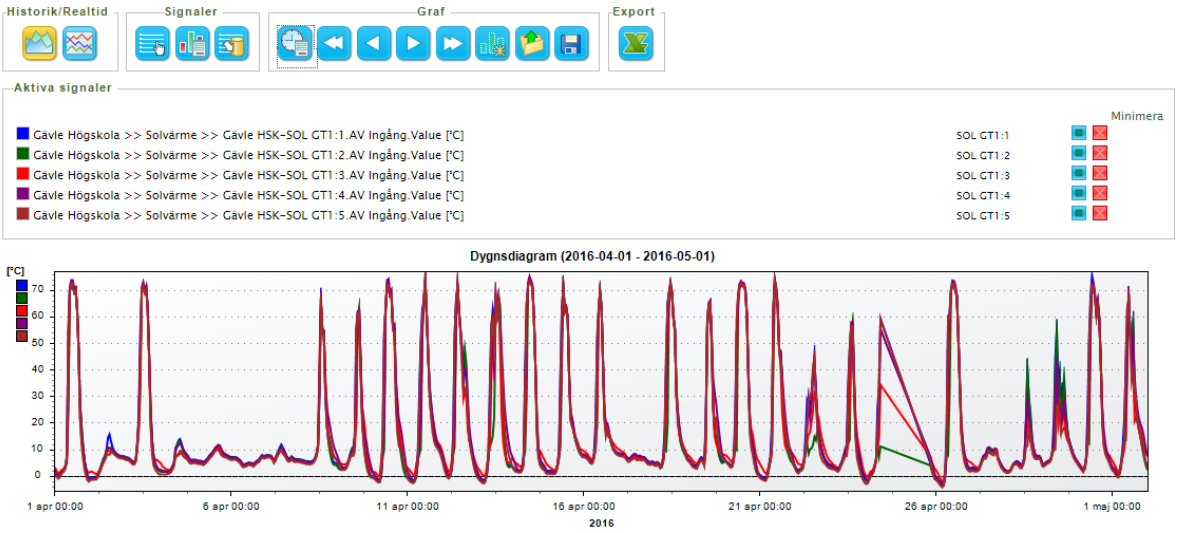

Figure 5.5. Example of diagram of chosen data

For getting the power output of the thermal system, the following equation has been used:

$$Q = \rho * \dot{V} * C_p * \Delta T \qquad \text{(eq. 6)}$$

Once knowing the parameters of the fluid, the only needed data for getting the thermal power output are the flow and the temperatures of the liquid entering and exiting the heat exchanger. For getting this data the sensors used are VP2-FM (1), VP2-GT2 (2) and VP2-GT3 (3), marked in green in Figure 5.6. It has to be noted that the flow meter is accumulative, so it can be known by variation of volume when the valve is open and the pump is working.

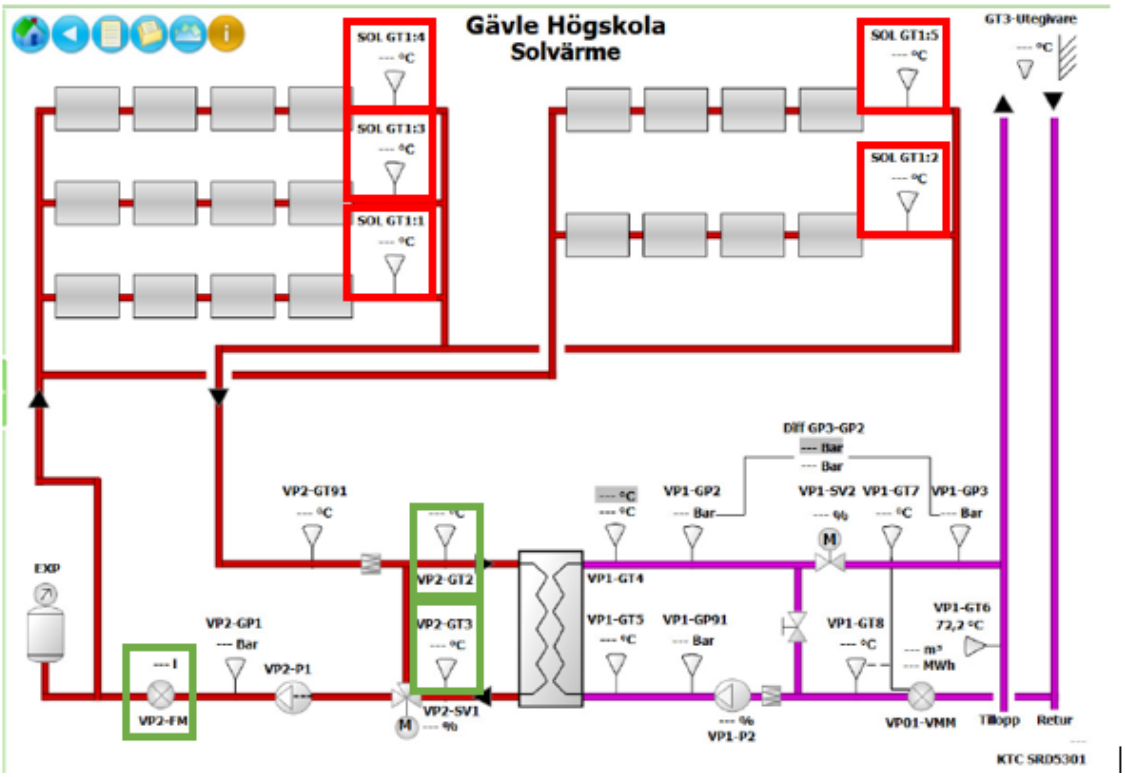

Figure 5.6. Thermal installation with the sensors

The data from the 5 sensors that are next to the collectors (marked in red in Figure 5.6) has been taken. With this data, it is possible to compare the temperature at which the fluid comes out of the collectors. These 5 flows come together afterwards, before entering the heat exchanger. Calculating the mean value of these 5 temperatures, and comparing this temperature with the one from the sensor VP2-GT2, the heat losses through the pipes are calculated with the equation (eq. 6).

5.2.2. Tigo

The electrical data of the system can be obtained from the webpage Tigo [46]. The webpage shows the energy produced in a period of time, which can be hourly values, daily values, monthly values and yearly values. An example of a monthly output is displayed in Figure 5.7.

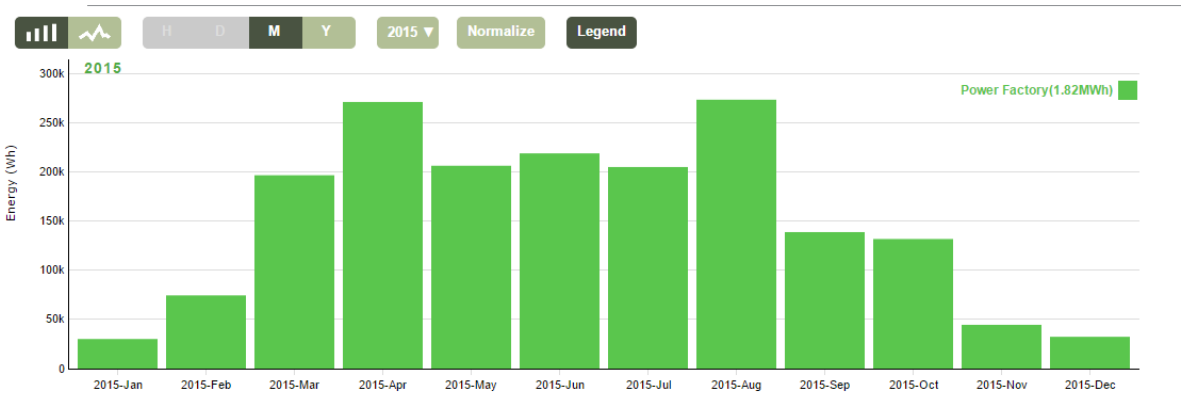

Figure 5.7. Example of monthly energy output in Tigo

The data has been taken manually as there was no option by downloading it into an excel file without a premium subscription. So by pointing each column, the value of the energy in that period of time is shown.

The webpage also shows the instant power provided by the installation in a certain time of the day as it is shown in Figure 5.8.

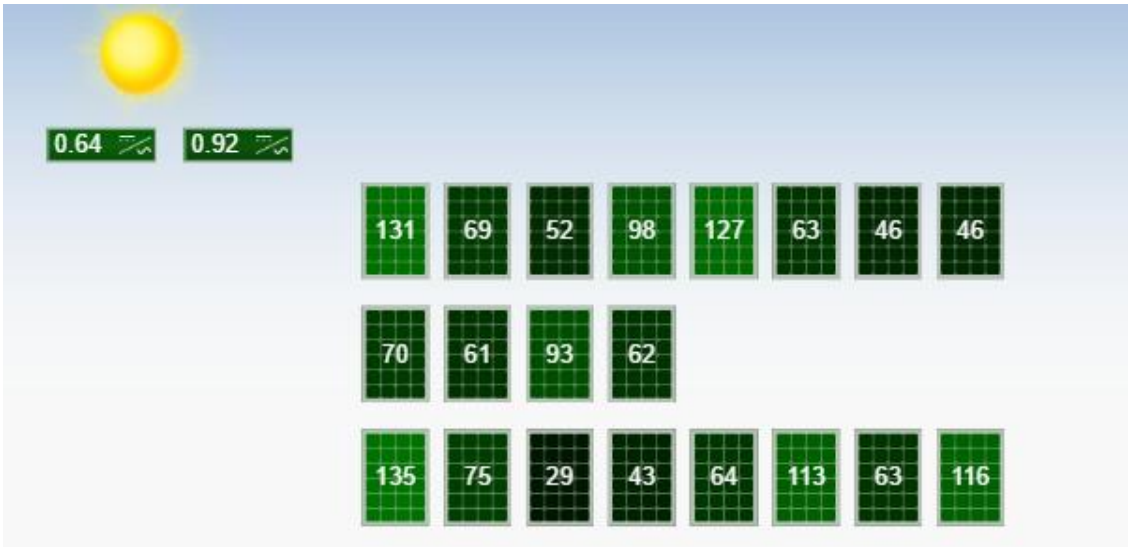

Figure 5.8. Power output of the different solar collectors at a certain time

5.2.3. Data Logger

Another way of getting the electrical data is using the data logger installed in the system. This data is provided by Elisabet Linden from the Hus 45 of HiG. There are three provided electrical data files, on for daily data, one for every 10 minutes, and another one for every minute. For simplicity and clearer understanding of the results, the daily data has been used. The interest in using the 10 minutes data or 1 minute data is to know when the collectors start producing electricity during the day at different seasons. But there is excessive information to process and not many conclusions would be achieved from its analysis.

5.2.4. Simulation

The simulation has been made using the Solarus standard simulation tool CEPT V1.4.2 which uses a 10 year average local climate data from Meteonorm. This simulation can differ from the actual performance based on the current weather. By using the local weather data for 2015 and 2016 and actual system temperatures, an actual expected performance can be determined. This last data has been taken from the website Shiny Weather Data [47].

5.3. Market review and competitor analysis

Although there are a lot of areas to be investigated and compared, the performed research is focused on the competitor's products. Obviously, there are a lot of companies providing PV panels or/and Thermal collectors, but there are fewer corporations offering both systems in the same collector as Solarus does.

The research is mostly dedicated to European companies and key characteristics are examined and analysed. In order to cover all the aspects of the collectors, the investigation is done in four main topics: price, size, PV part and thermal part. Each topic is briefly explained below.

- **Price:** surely one of the most important parameters to be competitive in the market. It takes into account production costs (raw material and labor costs) while transport and installation costs are excluded. But probably it is more important the price per m^2 of gross area to have a normalized parameter for comparison.
- **Size - Area:** it is based on three different areas.
    - Gross area: the total roof area of a collector.
    - Aperture area: also called "glazed area" due to it represents the total glazed area of a collector.
    - Absorber area: area occupied by the absorber in a collector.
- **PV part:** the characteristics reviewed are: type of cells, I_{sc}, I_{mp}, V_{oc}, V_{mp}, peak power, and the cells' efficiency.
- **Thermal part:** the parameters analyzed are: material of the absorber, maximum working pressure, maximum working temperature, peak power, and specific factors to characterize panel's efficiency expressed as (eq. 7) [48]:

$$\eta_{th} = \eta_0 - a_1 \cdot \frac{(T_m - T_a)}{G_T} - a_2 \cdot G_T \cdot \left(\frac{(T_m - T_a)}{G_T}\right)^2 \qquad \text{(eq. 7)}$$

It has to be stated that almost all the technical data of sizes, PV part and thermal part is found in datasheets but the price is a hidden parameter. Although there has been contact with the companies, in several cases it has not been possible to find it.

5.4. Production process guideline

First of all, once the main theoretical aspects of the collector were understood, a disassembly process and the consequent assembly procedure were performed in order to be more familiarized with the collector. As it is commonly considered, a manually hands-on process is extremely useful to understand and recognize all the parts of the collector that were studied in the theoretical background.

So, a C-PVT collector was completely disassembled piece by piece in the Solarus' workshop. After that, although it was a bit trickier, the reverse process was done, i.e. the assembly procedure. In fact, the authors took advantage of the situation and replaced one damaged gable and adjusted the shape of one reflector which was misplaced.

After this first important step, the authors went to visit another company, Absolicon Solar Collector AB, located in Härnösand together with other employees from Solarus. Absolicon also develops, manufactures and supplies solar energy systems and its designs are based on concentrating solar collectors. The purpose of the visit was to show the production process of a Solarus' prototype that was ongoing there, as well as to observe their workshop, machines and facilities.

In order to clarify the assembly process and standardize the operations that would take place during it, a guideline is made. One of the most relevant aspects is to classify all the tasks in sections where each component is attached. It has to be stated that it is an assembly process which means that each piece arrives at the company prepared and completely ready to be mounted.

So, the following list contains the steps that have been done in order to prepare the production process guideline for the actual collector:

- Identify the overall components of the collector and organize them in sections.
- Recognize all the tasks for each section/component.
- Determine the required material per section.
- Estimate the duration of each task, considering both operating and waiting times.
- Prepare explanatory images taken from SolidWorks® that represent the material and the procedures of attachment.
- Establish a timeline for the assembly process taking into account the durations of all the tasks.

The production process guideline is organized per sections. Each section has a brief description of the process and a list of the required material. After this the attachment procedure is explained with the help of images.

Chapter 6

Results

6.1. Design of the new C-PVT prototype

6.1.1. Solar cell cuts

Type 1

The first solar cell cut type is achieved by cutting the solar cell in 4 parts, cutting it in two from both directions as it can be seen in Figure 6.1. This way, as the initial solar cell has a measure of 156 mm x 156 mm, the resulted solar cell size is 78 mm x 78 mm, with two busbars per cell.

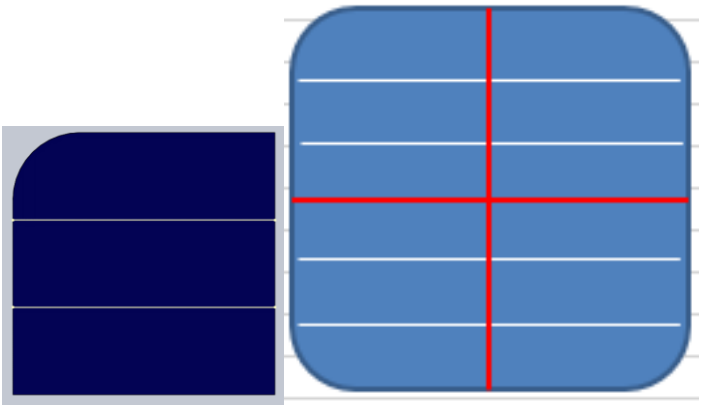

Figure 6.1. Type 1 solar cell 78 mm x 78 mm

The electrical characteristics of the type 1 cell cut are shown in Table 6.1.

Table 6.1. Electrical characteristics of type 1

Individual Type 1	
Isc	2,29 A
Imp	2,12 A
Voc	0,64 V
Vmp	0,54 V

Type 2

The second solar cell cut is obtained by cutting the solar cell in 8 parts, cutting in two pieces perpendicular to the busbars and cutting in 4 pieces parallel to the busbars as it can be seen in Figure 6.2. The size of the resulted solar cell is 78 mm x 39 mm, with only one busbar per cell.

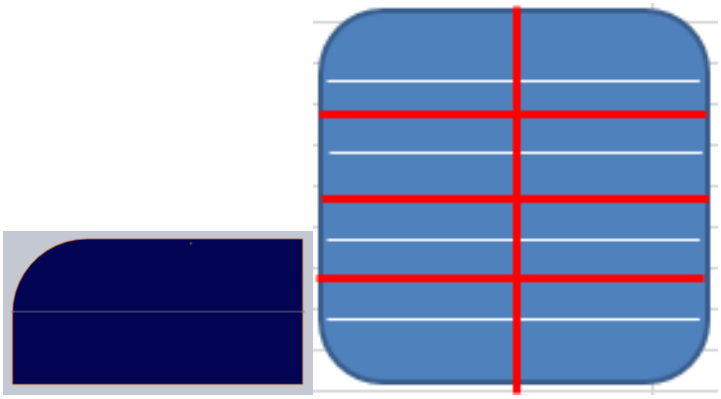

Figure 6.2. Type 2 solar cell 78 mm x 39 mm

The electrical characteristics of the type 2 cell cut are shown in Table 6.2.

Table 6.2. Electrical characteristics of type 2

Individual Type 2	
Isc	1,14 A
Imp	1,06 A
Voc	0,64 V
Vmp	0,54 V

Type 3

The last type of the solar cell cuts is made by cutting the solar cell in 4 pieces, but the cuts are made only in parallel with the busbars as seen in Figure 6.3. The size of the cell cut is then 156 mm x 39 mm with only one busbar per cell.

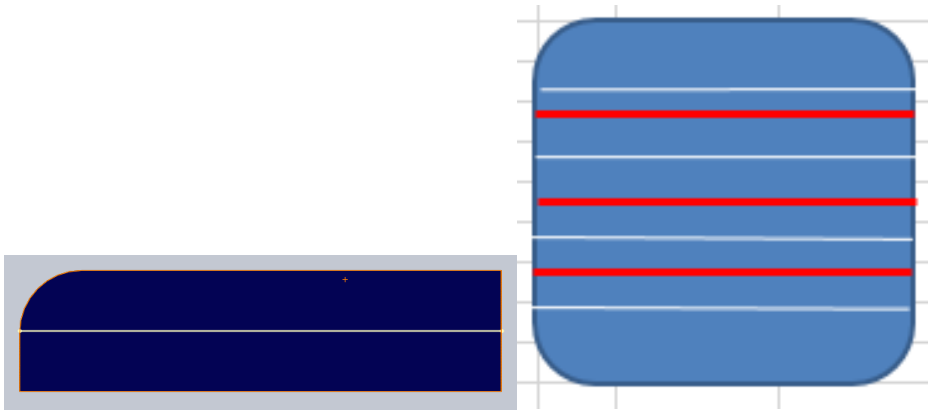

Figure 6.3. Type 3 solar cell 156 mm x 39 mm

The electrical characteristics of the type 3 cell cut are shown in Table 6.3.

Table 6.3. Electrical characteristics of type 3

Individual Type 3	
Isc	2,29 A
Imp	2,12 A
Voc	0,64 V
Vmp	0,54 V

6.1.2. Receiver

For calculating the size of the receiver, several measurements have to be taken into account: the spacing between the cells themselves; the gap between the cells and the sides; the string arrangement; the spacing between the strings; the gap between the cells and the sides. In the longitudinal direction, a similar length of the receiver is desired comparing with the actual one, so the cells arrangement is going to be conditioned partially by the length.

The distance left between the cells is 1,5 mm and the distance between the cells and the sides is 4 mm, as seen in Figure 6.4.

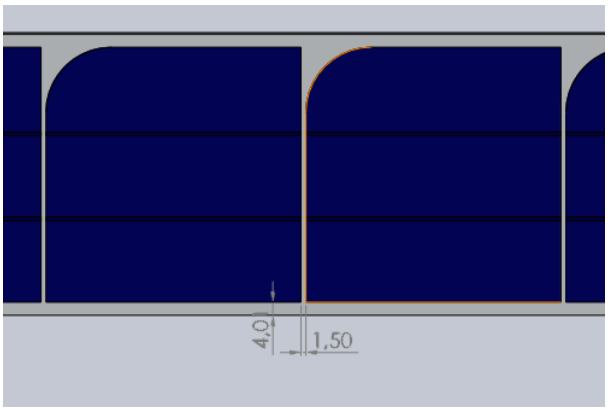

Figure 6.4. Distance between the cells and in the sides, example type 1

The distance between the strings is 16 mm and the distance in the edges is 20 mm for type 1 and 2 and 30 mm for type 3, as seen in Figure 6.5.

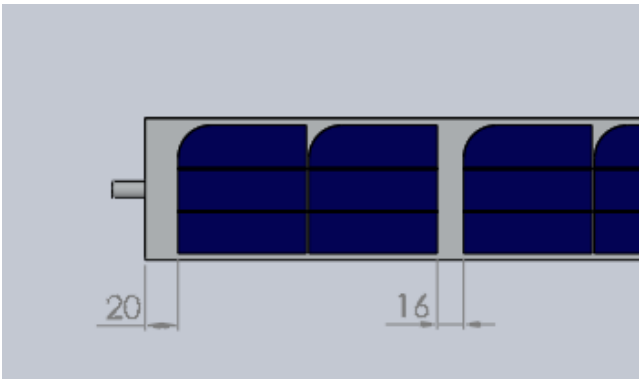

Figure 6.5. Distance between the strings and in the edges, example type 1

The string arrangement is going to be different with the different used cell cuts. All of the 3 type of receivers will consist of 5 strings of cell, being the string from the middle the one that contains most of the cells and the ones on the borders the ones with the fewest cells. The receiver then is symmetric from the centre, containing the string number 1 and 5 the same amount of cells, as it happens with string number 2 and 4. This is easier to see in the following images.

Type 1 receiver sheet

In the case of type 1 cell, the strings 1 and 5 contain two cells, the string 2 and 4 have five cells, while the string number 3 has fourteen cells as it can be seen in Figure 6.6. Summing up all this, the total amount of cells in a receiver sheet is 28. In the company's inventory, there are 800 type 1 cells so this means that 28 receiver's sheets of type 1 can be made.

Figure 6.6. Type 1 cell arrangement

Type 2 receiver sheet

In the case of type 2 cells, the width of the cells is smaller, being the width of the receiver smaller than the one of the type 1. But the length of the cells is the same so the string arrangement is the same as for the type one as seen in Figure 6.7.

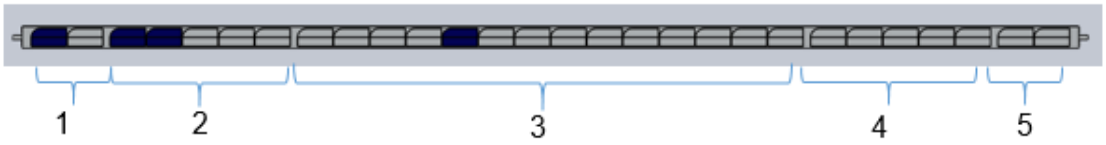

Figure 6.7. Type 2 cell arrangement

Type 3 receiver sheet

In the case of type 3, the width of the cells is the same as type 2, but the length varies. In consequence, the width of the receiver is also the same as in type 2. However, the string arrangement is different from the two previous ones because of the cell length. It is preferable to have all three receivers with the same the length, so the box which will contain them can be easily built. Moreover, in this way it is possible to take advantage of the existing and excess top glasses from other Solarus collectors. In this way, the box will be more compact, needing less material and being more manoeuvrable. So, in order to fit the length of the other receivers, fewer cells are used in one receiver. Being the length of the cells the double of the other types, half of the cells are used to build the receiver sheet. But because of the existence of less cells, there are less quantity of spaces between the cells, so this extra gap has to be added to the edges. This is the reason that the receiver from type 3 have a spacing of 30 mm instead of 20 mm as in the other types, Figure 6.8.

Figure 6.8. Type 3 cell arrangement

The size of the receivers is achieved by taking into account all the spacing and the arrangement. As said before, the length of all of them is the same, being it 2323 mm. The width of the receiver varies, being 86 mm for the type 1 and 47 mm for the types 2 and 3. The thickness in all the receiver sheets is 2 mm.

Cooling system

As the collectors are concentrator ones, the solar cells are going to be on both sides of the receiver. But a cooling system is included in the receiver also, so the whole receiver will consist of two reflector sheets (flat aluminum sheets) with the solar cells and a pipe for the thermal fluid between the sheets, having the receiver a triangular shape. The diameter of the pipe is 6 mm and 10 mm and will go through the whole length of the receiver Figure 6.9.

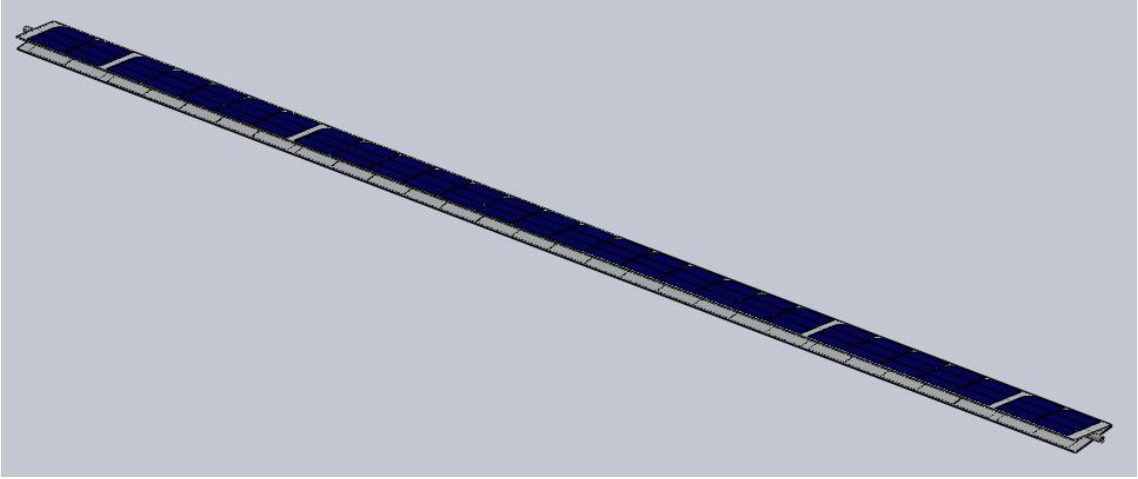

Figure 6.9. Type 1 receiver design with cooling and sheets in triangular shape

6.1.3. Collector box

Rib

Once the receiver is designed and all the measurements defined, the shape of the rib is designed so that the reflector can work properly. It consists, as stated before in 5.1.2, of a quarter of a circle and a parabola. The radius of the circle is 86 mm for type 1 and 47 mm for type 2 and 3. The equation has been given in (eq. 5) and Figure 6.10 and Figure 6.11 show the design of the rib.

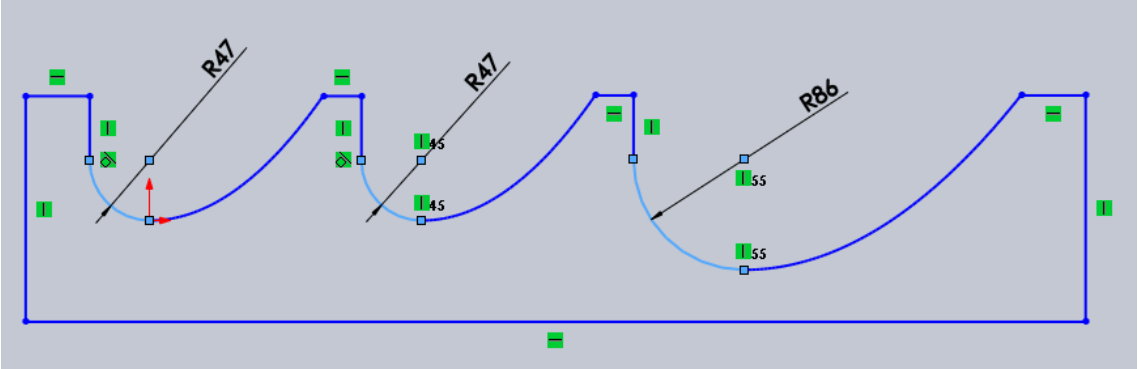

Figure 6.10. Sketch of the rib design with measurements

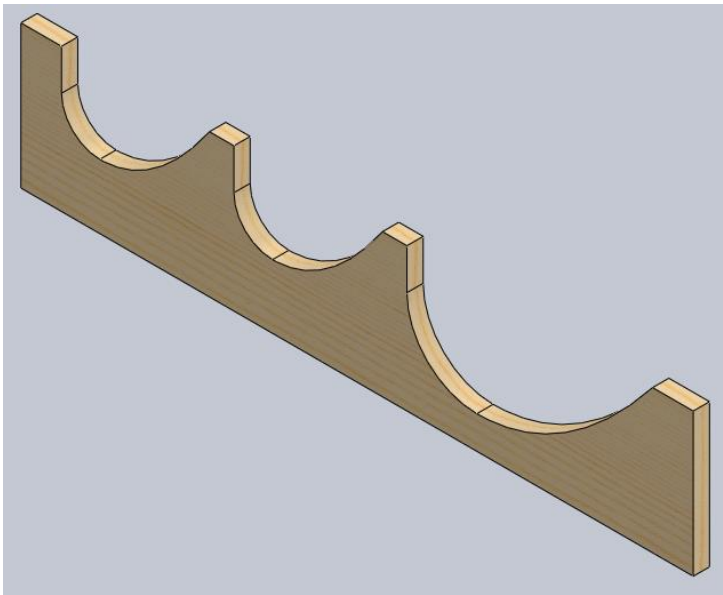

Figure 6.11. Design of the rib

The thickness of the rib is 18 mm to give the structure rigidity as it is made of wood, and it is important also that it has to be possible to drill the receiver holders to it.

Reflector

The shape of the parabola is the same as the rib Figure 6.12 and Figure 6.13, although in reality it consists of a flat sheet and the shape will be given by glue and pressure. The thickness of the reflector sheet is 0,5 mm.

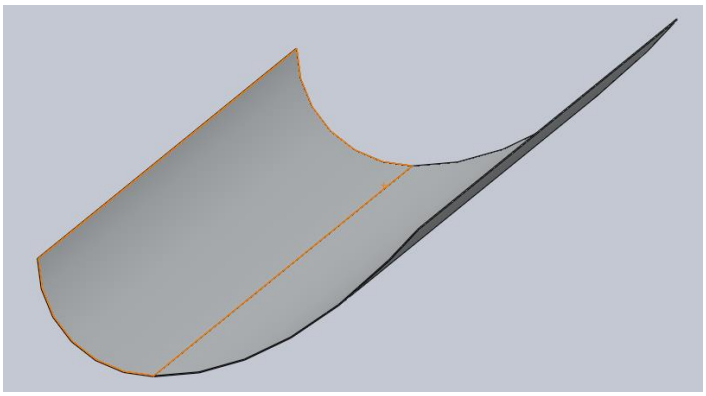

Figure 6.12. Shape of the reflector

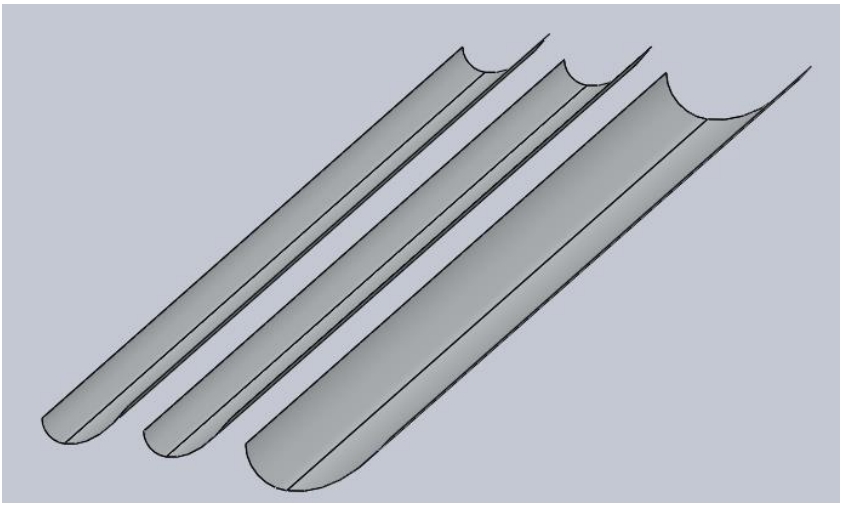

Figure 6.13. Reflectors for the three types

Receiver holders

The receiver holders will consist of metallic “L”-shaped sheets, they will look like in Figure 6.14.

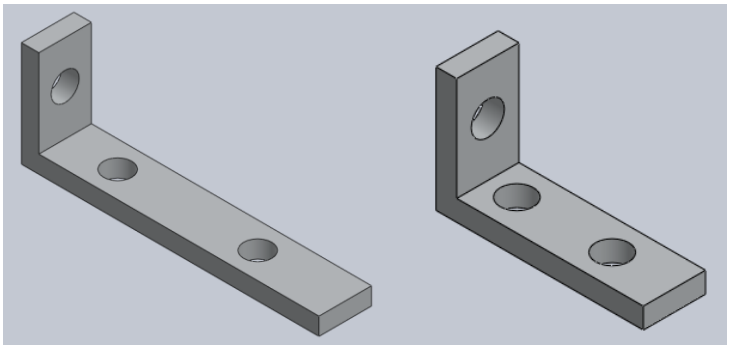

Figure 6.14. Receiver holders for type 1 (left) and for types 2 and 3 (right)

Building the collector

The whole solar collector is built using five ribs, and using two wooden sticks on each side to attach the ribs together, as it can be seen in Figure 6.15 and Figure 6.16.

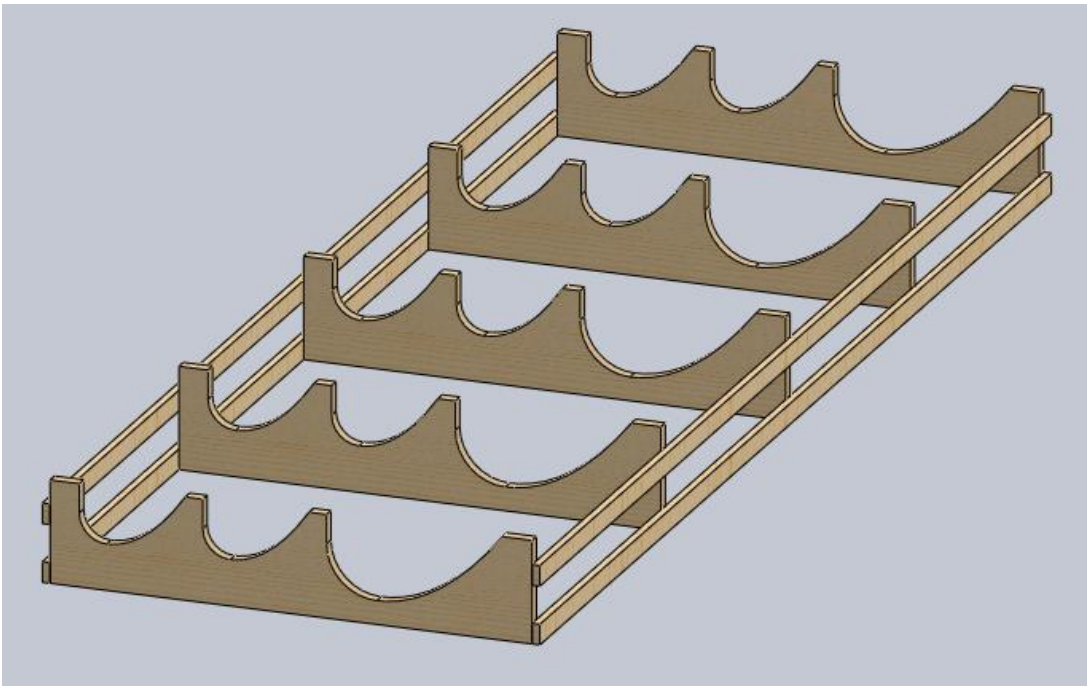

Figure 6.15. Asymmetric MaReCo wooden box

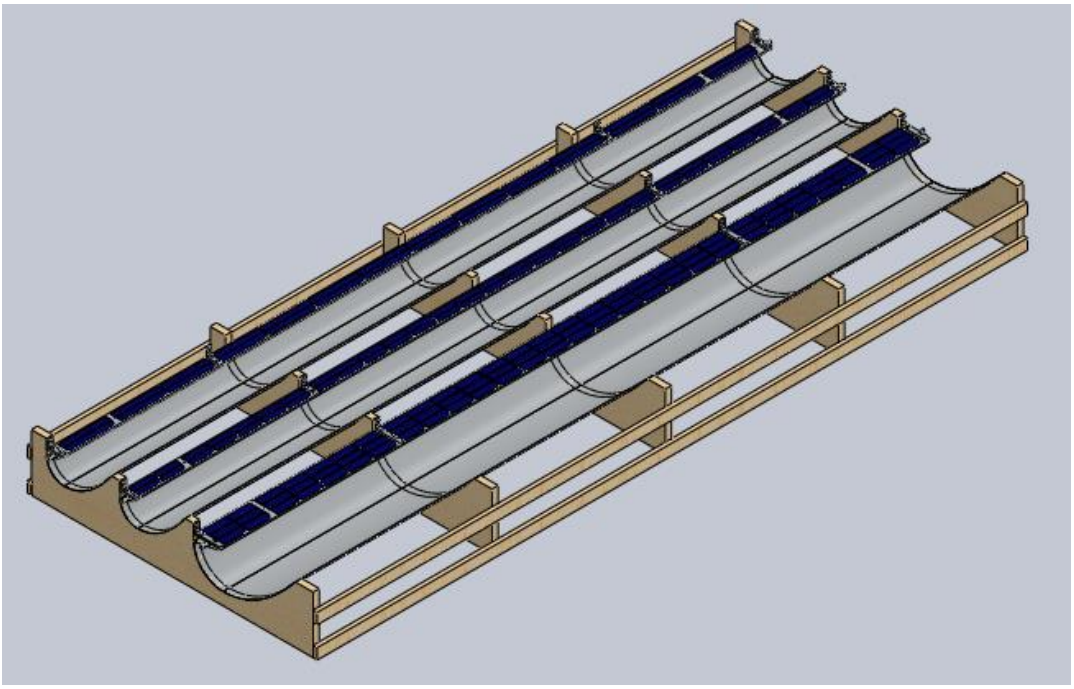

Figure 6.16. Solarus solar collector new design

6.1.4. Symmetric design

Rib

For the design of the rib, all the different reflector shapes have been designed in the same rib, for the same reason as it has been used in the MaReCo asymmetric design. In Figure 6.17, it can be easily differentiated which of the designs are symmetric MaReCo and which ones are pure parabola. The MaReCo designs (numerated as 1, 3 and 4) have a small arc on the bottom of the reflector, whereas the pure parabolas (numbers 2 and 5) do not have it.

The thickness of the rib is 18 mm also as in the other collector design Figure 6.18.

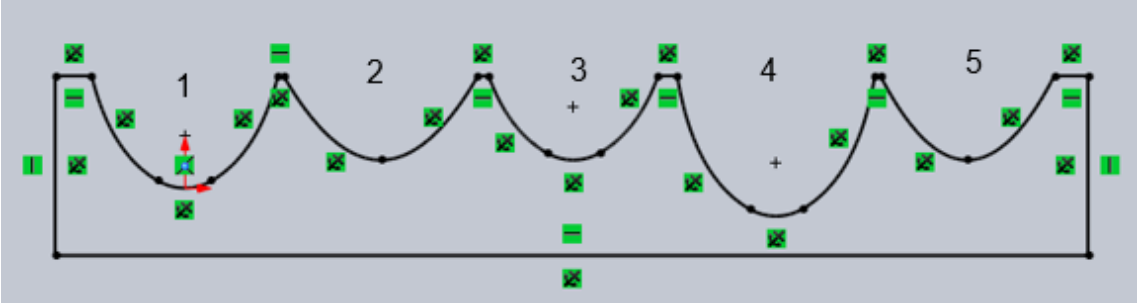

Figure 6.17. Sketch of the symmetric MaReCo-Pure parabola design

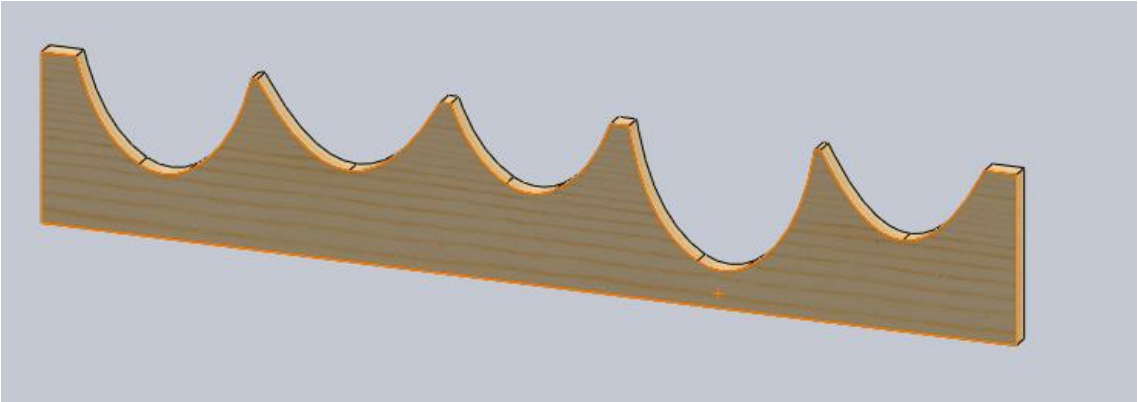

Figure 6.18. Symmetric MaReCo-Pure parabola rib design

Reflector

The shape of reflectors Figure 6.19 is determined by the shape of the rib as in the other design.

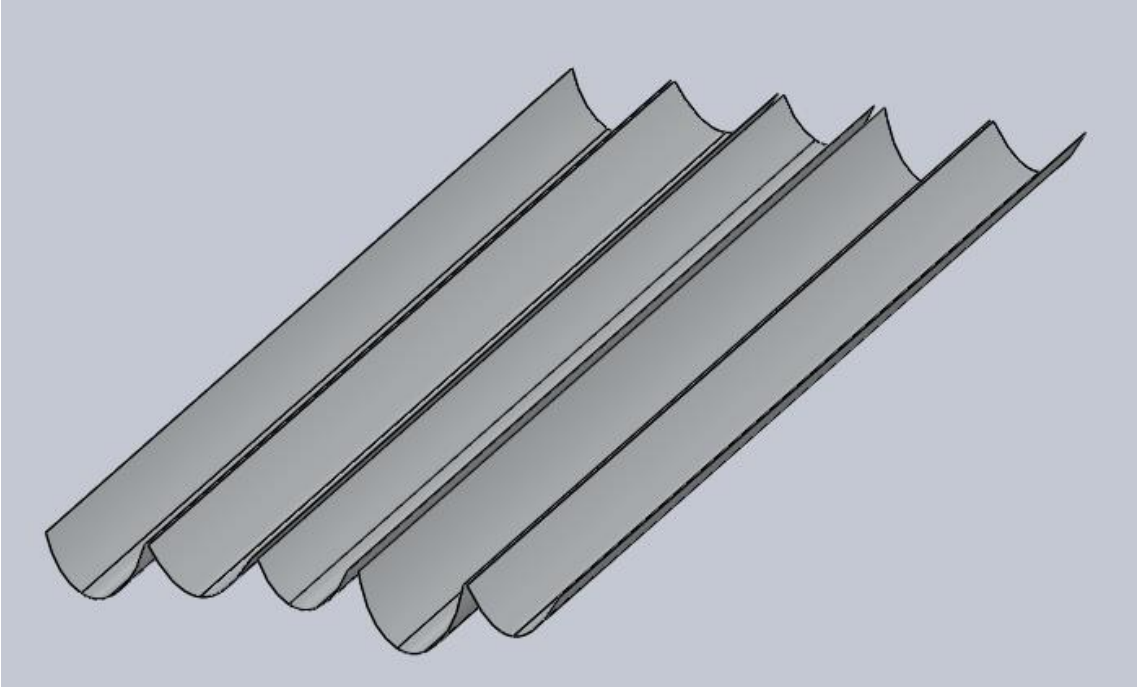

Figure 6.19. Shape of the reflectors in the symmetric MaReCo-Pure parabola design

Building the collector

The whole solar collector is also built with five ribs and four rib-attachments made of wood and it is presented in Figure 6.20 and Figure 6.21.

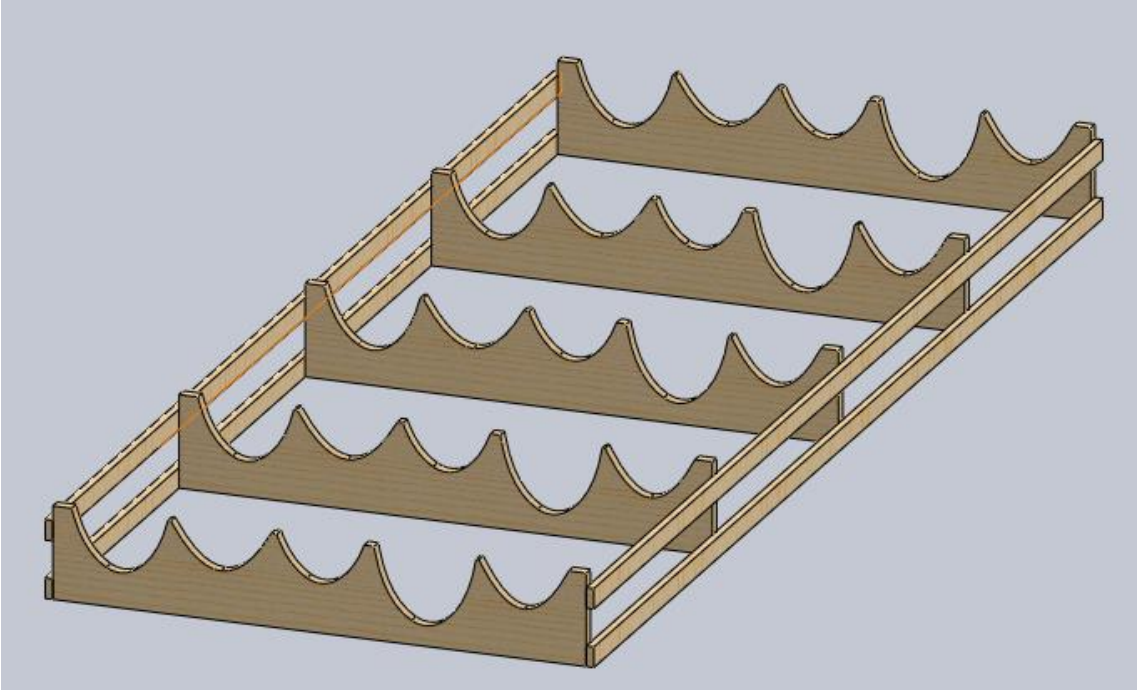

Figure 6.20. Collector wooden structure

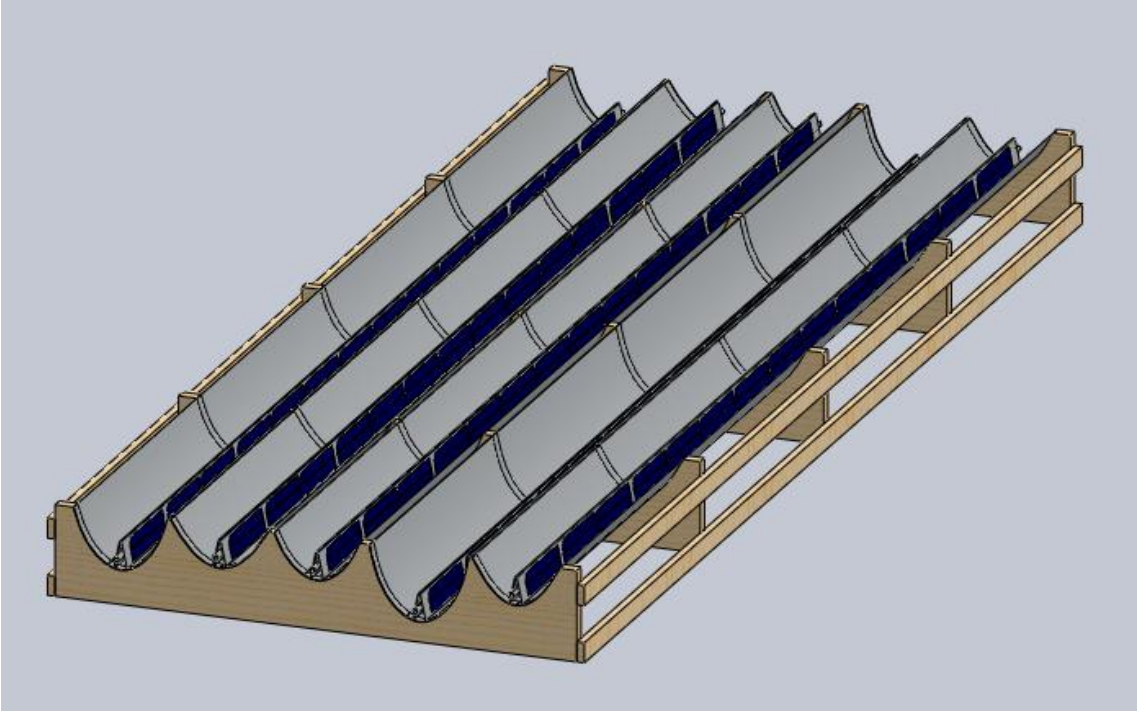

Figure 6.21. Complete symmetric MaReCo-Pure parabola collector

6.2. Analysis and evaluation of the HiG installation

6.2.1. Collectors thermal performance

The energy output of the collectors has been achieved by introducing the needed data in (eq. 6). The energy output has been divided for every month, to have a better insight of how the time of the year affects to the energy production. Results are shown in Table 6.4.

Table 6.4. Monthly thermal energy output and losses of the installation

	2015			2016		
Month	**Energy Output [kWh]**	**Energy per Gross Area [kWh/m2]**	**Losses [kWh]**	**Energy Output [kWh]**	**Energy per Gross Area [kWh/m2]**	**Losses [kWh]**
January	0,10	0,01	0,00	0,01	0,00	0,01
February	0,52	0,01	0,00	3,74	0,08	20,8
March	24,7	0,52	181	166	3,45	89,1
April	335	6,98	215	382	7,95	159
May	243	5,07	194			
June	425	8,85	236			
July	533	11,1	252			
August	1142	23,8	393			
September	273	5,69	182			
October	136	2,84	175			
November	3,06	0,06	13			
December	0,00	0,00	0,16			
Total	**3116**	**64,9**	**1840**			

These results can be better observed by drawing a diagram Figure 6.22.

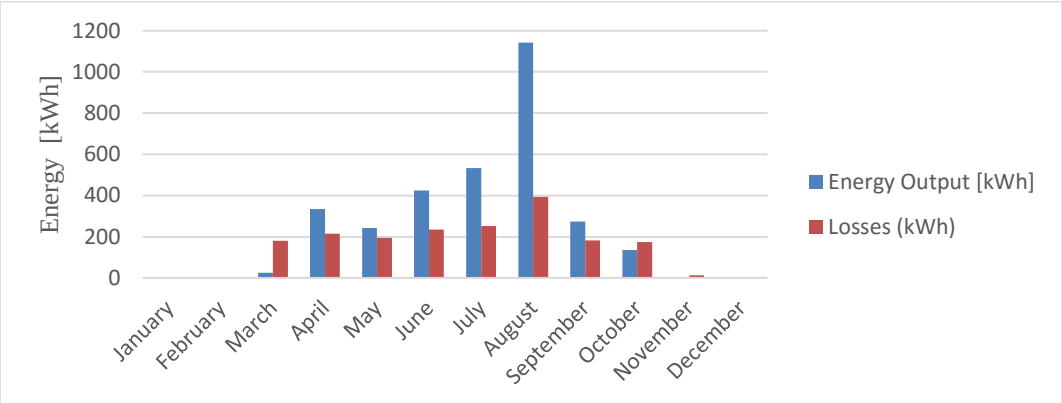

Figure 6.22. Monthly thermal energy output and losses of the installation in 2015

If the total production of the whole system is divided by the quantity of solar collectors (20 in this case), the power output per collector per year is obtained, which is 156 kWh/year*collector.

6.2.2. Collectors electrical performance in Tigo

The monthly electrical energy output was obtained directly from Tigo Table 6.5 and Figure 6.23.

Table 6.5. Monthly electrical energy output of the installation

Collectors electrical performance in kWh				
	2015		2016	
Month	Total production (kWh)	Production per gross area (kWh/m^2)	Total production (kWh)	Production per gross area (kWh/m^2)
January	30,1	0,63	8,41	0,18
February	74,5	1,55	70,5	1,47
March	197	4,10	109	2,26
April	271	5,65	154	3,21
May	206	4,30		
June	219	4,56		
July	205	4,27		
August	273	5,70		
September	139	2,89		
October	132	2,75		
November	44,5	0,93		
December	32,4	0,67		
Total	**1824**	**38**		

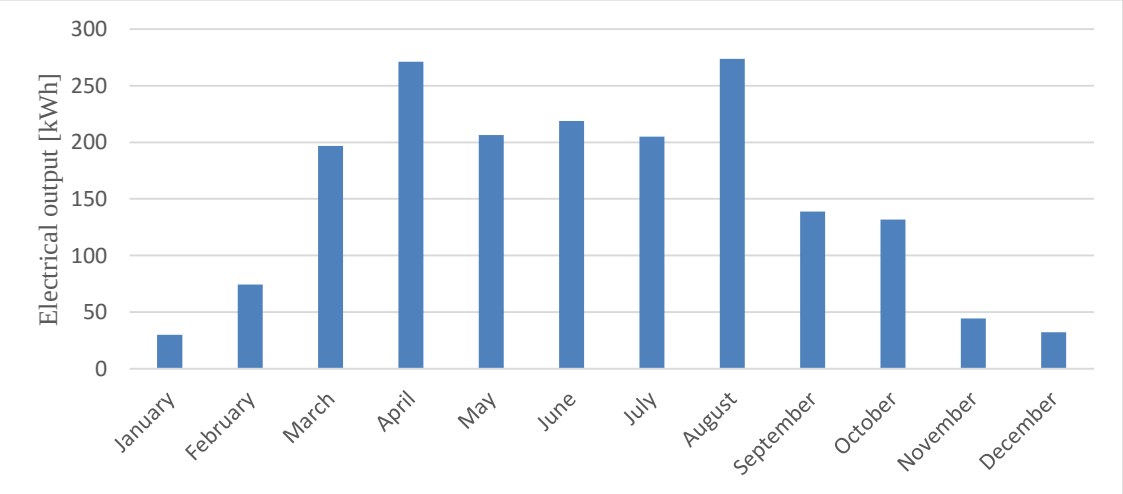

Figure 6.23. Monthly electric energy output of the installation in 2015

Dividing the yearly electrical production of all the collectors with the amount of them, the total annual electrical output of every collector can be obtained, which is 91,2 kWh/collector*year. But it has been seen in Figure 5.8, that the instant power of the different collectors is different with the same solar radiation. The annual energy production of every collector can be seen in Table 6.6.

Table 6.6. Electric energy output of each collector in the year 2015

	E1	E2	F1	F2	G1	G2	H1	H2	I1	I2	J1	J2
Energy (kWh)	113	70,4	99,1	70	106	62,5	99,3	86,5	118	124	86,3	81,8
	A1	**A2**	**B1**	**B2**	**C1**	**C2**	**D1**	**D2**				
Energy (kWh)	116	58,4	76,9	64,6	69,1	115	89,3	98,1				

It can be seen in Figure 6.24 which of the collector have the higher electrical production and which ones have the lowest ones, this way, it can be identified easily which ones are not working properly.

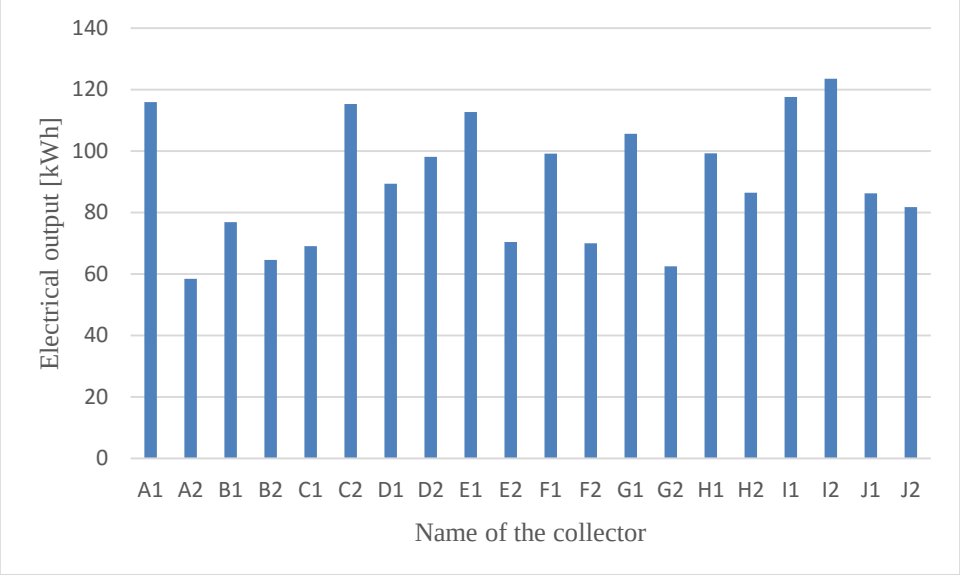

Figure 6.24. Electrical energy output from Tigo per each collector in 2015

6.2.3. Collectors electrical performance in data logger

The results obtained from the data logger are presented in the Table 6.7.

Table 6.7. Collectors electrical energy output from data logger

Collectors electrical performance in kWh						
	2014		2015		2016	
Month	Total production (kWh)	Production per gross area (kWh/m^2)	Total production (kWh)	Production per gross area (kWh/m^2)	Total production (kWh)	Production per gross area (kWh/m^2)
January	-	-	27,6	0,57	5,01	0,10
February	-	-	62,5	1,30	57,7	1,20
March	-	-	180	3,75	95,6	1,99
April	-	-	258	5,37	136	2,84
May	-	-	187	3,90	-	-
June	-	-	169	3,53	-	-
July	-	-	186	3,87	-	-
August	283	5,89	251	5,23	-	-
September	265	5,52	128	2,67	-	-
October	70,6	1,47	125	2,60	-	-
November	23	0,48	38,6	0,80	-	-
December	21,3	0,44	29,2	0,61	-	-
Total			**1642**	**34,2**		

6.2.4. Simulated and expected performance

The electrical and thermal output with the 10 year average local climate data from Meteonorm is shown in Table 6.8.

Table 6.8. Simulated electrical and thermal energy output for 2015

Month	$E_{electric}$ (kWh/m^2)	$E_{thermal}$ (kWh/m^2)
Jan 15	0,9	0,0
Feb 15	2,1	0,3
Mar 15	4,9	4,9
Apr 15	7,5	17,4
May 15	10,3	30,9
June 15	10,3	30,9
July 15	9,9	32,2
Aug 15	8,4	26,9
Sept 15	5,7	11,6
Oct 15	2,8	3,7
Nov 15	1,0	0,0
Dec 15	0,6	0,0
Total 2015	**64,4**	**159**

As expected, these results vary because the local climate has been determined by patterns. Taking real climate data from Shiny Weather Data [47], the expected energy output can be determined with the simulation, as seen in Table 6.9.

Table 6.9. Estimated electrical and thermal energy output

Month	$E_{electric}$ (kWh/m^2)	$E_{thermal}$ (kWh/m^2)
Jan 15	0,7	0,0
Feb 15	1,6	0,1
Mar 15	4,9	9,2
Apr 15	7,9	13,7
May 15	7,4	6,7
June 15	8,7	13,5
July 15	8,4	17,1
Aug 15	10,3	39,7
Sept 15	4,8	7,8
Oct 15	3,8	3,7
Nov 15	1,2	0,0
Dec 15	0,9	0,0
Total 2015	**60,6**	**112**
Jan 16	0,8	0,0
Feb 16	1,6	0,0

The local weather data of 2016 could be taken only for January and February and the data of March and April was missing. In spite of this fact, the data of 2015 should be enough to have an overall impression of the system's performance.

6.2.5. Comparison of the results

In this section, a summary of the results presented before is given. In this way, it is easier to compare all the results obtained from different software and simulations. The results are shown in Table 6.10 and Figure 6.25 for the thermal part, and in Table 6.11 and Figure 6.25 for the electrical performance. It has to be mention, that both are presented in energy per square meter during 2015 as it is the completed year.

Table 6.10. Simulated, estimated and real thermal data in kWh/m^2

Month	Simulated	Estimated	Styr och staller
Jan 15	0,0	0,0	0,01
Feb 15	0,3	0,1	0,01
Mar 15	4,9	9,2	0,52
Apr 15	17,4	13,7	6,98
May 15	30,9	6,7	5,07
June 15	30,9	13,5	8,85
July 15	32,2	17,1	11,1
Aug 15	26,9	39,7	23,8
Sept 15	11,6	7,8	5,69
Oct 15	3,7	3,7	2,84
Nov 15	0,0	0,0	0,06
Dec 15	0,0	0,0	0,00
Total 2015	**159**	**112**	**64,9**

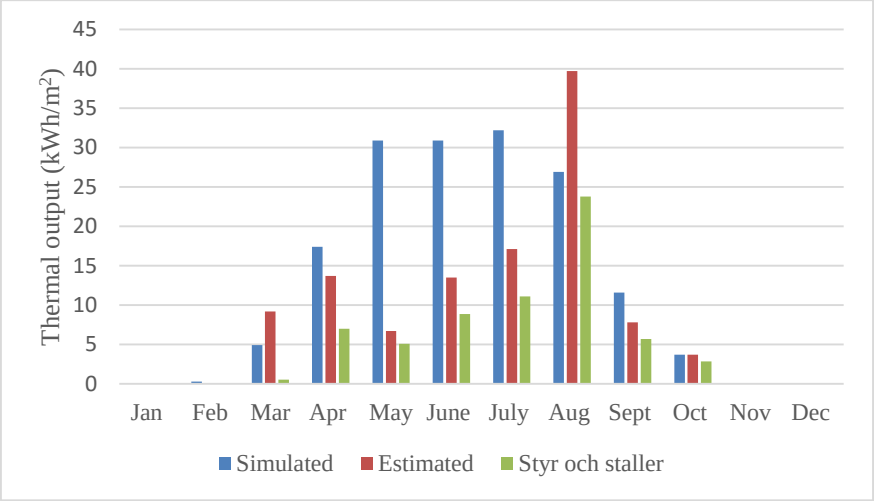

Figure 6.25. Simulated, estimated and real thermal data

Table 6.11. Simulated, estimated and real electrical data in kWh/m^2

Month	Simulated	Estimated	Tigo	Data Logger
Jan 15	0,9	0,7	0,63	0,57
Feb 15	2,1	1,6	1,55	1,30
Mar 15	4,9	4,9	4,10	3,75
Apr 15	7,5	7,9	5,65	5,37
May 15	10,3	7,4	4,30	3,90
June 15	10,3	8,7	4,56	3,53
July 15	9,9	8,4	4,27	3,87
Aug 15	8,4	10,3	5,70	5,23
Sept 15	5,7	4,8	2,89	2,67
Oct 15	2,8	3,8	2,75	2,60
Nov 15	1,0	1,2	0,93	0,80
Dec 15	0,6	0,9	0,67	0,61
Total 2015	**64,4**	**60,6**	**38**	**34,2**

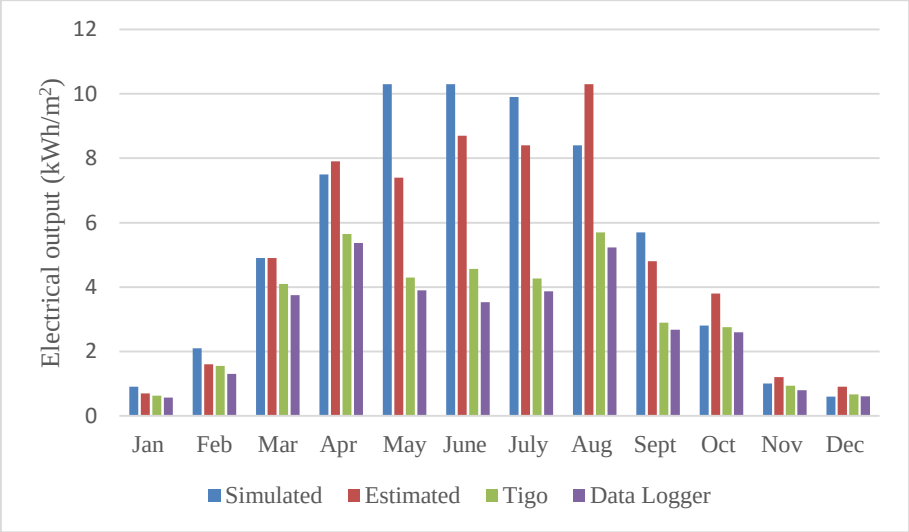

Figure 6.26. Simulated, estimated and real electrical data

6.3. Market review and competitor analysis

The following tables, Table 6.12 and Table 6.13, summarize the market review and competitors analysis of PVT collectors that has been done.

Table 6.12. Characteristics of competitor's products price, size and electrical data

Technology	COMPANY & PANEL MODEL	COUNTRY	PRICE [€]	PRICE [€/m²]	Size ([m²])			PHOTOVOLTAIC PART						
					Gross	Aperture	Absorber	Cell type	Current (A)		Voltage (V)		Power peak (W)	Efficiency (%)
									Isc	Imp	Voc	Vmp		
C-PVT	SOLARUS - Power Collector *	Sweden	550	229	2,40	2,17	0,65	Mono	4,1	3,7	51,0	40,0	250	19,2
PVT	Fototherm - Module FT275AL	Italy	850	518	1,64	1,58		Mono	9,62	8,83	39,10	31,10	275	16,70
PVT	Fototherm - Module FT250Cs	Italy	680	422	1,61	1,59	1,59	Poly	8,9	8,3	37,2	30,1	250	15,5
PVT	Dualsun Wave	France			1,66	1,58		Mono	8,6	8,2	38,5	30,7	250	15,4
PVT	Solimpeks - Volther powervolt	Turkey	360	263	1,37	1,36	1,30	Mono	5,7	5,4	46,4	36,8	200	17,8
PVT	Solimpeks - Volter powertherm	Turkey	390	273	1,43	1,42	1,40	Mono	5,4	5,0	44,6	36,2	180	16,0
PVT	TESGroup -TESZeus - 250 Mono	China			1,69	1,60	1,57	Mono	5,26	4,92	59,9	50,8	250	17,66
PVT	Meyer Burger- Hybrid 285-290	Switzerland			1,650			Mono	9,70	9,10	39,80	31,40	285	17,40
PVT	Sun System - PVT 240	Bulgaria	246	151	1,63	1,62		Poly	8,52	7,84	37,20	30,60	240	16,40
PVT	Minimise Generation Power Hybrid 240	UK			1,29	1,2656	1,26	Mono	5,85	5,51	52,40	43,70	240	21,60
PVT	BrandoniSolare - Hybrid SBP-250	Italy			1,66		1,44	Poly	8,57	8,09	38,58	30,09	250	
PVT	Smart clima - Solar PVT	China			1,63			Poly	8,96	8,14	37,40	30,70	250	16
PVT	Ensol - E-PVT2,0	Poland	400	198	2,02	1,86		Poly	8,78	8,15	45,31	36,82	300	
PVT	Pegoraro Energia - PVT H-NRG 250	Italy	350	211	1,66	1,52	1,46	Poly	8,9	8,67	37,79	29,27	250	15,06
PVT	Systovi - R-Volt	France			1,515		1,314	Mono	8,811	8,502	34,4	28,84	250	16,5
PVT	Nelskamp - HM 260 Mono Black	Germany			1,63	1,55		Mono		8,41		30,9	260	

Table 6.13. Characteristics of competitor's products weight and thermal data

Technology	COMPANY & PANEL MODEL	THERMAL PART							Weight (kg)
		ABSORBER							
		Material	Zero loss Efficiency (η0)	First order Coefficient (a1) (W/m2.K)	Second Order Coefficient (a2) (W/m2.K2)	Pressure (bar)	Max Temp (ºC)	Peak power (W)	
C-PVT	SOLARUS - Power Collector *	Aluminium	0,447	4,48	0,0034	10,00	180	1250	55
PVT	Fototherm - Module FT275AL	Copper	0,583	6,08	0,00		85,00	921,00	32,00
PVT	Fototherm - Module FT250Cs	Copper	0,560	9,12	0,00		85,00	888	27
PVT	Dualsun Wave	Copper	0,578	12,08	0,00	12	75	912	30
PVT	Solimpeks - Volther powervolt	Copper				10	101	460	24
PVT	Solimpeks - Volter powertherm	Copper				10	134	680	34
PVT	TESGroup -TESZeus - 250 Mono	Copper/ Aluminium	0,520				85,00		27,5
PVT	Meyer Burger- Hybrid 285-290		0,600			6	80	900	29
PVT	Sun System - PVT 240	Copper/Aluminium		9,12	0,00		85	900	28
PVT	Minimise Generation Power Hybrid 240	Copper/Aluminium	0,534	8,37	0,586	10	93	675	26
PVT	BrandoniSolare - Hybrid SBP-250	Aluminum	0,538	15,529	0,010	3	85	849	32,8
PVT	Smart clima - Solar PVT	Aluminium					85	550	30
PVT	Ensol - E-PVT2,0	Aluminium	0,555			6		1037	
PVT	Pegoraro Energia - PVT H-NRG 250	Aluminium	0,650	14,405	0,00	3	80	831	29
PVT	Systovi - R-Volt	Aluminium	0,500				85	450	20,7
PVT	Nelskamp - HM 260 Mono Black					6	85	719	25

6.4. Production process guideline

The complete guideline of the assembly process can be found in Appendix. Table 6.14 summarizes the tasks in each section with their corresponding workers, working time per task and the total time per station.

Table 6.14. Production process stations with their tasks, workers and times

Station	Step		Workers	Working time [s]	Total time per station [s]
1.Ribs	1.1	Put the ribs in their location and attach with clamps	2	60	60
2.Profiles	2.1	Put glue where the "n" profile goes	2	30	
	2.2	Attach the "n" profile	2	15	
	2.3	Put glue where the "A" profile of the border goes	2	30	
	2.4	Attach the "A" profile of the border	2	15	
	2.5	Put glue where the "A" profile of the middle goes	2	30	
	2.6	Attach the "A" profile of the middle	2	15	135
	2.7	Waiting time for the glue to get dry		1800	1935
3.Reflector	3.1	Put glue on the surfaces for one reflector	2	60	
	3.2	Attach a reflector plate	2	30	
	3.3	Put glue on the surfaces for the other reflector	2	60	
	3.4	Attach the other reflector plate	2	30	
	3.5	Put the press	2	60	240
	3.6	Waiting time for the glue to get dry		1800	2040
4.Receiver	4.1	Assemble 6 Receiver holders	2	90	
	4.2	Attach the two receivers	2	60	
	4.3	Connect the receivers each other	2	30	180
5.Gable	5.1	Put glue in the reflector and the ribs where one gable goes	2	30	
	5.2	Attach one gable	2	15	
	5.3	Repeat the same process for the other gables	2	135	180
	5.4	Waiting time for the glue to get dry		1800	1980
6.Top glass	6.1	Clean the box inside (last opportunity)	2	30	
	6.2	Glue the surface of the profiles and the gables	2	120	
	6.3	Put the glass on the top	2	30	180
	6.4	Waiting time for the glue to get dry		1800	1980
7.Side covers	7.1	Lift the module up from the wagon	2	15	
	7.2	Attach the side covers with clinching	2	60	75
8.Bottom plate	8.1	Lift the module up higher	2	15	
	8.2	Attach the bottom plate	3	60	75

It is also possible to present the timeline of the assembly process in which can be analyzed how the stations are planned and what improvements could be functional in order to decrease the total time that amounts up to 8145 s (136 min, i.e. 2h 16min). Table 6.15 shows start and end times per section represented in the timeline in Figure 6.27.

Table 6.15. Numerical summary of the assembly process timeline

Section name	Start time	End time	Duration [s]
1. Ribs	0	60	60
2. Profiles	60	1995	1935
3. Reflectors	1995	4035	2040
4. Receivers	2235	2415	180
5. Gables	4035	6015	1980
6. Top glass	6015	7995	1980
7. Side covers	7995	8070	75
8. Bottom plate	8070	8145	75

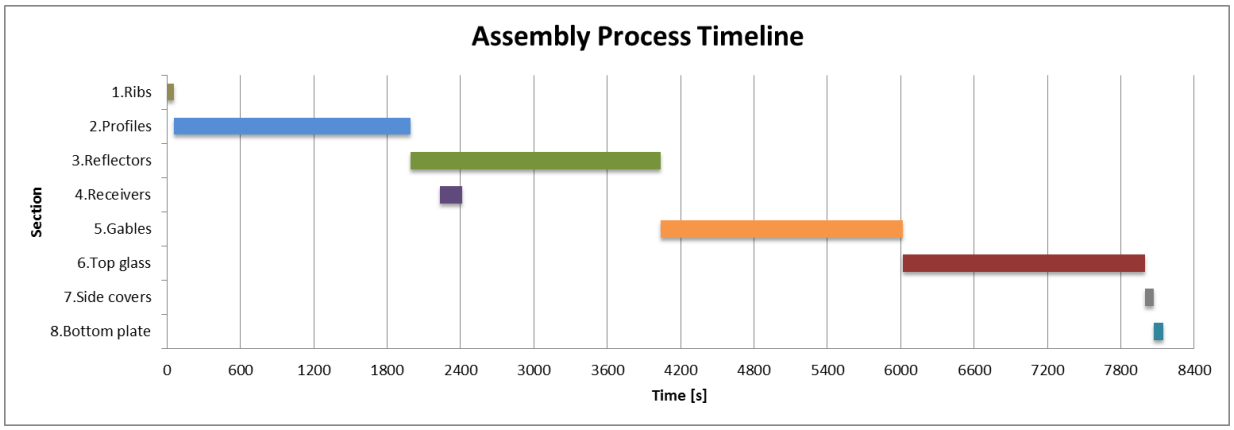

Figure 6.27. Graphical representation of the assembly process timeline

It has to be indicated that during the development of this specific study, a new design of the press has been developed. The idea came up when the visit to Absolicon Solar Collector AB was made. This company has two options to attach the reflector to the structure:

- Wooden solid press: it consists on using a wooden structure which is built by taking the complementary excess of wood when cutting the shape of the ribs. This type of press is shown in Figure 6.28. Obviously, it is considerably cheap but it has one main problem: the operators cannot work while the silicone is drying due to its solid structure and lack of free space in the collector.

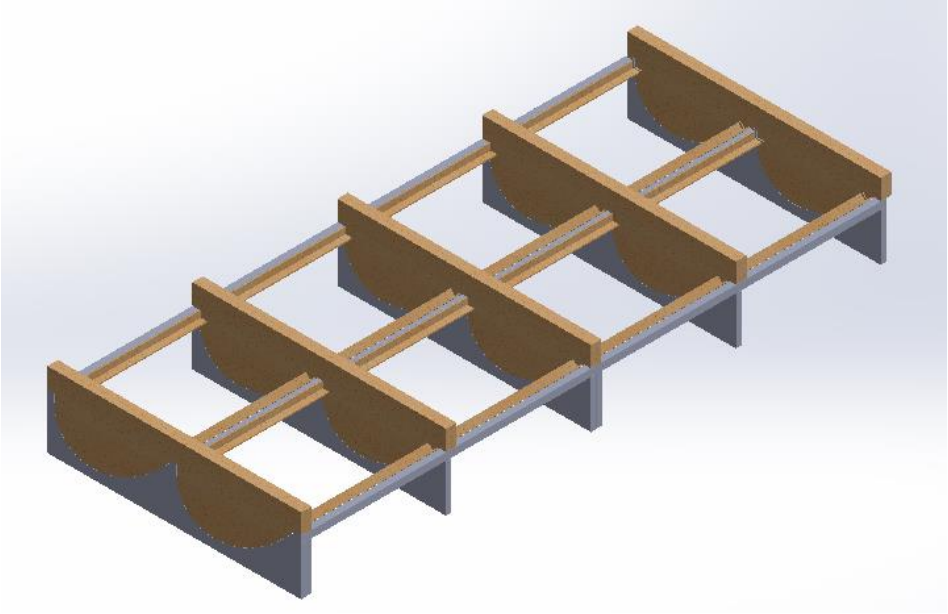

Figure 6.28. Wooden solid press used in Absolicon Solar Collector AB

- Vacuum machine: it is based in a more precise way to deposit the reflector and attach it to the collector. A representative image of this kind of machine can be observed in Figure 6.29. Evidently it is incredibly expensive but its performance is probably more accurate. It is also impossible to work during the drying time it happens in the wooden solid structure.

Figure 6.29. Vacuum machine similar as the one used in Absolicon Solar Collector AB [49]

So, a new design of the press has been created and it is based in the wooden structure's idea but allowing the workers to proceed to the installation of the receivers while the glue is drying. Its design is shown in Figure 6.30 and its application in Figure 6.31, where it can be seen that there is more free space to work in the collector. In this way it is possible to overlap the drying time of the silicone with the next task, reducing waiting time (see Figure 6.27).

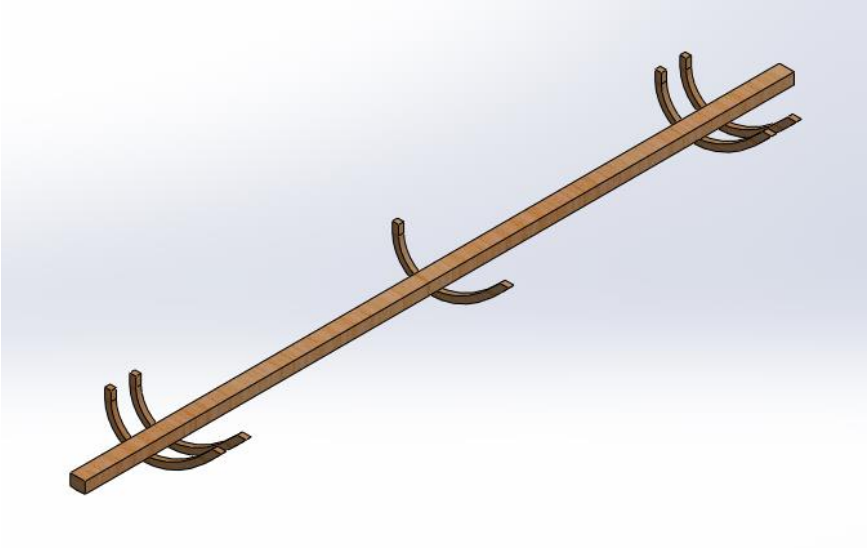

Figure 6.30. Design of the new wooden press

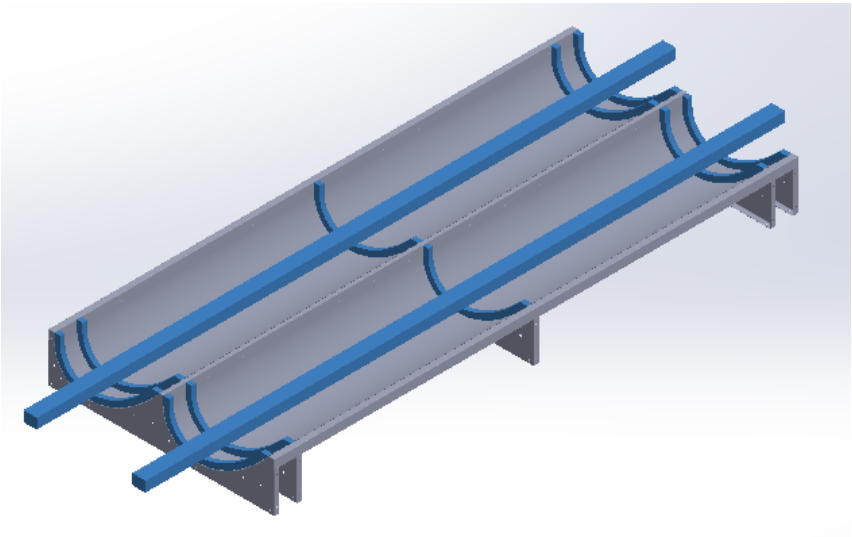

Figure 6.31. Application of the new wooden press

Chapter 7

Discussion

7.1. Design of the new C-PVT prototype

First of all, it is relevant to say that there have been many variations in the designs of the different parts since the first idea came up. At the beginning the plan was to design the receivers for analyzing only the electrical data. But later on, it was decided that it would be more interesting to build the prototypes for analyzing both the electrical and thermal data, so this made some variations to the dimensions of the boxes and the whole receiver was redesigned.

The designs have been developed taking into account that they would end up as a prototype and not as a design for mass production. This is the reason why the box is, for example, made of wood and the design of the holders is just a provisional solution for being able to build the collector. If the design results to be successful, a longer lasting design of the box should be made.

As the boxes are made of wood, the mounting process can be made by screwing the ribs to the attachments, and later on screwing the receiver holders to the ribs as well. The receivers will have to be screwed also to the holders, which is the reason why the placement of the ribs coincides with the spaces between the strings of the solar cells.

Regarding the shape of the pipes for the cooling system, the solution has been adopted as provisional because the heat transfer from the receiver to the fluid will probably perform worse than, for instance, a flat (rectangular) pipe that covers the whole surface of the receiver.

The solar cell cuts are already made and there are enough of them to be able to build the need receivers for the designed collectors. The most complicated part of the prototype is to solder the cells in strings. As they have no standard sizes, the cells have to be fitted manually in the machine that is in the Solarus' factory in Venlo. Soldering them by hand would end up with many broken cells and their performance would suffer a decrease in production so this is an undesirable method.

The proper design will be verified while building the prototypes. As the construction will be manual, it has been attempted to think beforehand about all the problems that could appear in the process of building the prototypes, but new problems may appear and some variations might be needed.

7.2. Analysis and evaluation of the HiG installation

First of all, comparing the simulated thermal output and its estimated output Table 6.10, it can be seen that the second one (111,5 kWh/m^2) is significantly lower than the first one (158,8 kWh/m^2). So, the estimated thermal output is about the 70 % of the simulated using the ten years average. But it is not only the total sum which varies, but also the distribution of the thermal performance Figure 6.22. It can be seen that during the summer (from May to August) the simulated results are much higher than the estimated ones except from August where there is a peak in the estimated output.

In addition, comparing the estimated thermal output with the real performance of the collectors extracted from "Styr och staller", it can be noticed that the performance is noticeably lower than the expected one, concretely 58 % of the total estimated value. But it can be noticed that the real results follow the almost the same distribution over the year as the estimated performance (i.e. different from the simulated).

It has been observed that there are a lot of losses throughout the pipeline and as it can be seen in Table 6.4, the losses correspond around 36 % of the produced heat in the collectors.

Concerning the electrical results obtained Table 6.11, its discussion is similar to the thermal part. The estimated output is slightly lower (60,6 kWh/m^2) than the simulated one (64,4 kWh/m^2), in other words, the estimated energy output is around 94 % of the simulated production. About the distribution, it can be seen in Figure 6.23 that its analysis is similar to the thermal performance, but the differences are minor as well as the peak difference in August.

Examining the real electrical results obtained, it can be determined that there is a slightly variation between the data from Tigo and the data from the logger (Table 6.6 and Table 6.7). Data logger's values are somewhat lower than the values from Tigo, concretely the total value is 10 % inferior. This may be due to the data in the logger has been taken after the inverter which obviously has its own efficiency.

Moreover, analysing more in depth the results from Tigo, it can be seen in Table 6.6 and in Figure 6.24 that the performance of the collectors is unequal among them. Some are not working properly and normally have lower performance than the others: these are the collectors A2, B2, C1, E2, F2 and G2 (below 70 kWh/year). On the other hand, there are a few of them that work always better than the other ones: these are A1, C2, E1, I1 and I2 (above 110 kWh/year).

In addition in Table 6.11, it is possible to compare the real electrical performance (37,99 kWh/m^2 or 34,20 kWh/m^2) with the estimated electrical output (60,6 kWh/m^2). This means that the real output is 62,7 % or 56,4 % of the estimated result, using Tigo or Data logger respectively.

It is obvious that in overall the real results are lower than the expected ones. There can be several factors that contribute to this fact and some are listed below.

- Uneven flow in receiver core. Having a bad flow in the receiver can cause electrical losses in the cells due to local heating. It can also reduce the thermal output due to elevated temperatures in the receiver compared to heat transfer fluid.
    - The Solarus' receiver has seven parallel channels for the flow. The inlet and outlet of these channels are clamped to induce a pressure drop that gives an even flow in all the channels. The production of the collectors for the HIG installation were done with a faulty tool that provided insufficient pressure drop which could lead to uneven flow in the receiver.
        - To evaluate this effect a collector with badly clamped receiver could be tested individually.
- Miss match of collectors
    - The HiG installation uses longer strings of collectors than any other Solarus installation. It is possible that the panels suffer from miss match.
        - To evaluate this effect the fill factor of single panels can be compared to the string fill factor.
- Stagnation issues
    - Recent tests have shown that the previous collector design may have problem with stagnation. After stagnation receiver strings have stopped producing entirely. Investigation into this problem is ongoing.
- Long cables of insufficient diameter
    - There are a lot of losses throughout the pipeline Table 6.4, maybe increasing the diameter of them might decrease the heat losses.
- Shading of collectors
    - It has been shown from testing that the receiver can hang down and cause low electrical production in some unexpected solar angles.

7.3. Market review and competitor overview

Observing Table 6.12 and Table 6.13, there are several conclusions that can be deduced from the most important parameters. To begin with, it has to be stated that the price per square meter of the Solarus' collector is one of the cheapest, which is a remarkable plus point.

The area of the collector is the biggest one due to it contains two troughs in the same module. This fact can be a drawback because the surface is typically the parameter which limits an installation. Nevertheless, the absorption area is the smallest one because the majority of the needed surface is used for concentrating and the competitors are not using concentrators.

The peak electrical power is on the average but two interpretations can be done. Comparing the peak power with the gross area, the efficiency is quite low compared to the competitor's collectors, but comparing it with the absorber area, it has the highest efficiency.

Regarding the thermal part, the solar panel from Solarus has the lowest efficiency of the market, but the peak power is the highest one. This circumstance might be because of the larger area of the module.

Lastly, talking about the weight of the collector, the collector from Solarus is the heaviest one by far but this is understandable taking into account that it is the one with the largest area. Being the heaviest can also be a handicap because it is harder to handle and the structure where it should be mounted has to be firmer and solider.

7.4. Production process guideline

The main conclusion that can be extracted from analyzing the assembly process (Table 6.14 and Figure 6.27) is that the attachments should be reconsidered because of the glue needs too much time and stretches on the process. The waiting time amounts up to 7200 seconds which represents an 88% of the overall time.

Obviously a modification in the manner of mounting all the parts would imply a redesign of several components. For instance, using screws would probably involve higher costs in the production of the components and more labor of mounting but it would evidently remove the waiting time and it would make easier to repair the modules, in case of need.

Moreover, this could be the first step to automate the assembly process. This would make sense if the production increases extensively. Then, prices could be greatly reduced as well as the time of production taking into account that the measure would require a high initial cost to buy all the machines and adapt them to the necessities.

Another way to improve the process would be to produce a huge quantity of collectors at the same time. In this way, during waiting time of one collectors the operators could work mounting other components in another collector until they reach the glue drying time in the other one as well. However, this measure would imply more required space in the workshop.

Chapter 8

Conclusions

After having described all the work performed in the Master Thesis, conclusions have been deducted and summarized per each main topic. In addition, it has been thought that presenting future work and recommendations would be really useful to go straight on with the projects. Thus, some suggestions and possible upcoming tasks are defined in this chapter.

8.1. Design of the new C-PVT prototype

8.1.1. Future work

Once the prototypes have been designed, it is time to build them. In order to do it, some contacts with possible suppliers have been already made, asking for estimated budgets and approximate delivery times. So, the first step would be to come to an agreement with the suppliers and give the final OK to them so that they can start producing the components.

While the components will be manufactured, it could be useful to start preparing the test equipment and organize all the needed tools. After that, and once the components will be received, the PV cells should be laminated and soldered. Then, it would be time to build the prototype manually in the Solarus' workshop.

At this time, the potential comparisons that could be done with the prototypes have been planned. In Table 8.1 and Table 8.2, the designs of boxes and designs of receivers that have been presented during the Master Thesis are characterized.

Table 8.1. The different boxes designs

Design Number	Reflector Design	Arc circle angle / focus length	Reflector height (mm)
1	Standard Solarus	-	86
2	Standard Solarus	-	47
3	Standard Solarus	-	47
4	Symmetric MaReCo	30º	100
5	Pure Parabola	25mm	75
6	Symmetric MaReCo	30º	75
7	Symmetric MaReCo	30º	125
8	Pure Parabola	20mm	75

Table 8.2. The different receiver designs

Design Letter	Cell size (mm)	Receiver (mm)	Pipe size (mm)	Receiver type
A	78*78	2323*86	6	Triangular
B	78*39	2323*47	6	Triangular
C	156*39	2323*47	6	Triangular
D	78*39	2323*47	6	Non-Triangular
E	78*39	2323*47	10	Triangular

Taking into account that it is possible to change the trough (box design) in which the receivers are placed, the planned comparisons are:

- **Cell sizes**
  - Comparison: 1A vs 2B vs 3C
  - Results to take out: Direct comparison of electrical peak power per m^2 and IAM [50].
- **Pipe dimensions**
  - Comparison: B vs E (using the same box design)
  - Results to take out: Direct comparison between thermal performance of 6mm and 10mm pipe diameter.
- **Type of receiver**
  - Comparison: B vs D (using the same box design)
  - Results to take out: Direct comparison between thermal performance of Triangular and Non-Triangular receivers. Do the thermal efficiency curve and the thermal IAM.
- **Reflector shapes**
  - Comparison: 1-2-3 vs 4-5-6-7-8 (using the same receiver)

- Results to take out: Direct comparison of the design in terms of electrical performance (peak power and IAM) and thermal performance (IAM and thermal efficiency curve).

In order to perform the tests, it can be useful to investigate and observe previous experimental setups, for instance [30,[51].

8.2. Analysis and evaluation of the HiG installation

8.2.1. Conclusions

The principal conclusion of its evaluation is that there are many aspects that should be modified in order to enhance the overall performance. Nowadays, the installation is not operating as it is supposed to be, thus it is necessary to implement some improvements.

Concerning the thermal part, it has been noticed that the performance during 2015 is concretely 58 % of the total estimated value. Moreover it has been perceived that there are disproportionate losses in the pipes which decrease considerably the performance of the installation. An in depth revision should be executed and the insulation of the pipes should be upgraded.

Regarding the electrical part, the real output is 62,7 % or 56,4 % of the estimated result, using Tigo or Data logger respectively. Data logger's values are 10 % lower than the values from Tigo, may be due to the presence of the inverter. In addition, the performance of the collectors varies greatly among them, even though they receive practically the same radiation and they are identical. This means that the conditions of several receivers is unacceptable and affects their performance. There are various possible causes, for instance the existence of broken cells and dirt, presence of shading and stagnation issues. So, some measures must be applied in order to improve the quality of the installation.

8.2.2. Future work

- Test a collector with badly clamped receiver to evaluate the flow in the receiver core.
- Compare the fill factor of single panels to the string fill factor of Solarus collectors, to see if the panels suffer from miss match.
- Investigate stagnation issues.
- Improve the pipeline insulation or make a new design.

8.3. Market review and competitor analysis

8.3.1. Conclusions

As it has been explained in section 7.3, the conclusions are that the price per square meter is low, while the electrical and thermal peak powers are high. Both characteristics are advantageous for the Solarus' collector but the main drawback is that the needed area and its weight are significantly higher because of the conception of the design which includes a reflection area.

8.3.2. Future work

It is obvious that the main important aspect to improve is the acquirement of more information about the competitors due to there are several characteristics to fill in. The principal lack of data comes from the prices and some thermal parameters.

On the other hand, it is not only important to complete the data but also to update all the others characteristics due to the solar market is changing rapidly during these years because of its expansion and growth.

8.4. Production process guideline

8.4.1. Conclusions

As said in section 7.4, the first conclusion is that instead of using glue for the attachments, another technique should be used (if possible) as for example screws. It has to be pointed out that the actual waiting time during the assembly process accounts for the 88 % of the total time. In this way, apart from reducing extremely the delay time, it would become more effortless for maintenance and reparations in case of needed.

At the same time, more overlapped processes should be planned in order to achieve the same goal: time reduction. Moreover, it has to be stated that adding screws may add a bigger initial investment, but it would be really useful if it is desired to increase the production in the near future.

8.4.2. Future work

The graph about the production process guideline Figure 6.27 shows that most of the time spent for building a collector is the waiting time for the glue to be able to handle it. So the first aspect to change is to switch from glue to screws wherever is possible (for example the reflector has to be attached to the rib with glue). In this way, the waiting time, and consequently the production time, will be decreased drastically.

For increasing the production of the factory, a line production is recommended so that in each stage a different process is made. Depending on the desired production, more than one line can be made to get a higher production, but the needs of the market have to be taken into account.

Bibliography

[1] K. Kaygusuz, "Energy for sustainable development: Key issues and challenges," *Energy Sources Part B Econ. Plan. Policy*, no. 1, 2007.

[2] W. B. Stine and M. Geyer, "Power From The Sun :: Chapter 2," *Power From The Sun*, 2001. [Online]. Available: http://www.powerfromthesun.net/Book/chapter02/chapter02.html. [Accessed: 24-May-2016].

[3] C. Good, "Environmental impact assessments of hybrid photovoltaic–thermal (PV/T) systems – A review," *Renew. Sustain. Energy Rev.*, vol. 55, pp. 234–239, Mar. 2016.

[4] "photovoltaic effect | physics," *Encyclopedia Britannica*. [Online]. Available: http://global.britannica.com/science/photovoltaic-effect. [Accessed: 24-May-2016].

[5] Y. Xing, P. Han, S. Wang, P. Liang, S. Lou, Y. Zhang, S. Hu, H. Zhu, C. Zhao, and Y. Mi, "A review of concentrator silicon solar cells," *Renew. Sustain. Energy Rev.*, vol. 51, pp. 1697–1708, Nov. 2015.

[6] "How Solar Systems Work & Produce Electricity | Solar TechSolarTech." [Online]. Available: http://solartechonline.com/resource-library/how-does-solar-work/. [Accessed: 24-May-2016].

[7] L. Mearian, "Panasonic surpasses SolarCity with world's most efficient solar panel," *Computerworld*, 06-Oct-2015. [Online]. Available: http://www.computerworld.com/article/2989813/sustainable-it/panasonic-surpasses-solarcity-with-worlds-most-efficient-solar-panel.html. [Accessed: 24-May-2016].

[8] O. Z. Sharaf and M. F. Orhan, "Concentrated photovoltaic thermal (CPVT) solar collector systems: Part I – Fundamentals, design considerations and current technologies," *Renew. Sustain. Energy Rev.*, vol. 50, pp. 1500–1565, Oct. 2015.

[9] J. J. Michael, I. S, and R. Goic, "Flat plate solar photovoltaic-thermal (PV/T) systems: A reference guide," *Renew. Sustain. Energy Rev.*, p. 62, 2015.

[10] F. Shan, F. Tang, L. Cao, and G. Fang, "Performance evaluations and applications of photovoltaic–thermal collectors and systems," *Renew. Sustain. Energy Rev.*, vol. 33, pp. 467–483, May 2014.

[11] T. t. Chow, "A review on photovoltaic/thermal hybrid solar technology," *Appl. Energy*, vol. 87, pp. 365–379, Jan. 2010.

[12] V. v. Tyagi, S. c. Kaushik, and S. k. Tyagi, "Advancement in solar photovoltaic/thermal (PV/T) hybrid collector technology," *Renew. Sustain. Energy Rev.*, vol. 16, pp. 1383–1398, Apr. 2012.

[13] A. Makki, S. Omer, and H. Sabir, “Advancements in hybrid photovoltaic systems for enhanced solar cells performance,” *Renew. Sustain. Energy Rev.*, vol. 41, pp. 658–684, Jan. 2015.

[14] “Combination Hot Water & PV - BOSS SOLAR • Toronto.” [Online]. Available: http://www.bosssolar.com/combination-hot-water-pv/. [Accessed: 19-Mar-2016].

[15] M. Li, X. Ji, G. Li, S. Wei, Y. Li, and F. Shi, “Performance study of solar cell arrays based on a Trough Concentrating Photovoltaic/Thermal system,” *Appl. Energy*, vol. 88, pp. 3218–3227, Jan. 2011.

[16] M. Li, X. Ji, G. l. Li, Z. m. Yang, S. x. Wei, and L. l. Wang, “Performance investigation and optimization of the Trough Concentrating Photovoltaic/Thermal system,” *Sol. Energy*, vol. 85, pp. 1028–1034, Jan. 2011.

[17] S. Nordlander Author and A. I. och samhälle Högskolan Dalarna Miljöteknik, Originator, “Load Adapted Solar Thermal Combisystems - Optical Analysis and Systems Optimization,” Uppsala Universitet, Uppsala, 2004.

[18] M. Adsten 1972-, Author and T. vetenskapsområdet Uppsala universitet Tekniska sektionen, Institutionen för teknikvetenskaper, Materialvetenskap, Originator, “Solar Thermal Collectors at High Latitudes: Design and performance of non-tracking concentrators,” Acta Universitatis Upsaliensis, Uppsala, 2002.

[19] A. Cuevas and S. López-Romero, “The combined effect of non-uniform illumination and series resistance on the open-circuit voltage of solar cells,” *Sol. Cells*, vol. 11, pp. 163–173, Jan. 1984.

[20] H. e. i. Khonkar and A. a. m. Sayigh, “Raytrace for compound parabolic concentrator,” *Renew. Energy*, no. 1, p. 376, 1994.

[21] E. Dresel, “Development and Characterization of a Light Diffuser for a Concentrating PV Collector,” 2011.

[22] W. B. Stine and M. Geyer, “Power From The Sun :: Chapter 9,” *Power From The Sun*, 2001. [Online]. Available: http://www.powerfromthesun.net/Book/chapter09/chapter09.html. [Accessed: 18-May-2016].

[23] M. Adsten, A. Helgesson, and B. Karlsson, “Evaluation of CPC-collector designs for stand-alone, roof- or wall installation,” *Sol. Energy*, vol. 79, pp. 638–647, Jan. 2005.

[24] W. T. Welford, *High Collection Nonimaging Optics*. Elsevier, 2012.

[25] J. A. Duffie and W. A. Beckman, *Solar Engineering of Thermal Processes*. Wiley, 1991.

[26] “10-004 | News release | Dexerials Corporation.” [Online]. Available: http://www.dexerials.jp/en/news/2010/news10004.html. [Accessed: 19-Mar-2016].

[27] S. Guo, J. P. Singh, I. M. Peters, A. G. Aberle, T. M. Walsh, S. Guo, J. P. Singh, I. M. Peters, A. G. Aberle, and T. M. Walsh, “A Quantitative Analysis of Photovoltaic Modules Using Halved Cells, A Quantitative Analysis of Photovoltaic Modules Using Halved Cells,” *Int. J. Photoenergy Int. J. Photoenergy*, vol. 2013, 2013, p. e739374, Sep. 2013.

[28] S. Guo, J. Schneider, F. Lu, H. Hanifi, M. Turek, M. Dyrba, and I. M. Peters, “Investigation of the short-circuit current increase for PV modules using halved silicon wafer solar cells,” *Sol. Energy Mater. Sol. Cells*, vol. 133, pp. 240–247, Feb. 2015.

[29] “Solar Power - MITSUBISHI ELECTRIC.” [Online]. Available: http://www.mitsubishielectric.com/bu/solar/pv_modules/monocrystalline/technologies.html. [Accessed: 19-Mar-2016].

[30] J. Gomes, L. Diwan, R. Bernardo, and B. Karlsson, “Minimizing the Impact of Shading at Oblique Solar Angles in a Fully Enclosed Asymmetric Concentrating PVT Collector,” *Energy Procedia*, vol. 57, pp. 2176–2185, Jan. 2014.

[31] “Solarus | Sunpower for the people.” [Online]. Available: http://solarus.com/. [Accessed: 18-May-2016].

[32] “LOW IRON SOLAR GLASS,” *Sunarc*. [Online]. Available: http://www.sunarc.net/index.php/glass/lowironsolarglass. [Accessed: 18-May-2016].

[33] L. r. Bernardo, B. Perers, H. Håkansson, and B. Karlsson, “Performance evaluation of low concentrating photovoltaic/thermal systems: A case study from Sweden,” *Sol. Energy*, vol. 85, pp. 1499–1510, Jan. 2011.

[34] “ALANOD |.” [Online]. Available: http://alanod.com/en. [Accessed: 18-May-2016].

[35] J. Moreno Puerto, “Performance Evaluation of the Solarus AB Asymmetric Concentrating Hybrid PV/T Collector,” Master Thesis, 2014.

[36] “Solar Cell, Mono Cell, Poly Cell Manufacturer - BIG SUN Energy Technology Inc.” [Online]. Available: http://www.bigsun-energy.com/en/. [Accessed: 18-May-2016].

[37] “ACC Silicones manufacture silicone RTV, adhesive, sealant, moulding rubber, gels and fluids.” [Online]. Available: http://www.acc-silicones.com/. [Accessed: 18-May-2016].

[38] “Solidworks.” [Online]. Available: http://www.solidworks.es/. [Accessed: 11-Mar-2016].

[39] M. Bergen and M. A. Peteraf, “Competitor identification and competitor analysis: a broad-based managerial approach,” *Manag. Decis. Econ.*, vol. 23, no. 4–5, pp. 157–169, Jun. 2002.

[40] T. O’Connor, *Strategic Planning for Distributors: Execution Isn’t Everything--It’s the Only Thing!* Natl Assn Wholesale-Distr, 2010.

[41] M.-N. Nguyen and N.-H. Do, “Re-engineering Assembly Line with Lean Techniques,” *Procedia CIRP*, vol. 40, pp. 590–595, 2016.

[42] R. Álvarez, R. Calvo, M. M. Peña, and R. Domingo, “Redesigning an assembly line through lean manufacturing tools,” *Int. J. Adv. Manuf. Technol.*, vol. 43, no. 9–10, pp. 949–958, Oct. 2008.

[43] H. Gajbert, *Solar thermal energy systems for building integration*. Lund: KFS AB, 2008.

[44] L. Bonfligio and C. Giovinazzo, “Alternative reflector shapes for stationary concentrating PV/T collectors.” 2015.

[45] “Manodo Server - Login.” [Online]. Available: http://styrochstaller.ktc.se/Portal/Login/Login.aspx?ReturnUrl=%2fPortal%2f. [Accessed: 16-May-2016].

[46] “User Login - Tigo Energy.” [Online]. Available: https://installations.tigoenergy.com/base/login/login. [Accessed: 16-May-2016].

[47] “Shiny weather data.” [Online]. Available: https://rokka.shinyapps.io/shinyweatherdata/. [Accessed: 16-May-2016].

[48] EUROPEAN SOLAR THERMAL INDUSTRY FEDERATION, “Objective methodology for simple calculation of the energy delivery of (small) Solar Thermal systems.” 2007.

[49] “intercomercial-aog-1962-sistema-de-elevacion-por-vacio-el-sistema-de-elevacion-por-vacio-tawigrip-puede-elevar-voltear-y-girar-paneles-de-metal-vidrio-y-laminados-701036-FGR.jpg (350×350).” [Online]. Available: https://www.logismarket.es/ip/intercomercial-aog-1962-sistema-de-elevacion-por-vacio-el-sistema-de-elevacion-por-vacio-tawigrip-puede-elevar-voltear-y-girar-paneles-de-metal-vidrio-y-laminados-701036-FGR.jpg. [Accessed: 18-May-2016].

[50] Bernardo Ricardo, Davidsson Henrik, Gentile Niko, Gomes João, Gruffman Christian, Chea Luis, Mumba Chabu, and Karlsson Björn, “Measurements of the Electrical Incidence Angle Modifiers of an Asymmetrical Photovoltaic/Thermal Compound Parabolic Concentrating-Collector,” *Engineering*, no. 1, p. 37, 2013.

[51] J. Nilsson, H. Håkansson, and B. Karlsson, “Electrical and thermal characterization of a PV-CPC hybrid,” *Sol. Energy*, vol. 81, pp. 917–928, Jan. 2007.

Appendix - Production Process Guideline

1. Ribs

Description: The first step for the solar panel is the construction of the foundations of the structure. First 5 ribs made out of steel are needed, for making the basis of the structure. The geometry of the ribs is quite complex because it is defined by the desired shape of the reflector, which is a parable-circumference.

Material: 5 steel ribs (1mm thickness), mounting jig, clamps

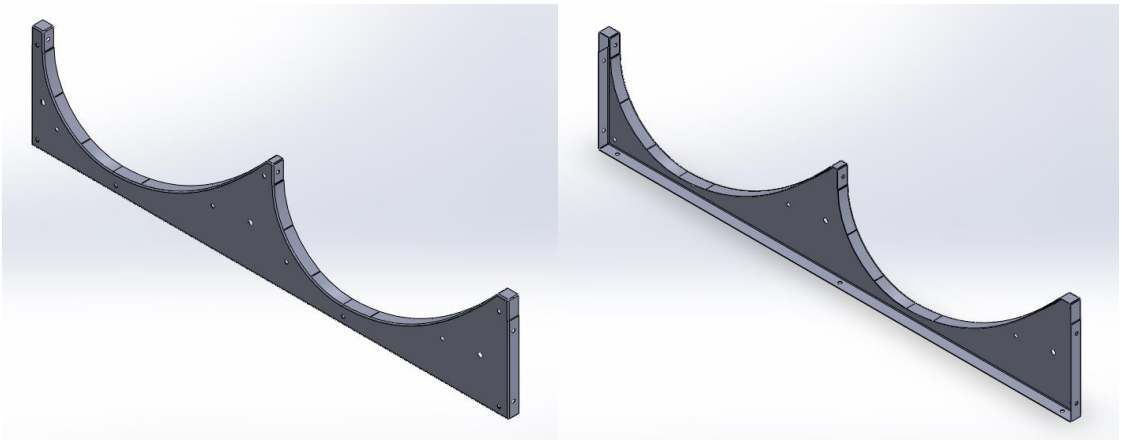

Figure A-1. Design of the ribs

Attachment:

I. For mounting the five ribs, the distance between the two exterior ribs is 2’3 meters. Two other ribs go 10 cm away to the centre from the exterior ones. The last rib goes in the exact middle point. They are to be attached by clamps.

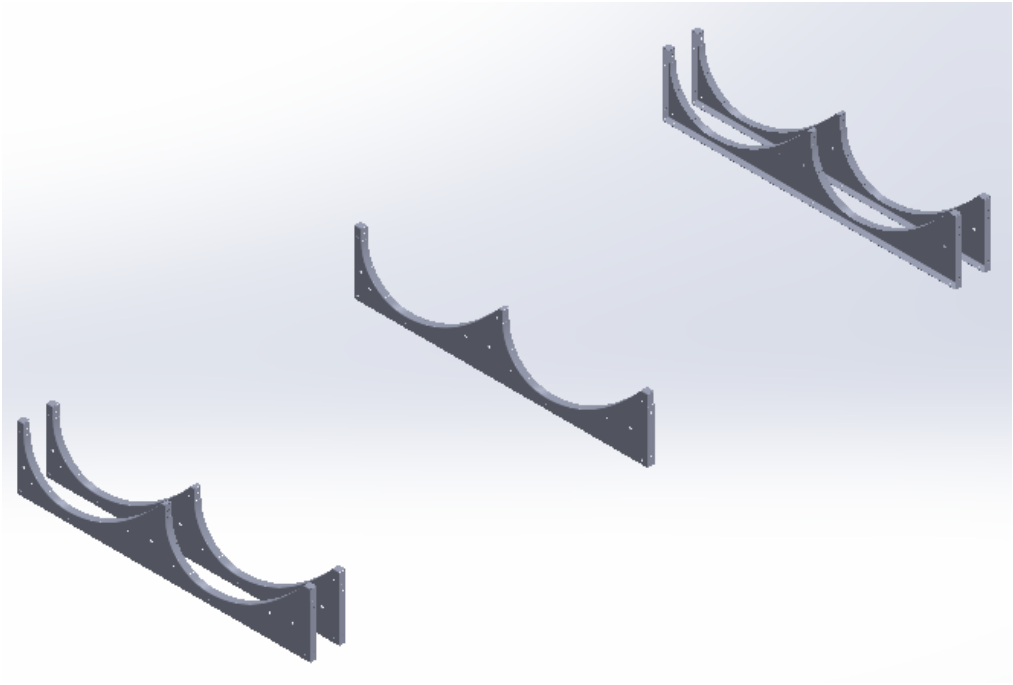

Figure A-2. Rib deployment for the collector

2. Two “A” profile & one “n” profiles

Description: In this step the ribs are attached to each other with the help of 3 metal covers with different profiles. The shape of two of the covers will be an “A” profile and they will be set at one end of the rib and in the middle. The shape of the other cover will be an “n” profile and it will connect the other end of the five ribs.

Material: 2 different (symmetric) “A” profiles and 1 “n” profile made out of steel with 1mm thickness, glue

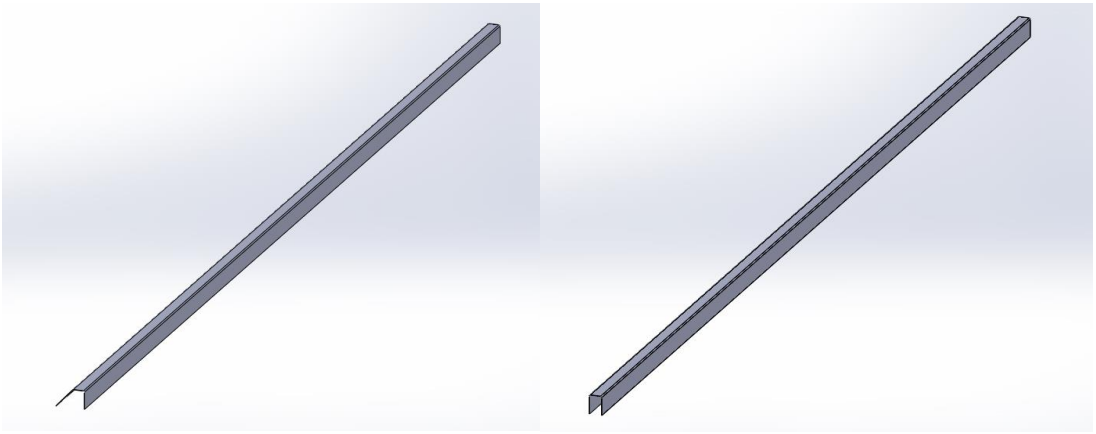

Figure A-3. Design of the “A” and “n” profiles

Attachment:

I. Put glue on the top surfaces of the ribs

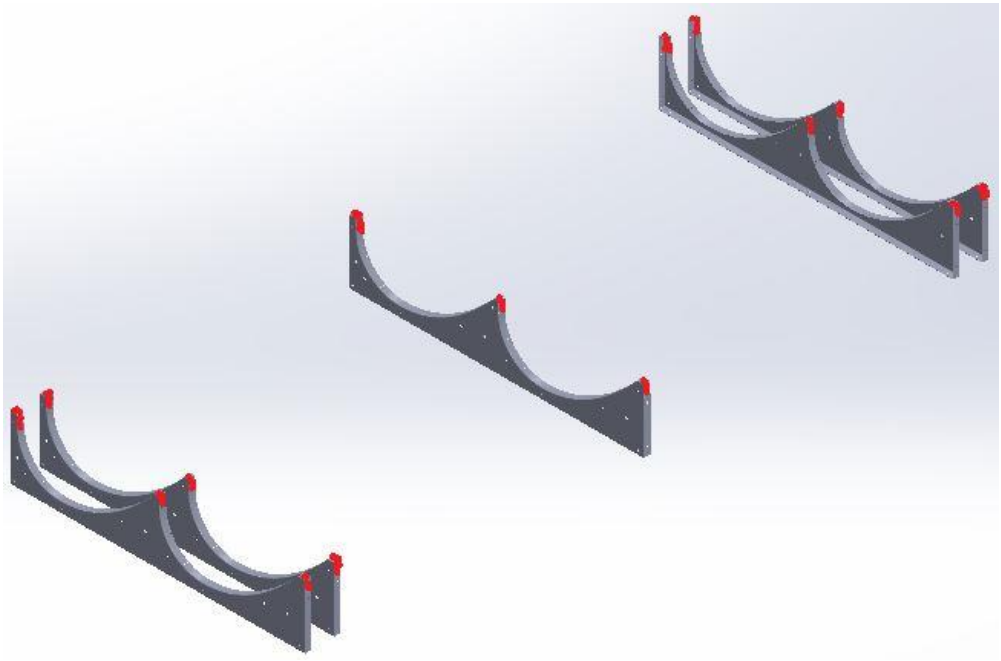

Figure A-4. Location for the glue

II. Attach the “n” profile in its defined location

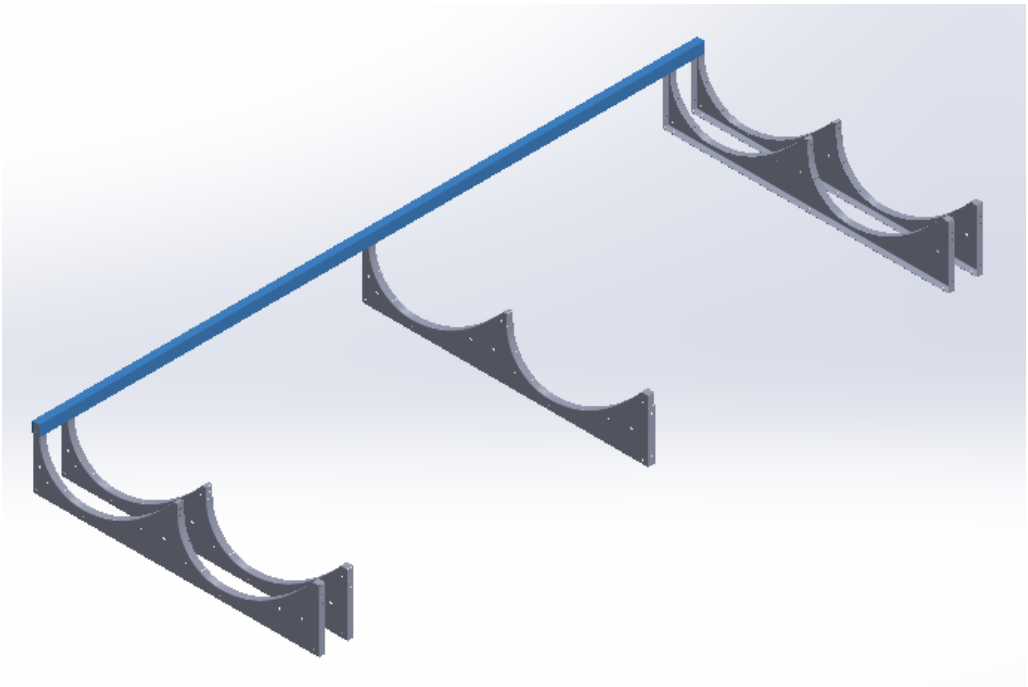

Figure A-5. Attachment of the “n” profile

III. Attach the “A” profile of the opposite position of the ribs

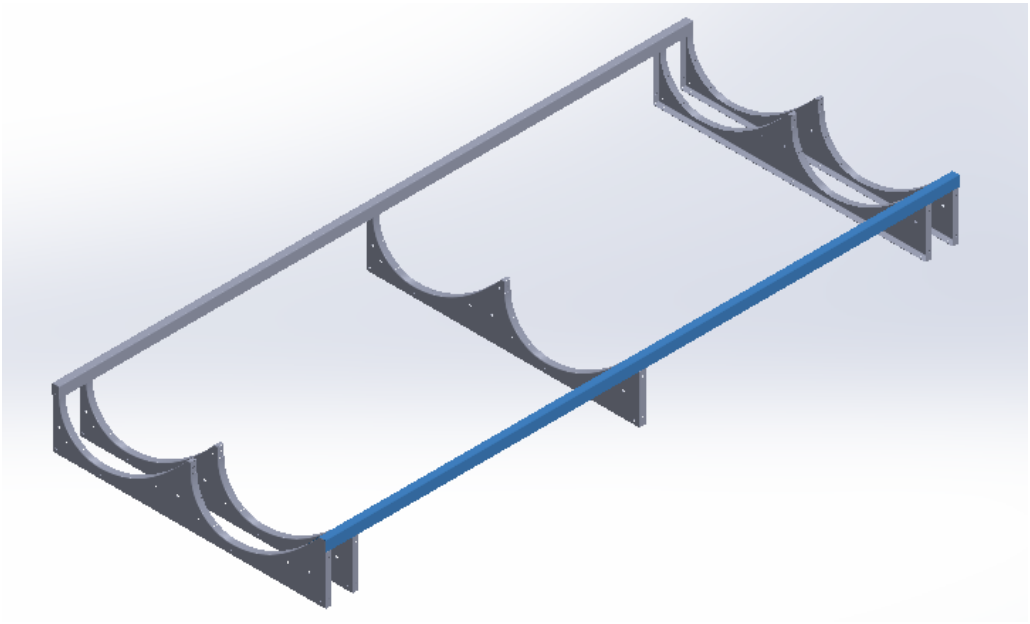

Figure A-6. Attachment of the “A” profile of the side

IV. Attach the other “A” profile that goes in the middle of the ribs

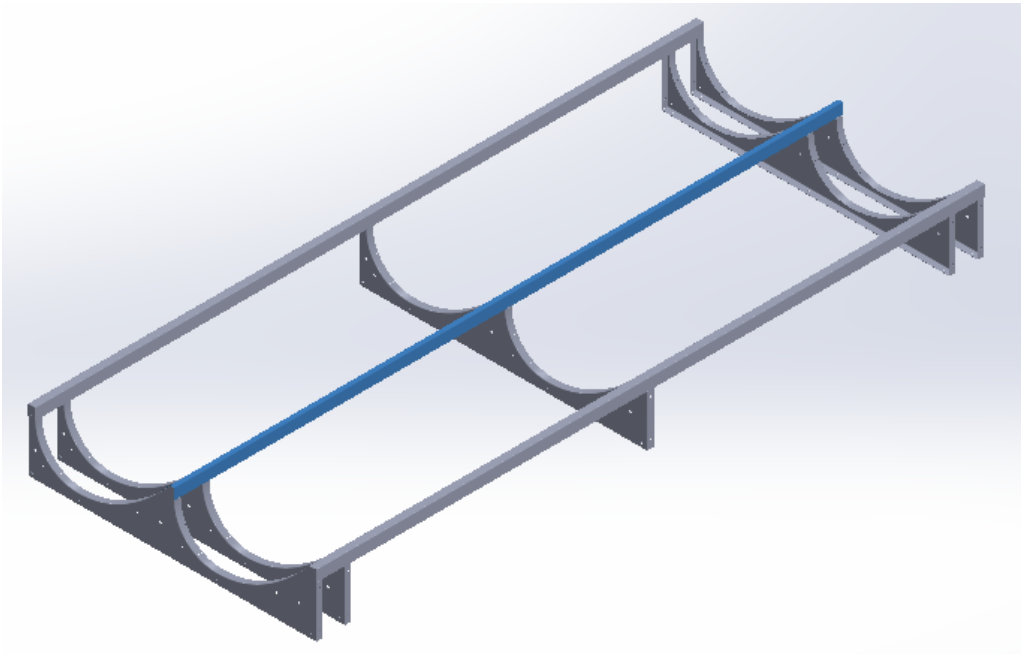

Figure A-7. Attachment of the “A” profile of the middle

3. Reflectors

Description: Two large reflector plates are pressed and glued in this step to the ribs with the proper geometry so that they can concentrate the solar radiation in the receivers. The reflectors are long metal sheets that thanks to the pressure and the form of the ribs, take the desired shape. The reflector plate will have some holes, which some are needed to put the holders of the receivers and some to lead the cables under the reflector.

Material: 2 reflectors plates (0,5 mm thickness), glue, pressing tool

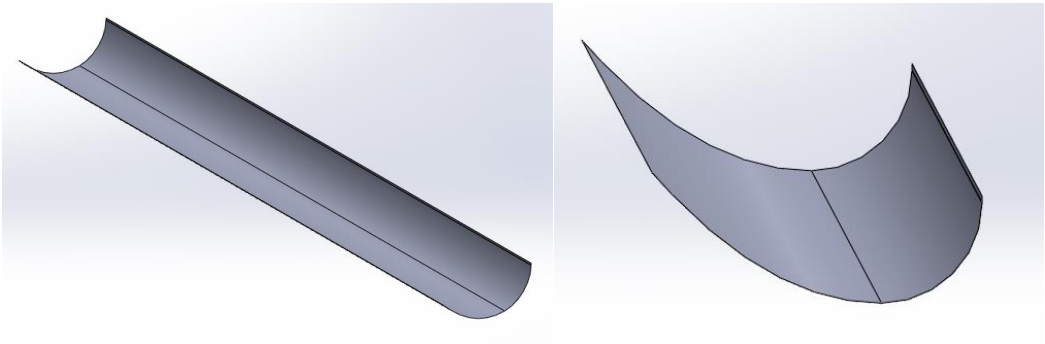

Figure A-8. Design of the reflector

Attachment:

I. The surface of the parable-circumference of the ribs is glued to attach the reflector on it.

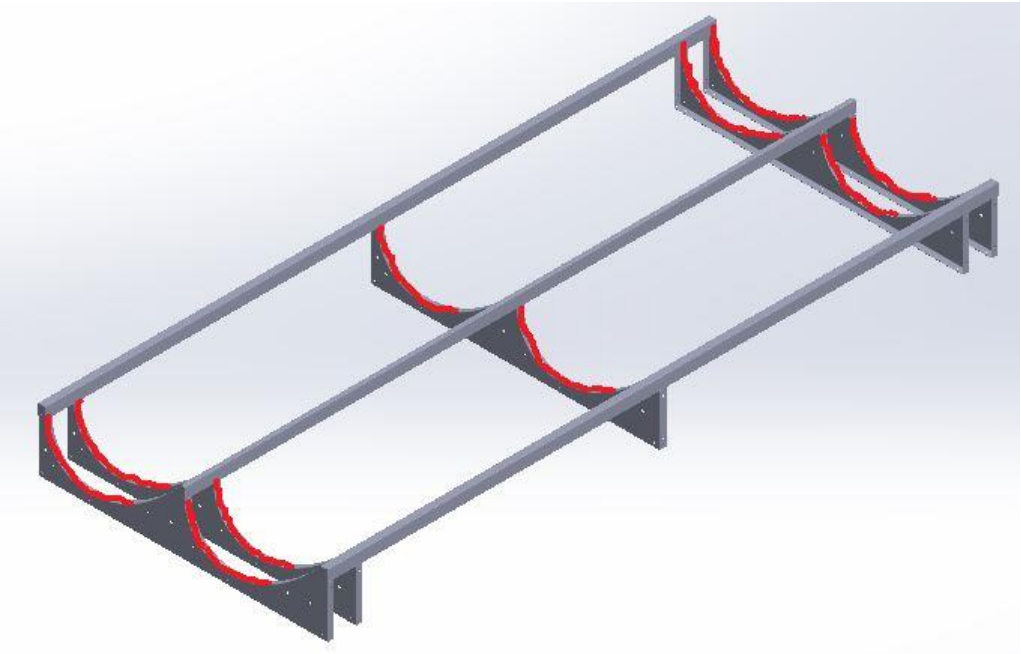

Figure A-9. Location of the glue for the reflector on the ribs

II. The reflector plates are attached to the ribs.

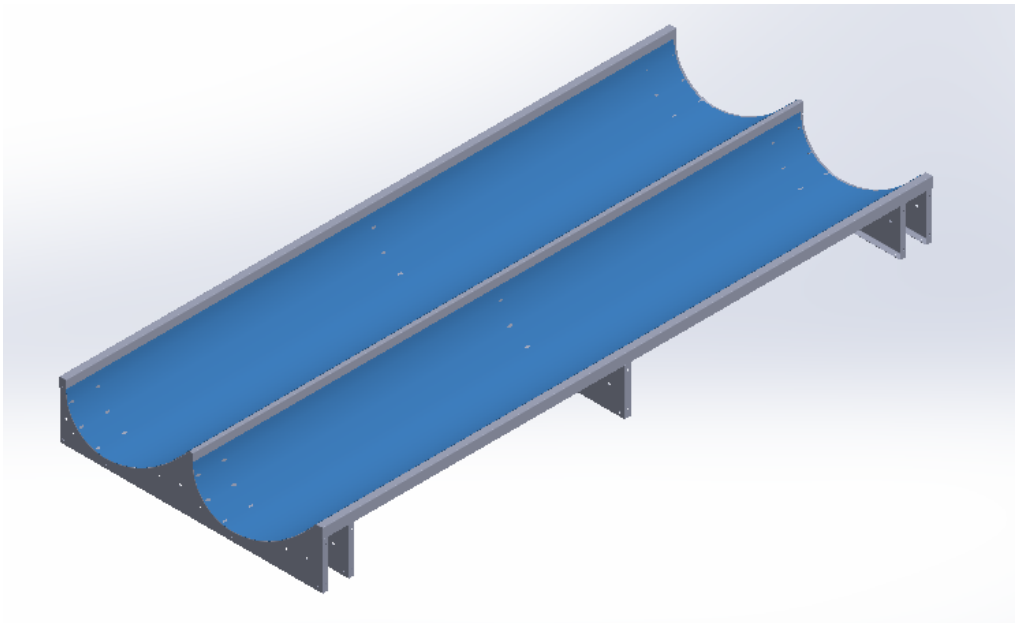

Figure A-10. Attachment of the reflectors

III. Pressure is made from the top to make sure that the reflector is well attached to the ribs and the profiles.

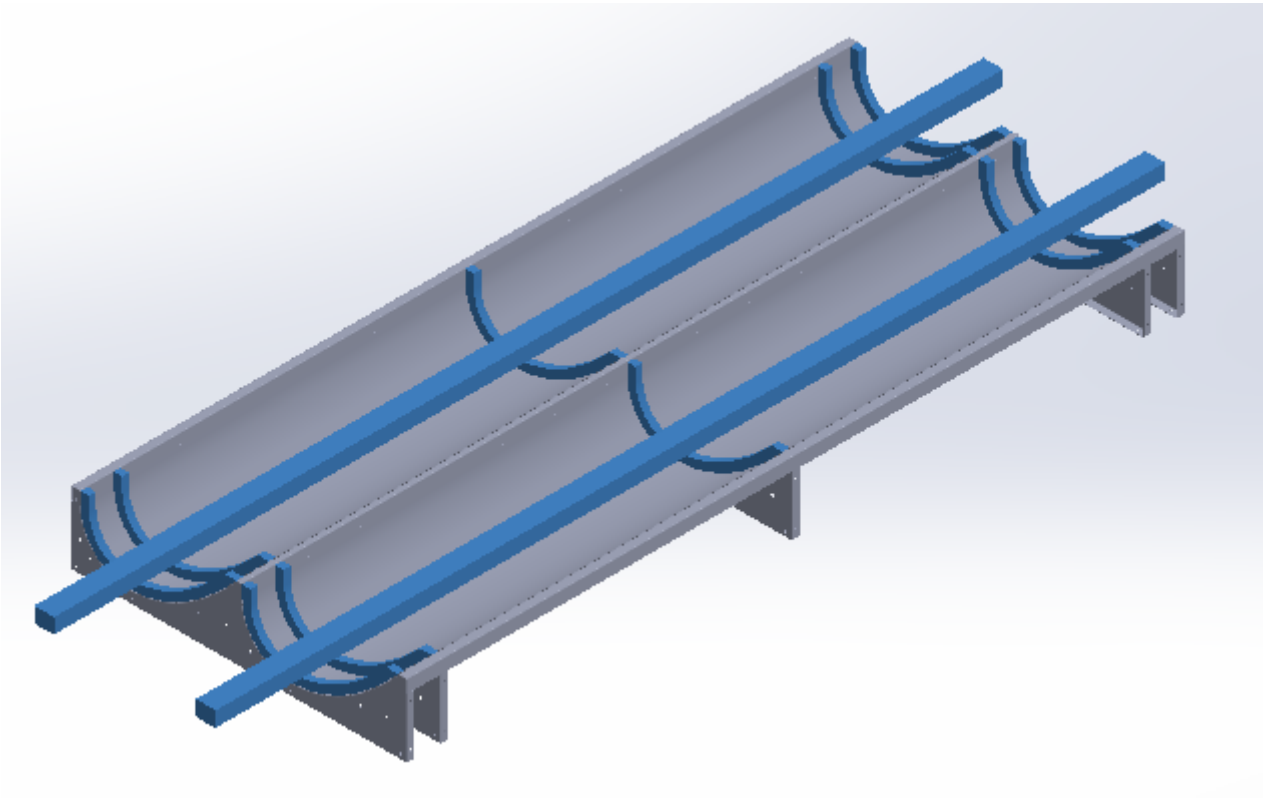

Figure A-11. Design of the press for the reflector

“Waiting time”: After this third step it is necessary to wait 30 minutes for the glue to make effect and get dry so that is possible to start with the next steps. The glue is completely dry after 24 hours but it is possible to handle within 30 minutes. So this pressing tool should let putting the receiver holders and the receivers themselves.

4. Receivers

Description: Before the receivers are attached to the construction, it is necessary to assemble three holders on the construction. The holders are attached in the three interior ribs with screws. After this step you can put the receiver in the holder to assemble it. This step is the same for both sides of the parable-circumference.

Material: 2 receivers, 6 receiver holders

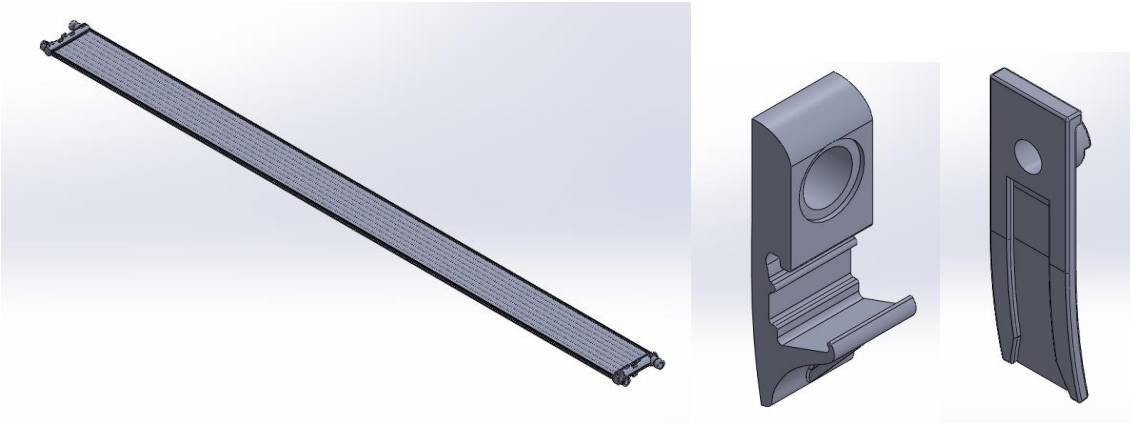

Figure A-12. Receiver and receiver holders

Attachment:

I. The six holders are screwed to the three ribs located in the middle

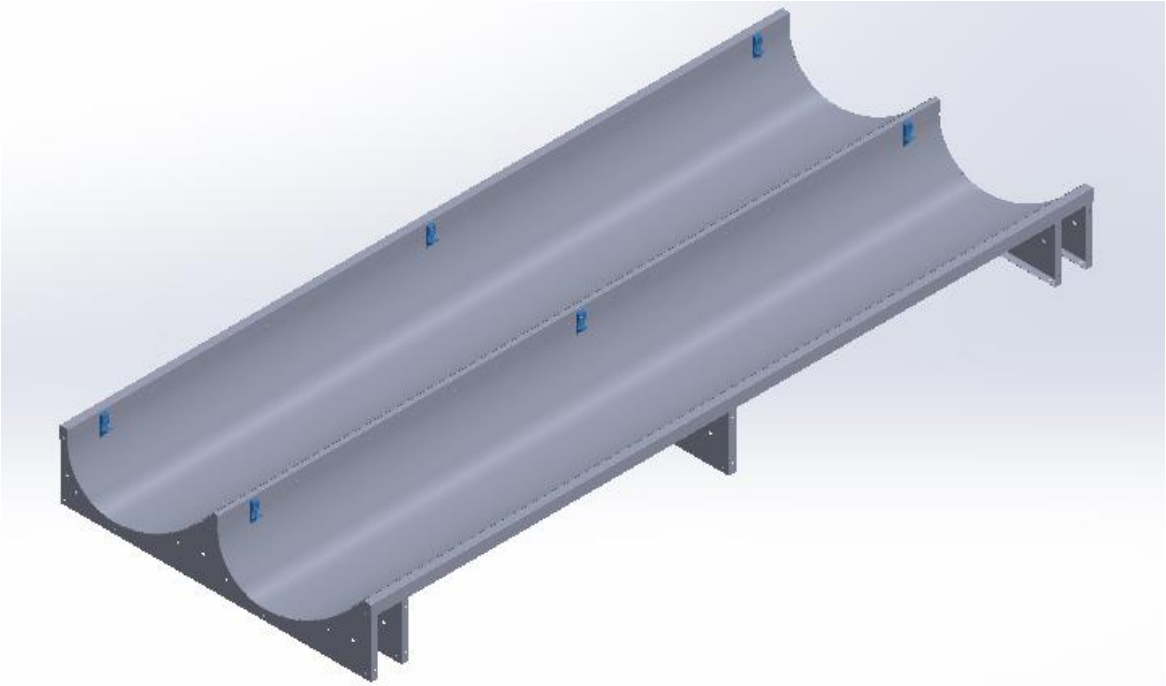

Figure A-13. Location of the holders

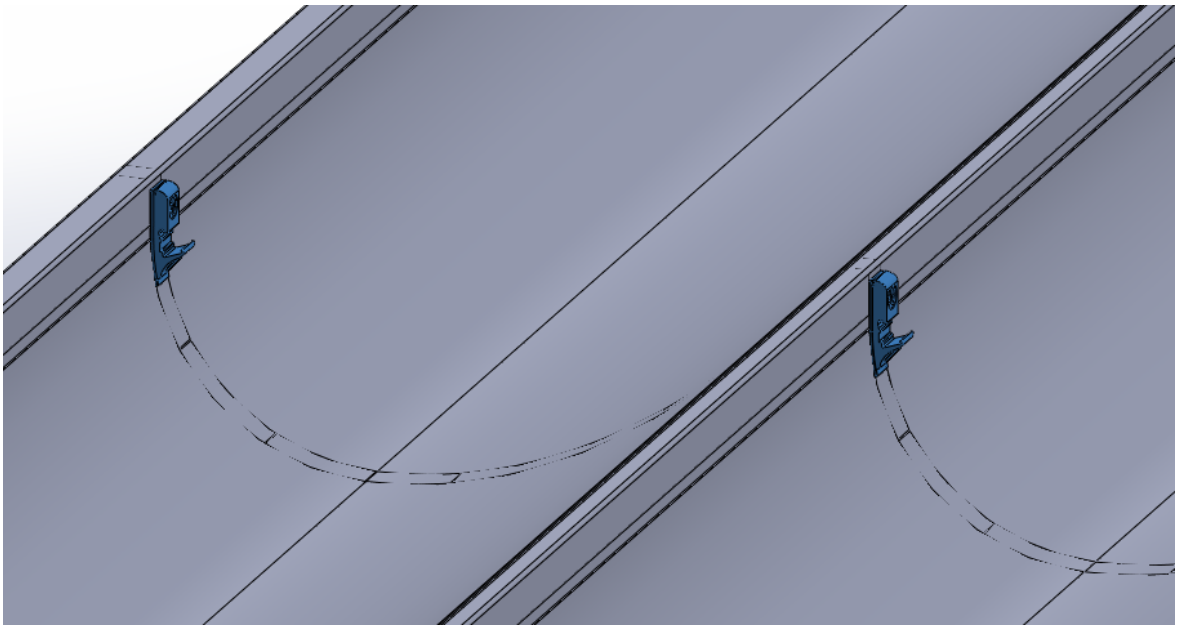

Figure A-14. Attachment of the holders

II. Receiver is attached to the holder

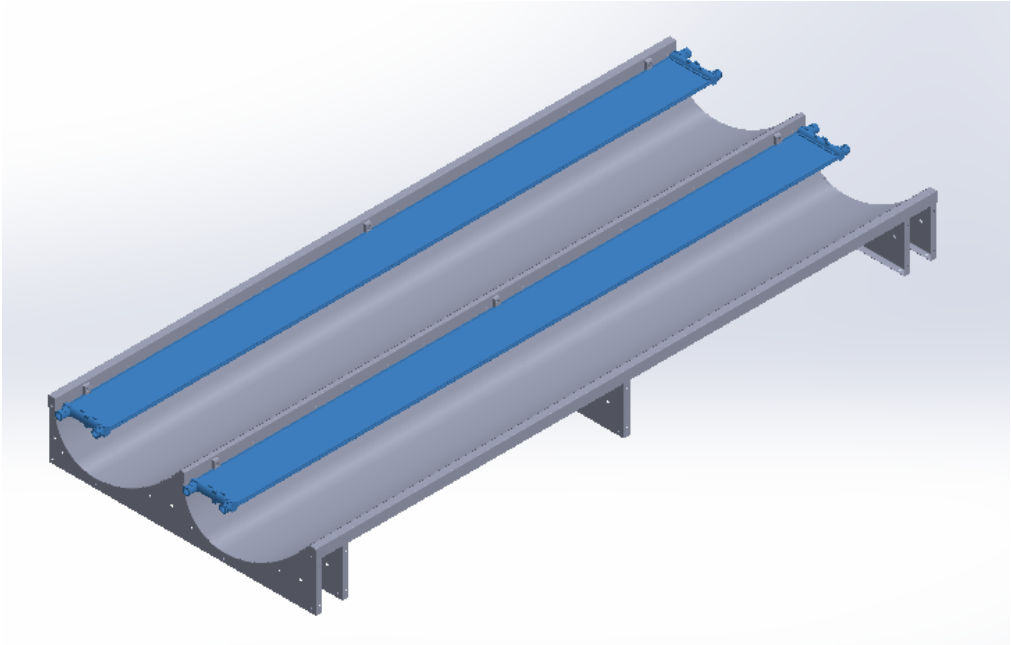

Figure A-15. Attachment of the receivers

III. The electrical connection between the two receivers is made.

5. Gables

Description: In step two gables are used to cover both sides of the receivers and to hold the receivers from the sides at the same time. The gable is made out of plastic and is attached with glue on the side of the ribs. The holes of the gables will hold the receiver, the gables will work as a protection of the receivers and will have some grommets to attach the receiver to them.

Material: 4 gables (plastic), glue, grommet (rubber)

Attachment: In the first step the receiver has to be fit in the holes of the gables. Afterwards glue is put in the reflector and the gable is attached to it.

6. Top glass

Description: After every work inside the box is completed, it is covered with a glass at the top to protect the collector against stresses and strains from outside, for example: rain, hail and so on.

Material: low iron glass plate (4 mm thickness), glue

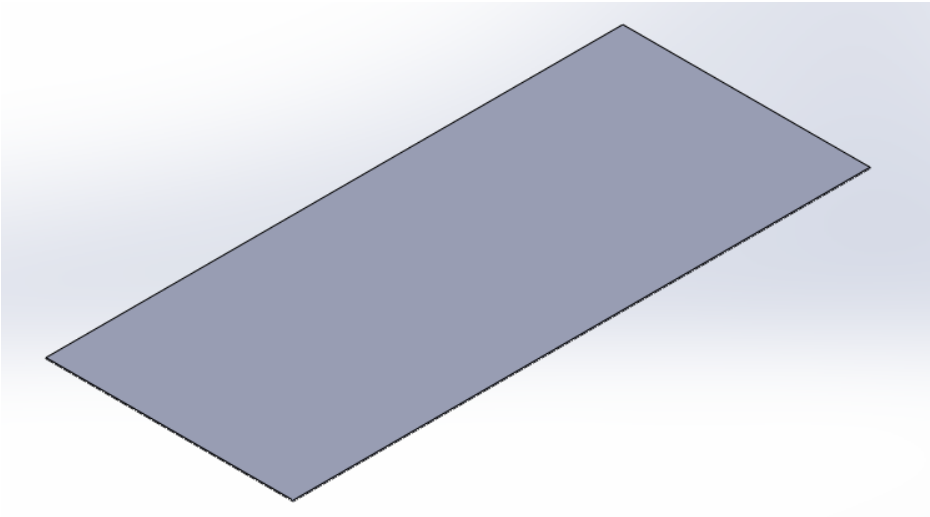

Figure A-16. Design of the top glass

Attachment:

I. Put glue at the top of the three profiles and the gables

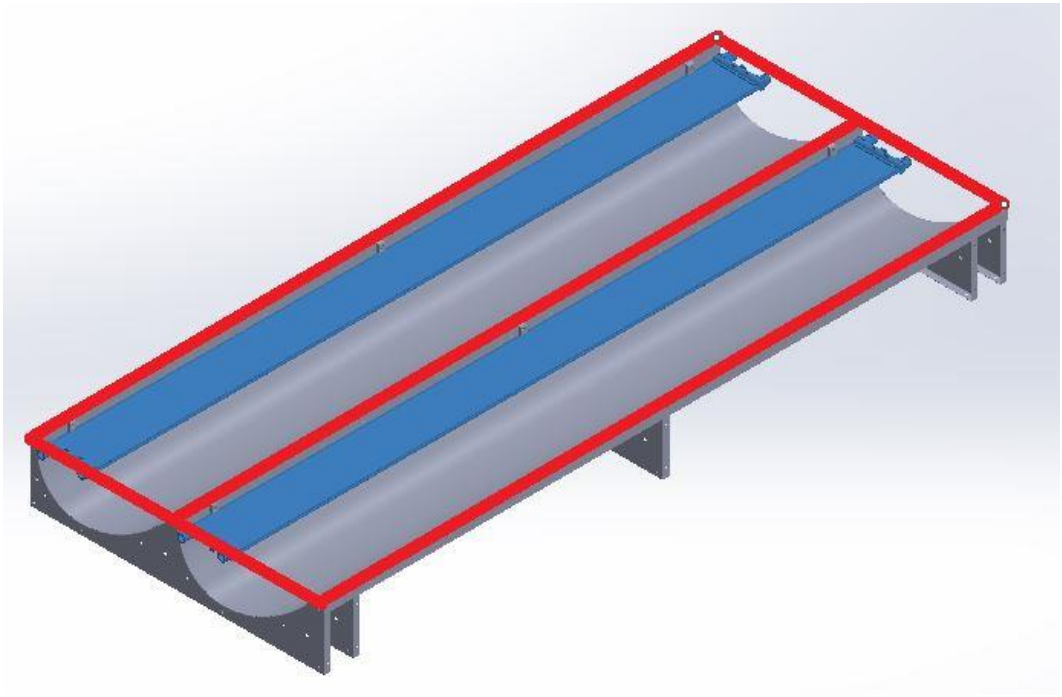

Figure A-17. Location of the glue for the glass

II. Put the glass plate on top

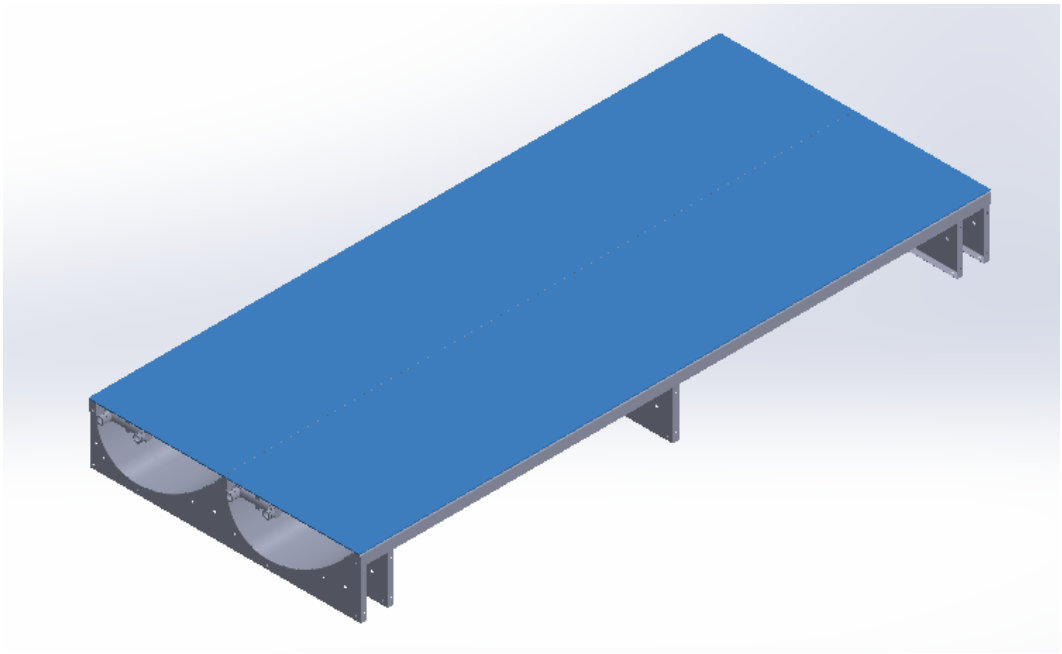

Figure A-18. Attachment of the glass

7. Protective cover on the side

Description: In this step two covers are attached on the long side of the construction as a safety measure against precipitations. The cover is made out of steel and has a “U” profile.

Material: 2 steel covers (1 mm thickness)

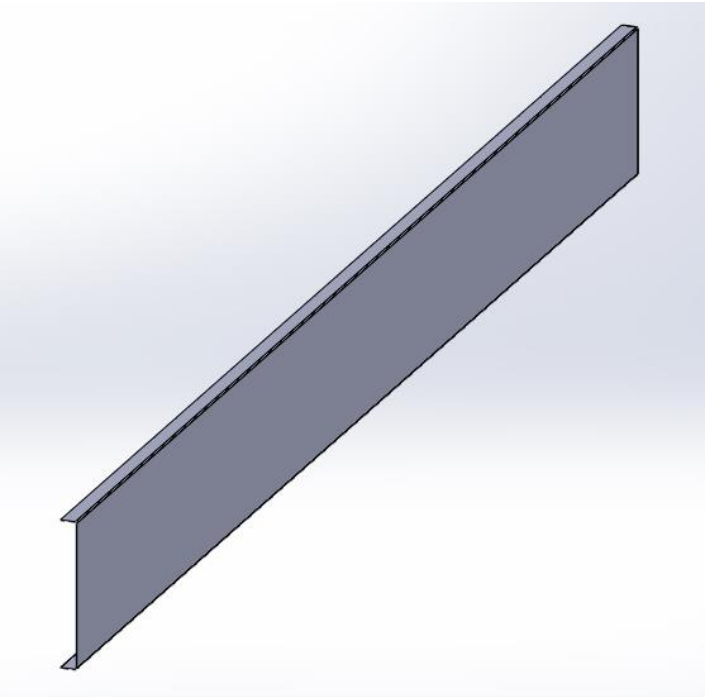

Figure A-19. Design of the protective cover of the side

Attachment: The idea to attach the covers on the side is with the procedure of “clinching”. Clinching also referred as Press-Joining" is a bulk-sheet metal-forming process aimed at joining thin metal sheet without additional components. In this case is it an advantage to lift the construction with a crane to edit the underside better.

I. Lift the module and attach the side covers with clinching

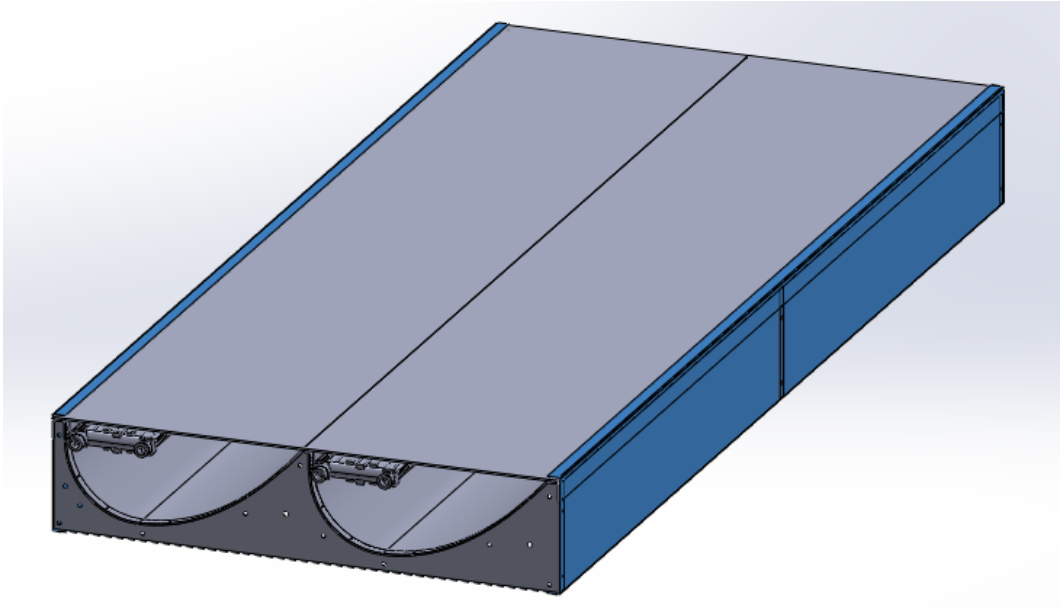

Figure A-20. Attachment of the protective cover on the side

8. Protective bottom plate

Description: In this step a bottom plate is attached in order to prevent ground moisture or other unfavourable conditions that could get the collector dirty. The bottom plate is made of steel and has the same size as the glass on the top.

Material: steel plate (1 mm)

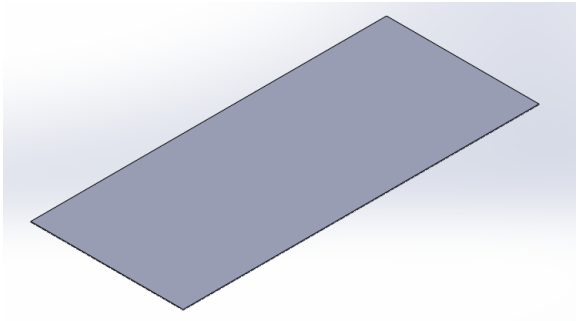

Figure A-21. Protective bottom plate

Attachment: The way of attaching the bottom plate is with the procedure of "clinching". In this case the construction should be lift with a crane.

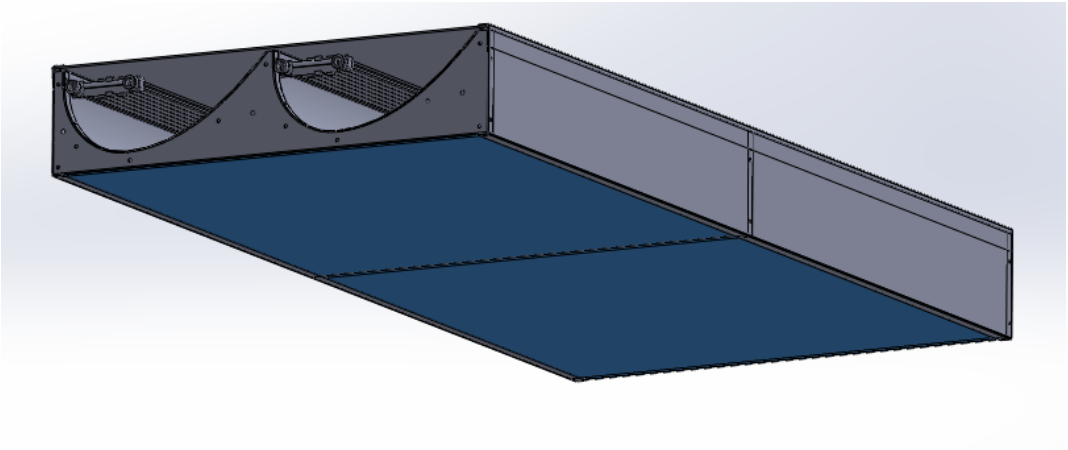

Figure A-22. Attachment of the protective bottom plate

- After the last step the construction should dry for 24 hours to get hardened -